Luminescent 1-Chalcogeno-1,3-butadiene: Elucidation of Photophysical Properties and Application to Hydrogen Sulfide Sensor

Graduate School of Science and Engineering

Course in Material Sciences

Saitama University

Tatsuro Annaka

March, 2015

Contents

Chapter 1

General Introduction

1–1 Introduction

Luminescent organic compounds have attracted considerable attention in the fields of biochemistry[1] and materials science as exemplified by organic light-emitting devices (OLEDs).[2] Organic compounds possess higher solubility to organic solvents than inorganic ones, leading to application for probes in the body and devices prepared by printing[3] and spin-coating[4] process. Although extended π-conjugative aromatic hydrocarbons, for example, anthracene, pyrene, pentacene, and their π-extended derivatives,[5] played a central role as organic fluorophore, they have several problems such as difficulties of tuning photophysical properties, low solubility, and instability.

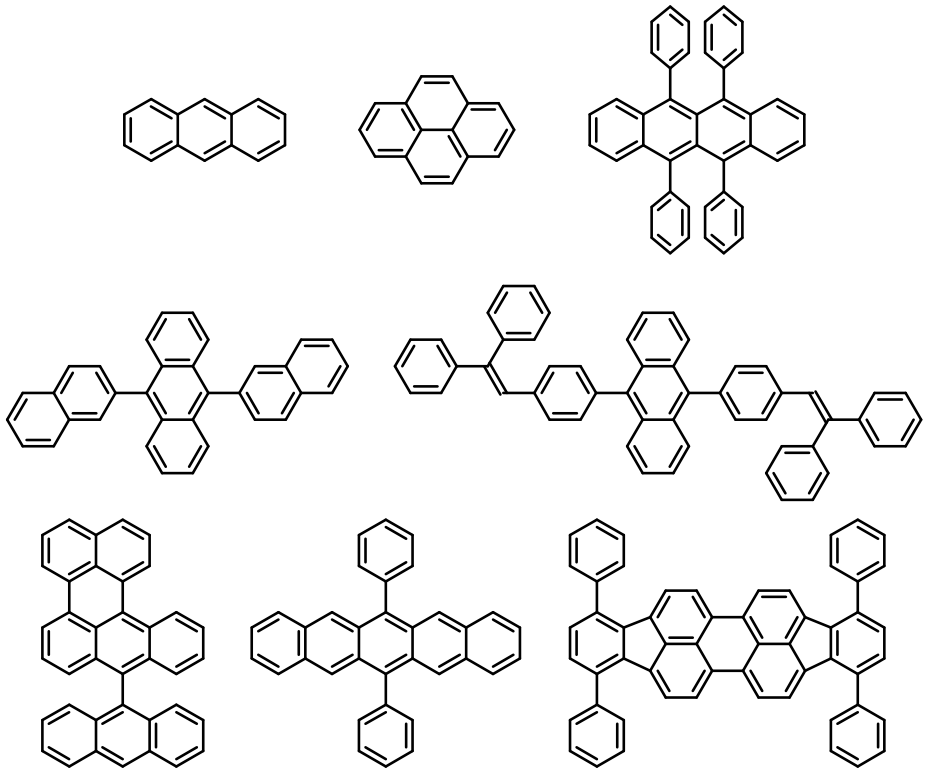

Figure 1–1. Hydrocarbon fluorophores.

1–2 Fluorescent Compounds Containing Heteroatom

In recent years, several types of fluorescent compounds containing heteroatom, such as boron,[6] silicon,[7] and phosphorus,[8] incorporated in a conjugated system have been reported. The heteroatom provide crucial perturbations to the electronic nature of the HOMO and/or the LUMO of the corresponding carbon counterparts.[9] A significant characteristic of these compounds is the drastic change in photophysical properties given by the chemical modification of heteroatom as shown in Figure 1–2–1.

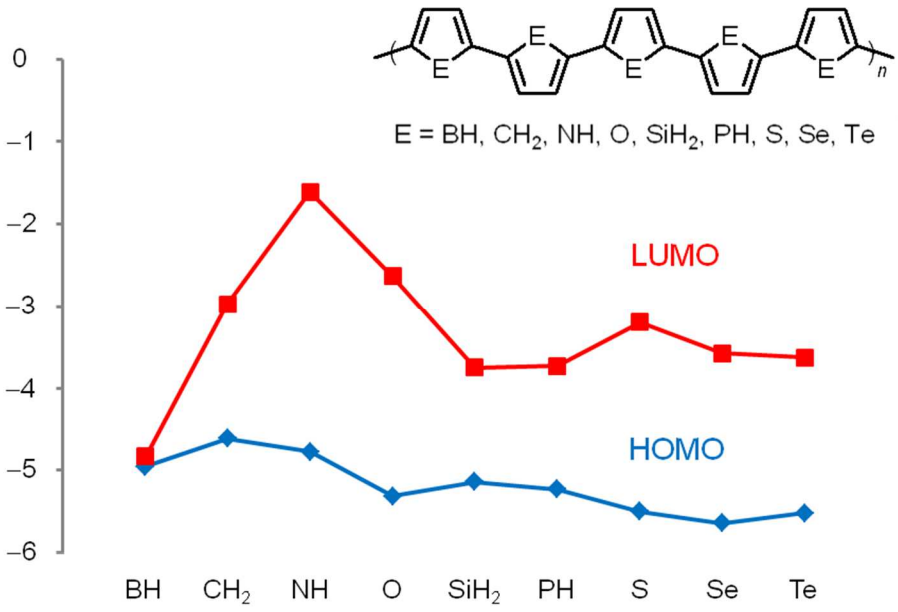

Figure 1–2–1. Calculated electronic structure of parent polyheteroles.

Boron compounds have acceptor character, leading to high reactivity with electrophilic species. Introduction of a silicon atom into π-conjugative compound reduces LUMO energy level due to the σ*(Si–C)–π* interaction and can increase fluorescence quantum

yield empirically. A donor character of phosphorus atom can control physical properties by the reaction with Lewis acid and transition metal.

para: CN^- sensor
ortho: F^- sensor
Mes = 2,4,6-trimethylphenyl

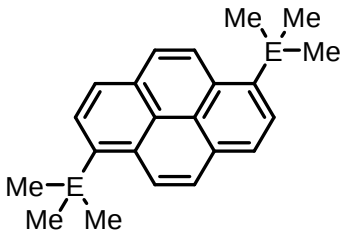

E = C (λ_{abs} = 348 nm, Φ_F = 0.34)
E = **Si** (λ_{abs} = 354 nm, Φ_F = 0.50)
in CH_2Cl_2

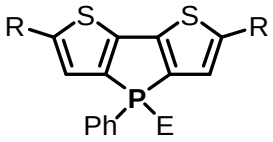

E = lp, O, S, BH_3, *Pd*, *Pt*, *Au*, *Rh*, *W*, *Fe*
lp = lone pair

Figure 1–2–2. Fluorescent compounds containing heteroatom.

1–3 Organochalcogen Compounds

Organochalcogen compounds, especially thiophene derivatives, have been studied as organic semiconductor.[10] In contrast, fluorescent organochalcogen compounds are still less known than other heteroatom compounds as mentioned above.[11] An acceptor character of chalcogen can be significantly increased by oxidation on chalcogen atom, changing electronic structure of the compound.[12] For example, oxidation of pentathienoacene working as p-type semiconductor gave corresponding oxide, which shows n-type semiconducting character.[12d] Fluorescence wavelength of poly(phenylene ethnylene) containing four sulfur atoms is shifted bathochromically as increasing oxidation number of sulfur.[12e]

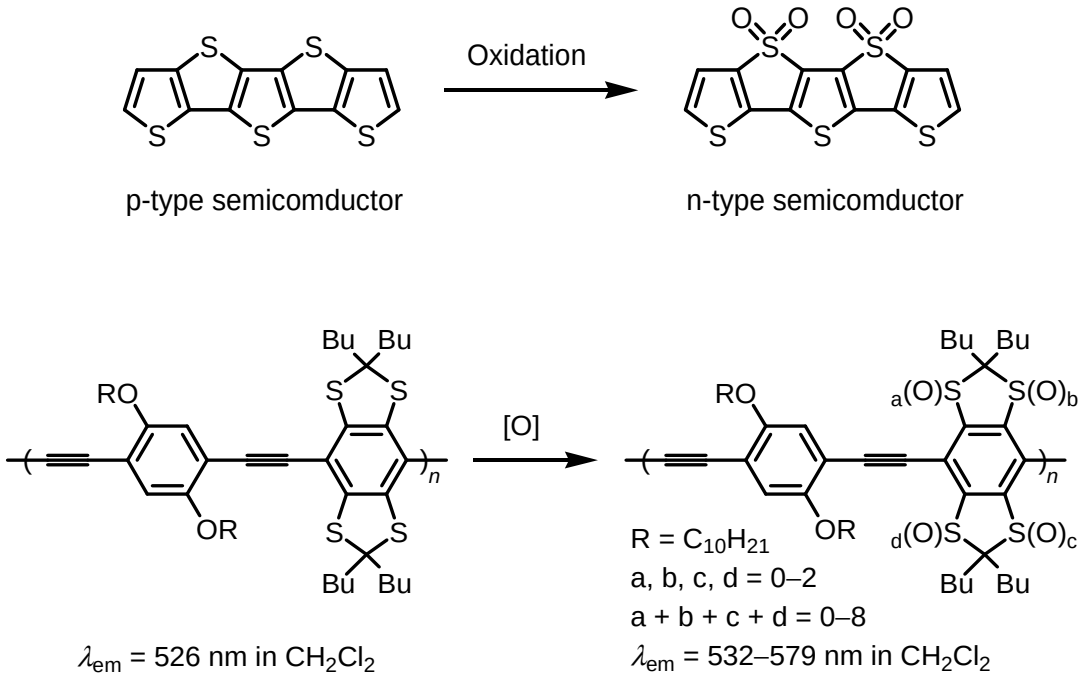

Figure 1–3. Exchange of properties before and after oxidation.

1–4 Heavy-atom Effect

Heavy-atom effect often plays a crucial role for nonradiative deactivation in a series of luminescent organic compounds or phosphorescence emission of transition metal complexes.[13] The effect induces the intersystem crossing from a exited singlet state to a triplet state caused by spin-orbit interaction of heavy atoms. It has been documented that chalcogen-containing heteroaromatics such as benzo[b]chalcogenophenes,[14] dibenzo[b,d]chalcogenophenes,[15] benzo[1,2-*b*:5,4-*b'*]dichalcogenophenes,[16] and chalcogenorhodamine derivatives[17] exhibit remarkable decrease of fluorescent quantum yields by changing oxygen to sulfur, selenium, and tellurium.

Table. Fluorescence quantum yields of organochalcogen compounds in ethanol (*in THF)

E	Φ_F	E	Φ_F	E	Φ_F
O	0.63	O	0.40	O	0.43
S	0.02	S	0.025	S	0.14
Se	0.0005	Se	0.001	Se*	0.00025
Te	<0.0005	Te	<0.0005	Te	No Data

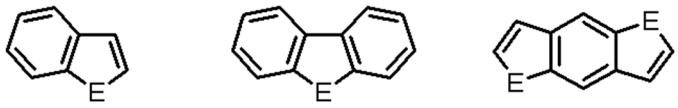

Figure 1–4–1. Heavy-atom effect in chalcogen-containing heteroaromatics.

On the other hand, heavy-atom effect is not always effective when the energy difference between S_1 and the accepting triplet state is not small enough for intersystem crossing;[18] perylene and the 3-bromo- and 3,9-dibromo derivatives show fluorescent quantum yields more than 0.95 at 295 K.[19]

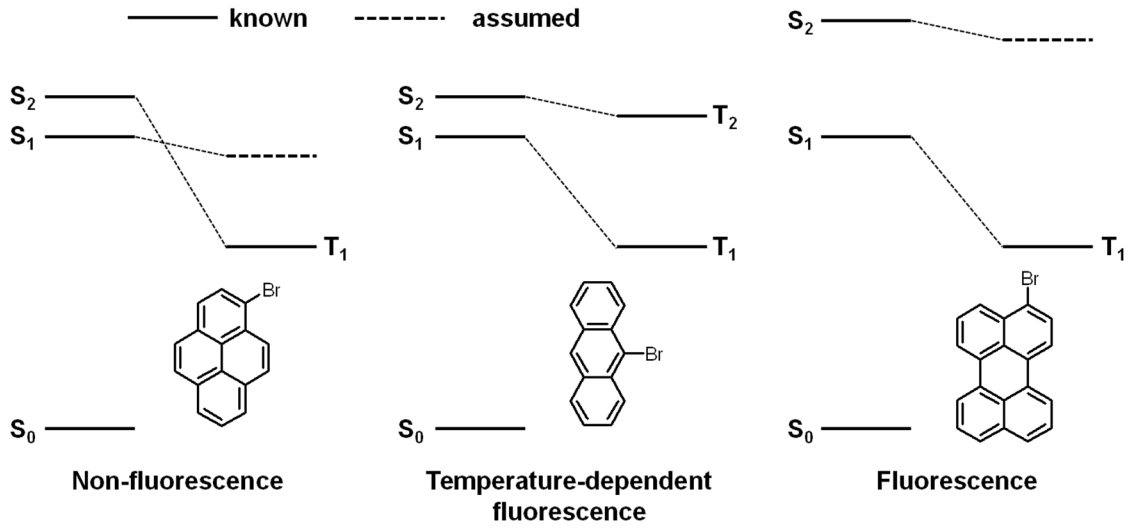

Figure 1–4–2. Energy diagram of aromatic compounds including bromine atom.

1–5 Chalcogenaplatinacycles and 1-Chalcogeno-1,3-butadienes

In our laboratory, chalcogenaplatinacycles incorporated in a dibenzobarrelene and a triptycence skeleton have been synthesized by the cyclization of corresponding hydrido(chalcogenolate) platinum(II) complexes or the reaction of corresponding dichalcogenides with platinum(0) complexes.[20] The cycles showed strong solid-state phosphorescence by the prevention of intermolecular interaction owing to the bulky dibenzobarrelene and triptycene skeleton [λ_P = 493–659 nm, Φ_P = 0.01–0.81 in the solid state]. The intermolecular interaction often leads to luminescence quenching by the Dexter type energy transfer,[21]

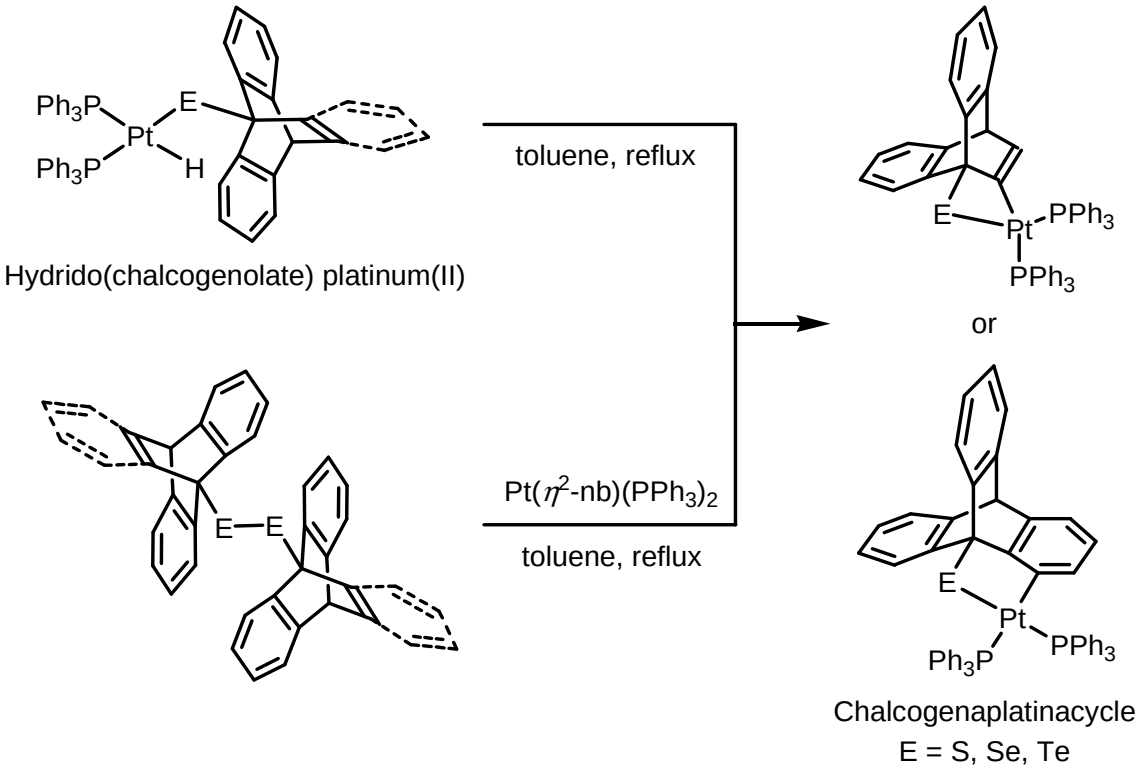

Scheme 1–5–1. Synthesis of chalcogenaplatinacycles.

The reaction of chalcogenaplatinacycles with dimethyl acetylenedicarboxylate (DMAD) or corresponding dichalcogenides with DMAD and stoichiometric palladium(0) complex gave 1,2-bis(methoxycarbonyl)-1-chalcogeno-1,3-butadiene derivatives.[20,22] Interestingly, sulfur and selenium analogues revealed strong fluorescence in spite of heavy-atom effect [E = S: $\Phi_F(CH_2Cl_2)$ = 1.00, Φ_F(solid) = 0.30, E = Se: $\Phi_F(CH_2Cl_2)$ = 0.86, Φ_F(solid) = 0.03], in which the 1-chalcogeno-1,3-butadiene conjugated system behaves as the main contributor to the fluorescence.

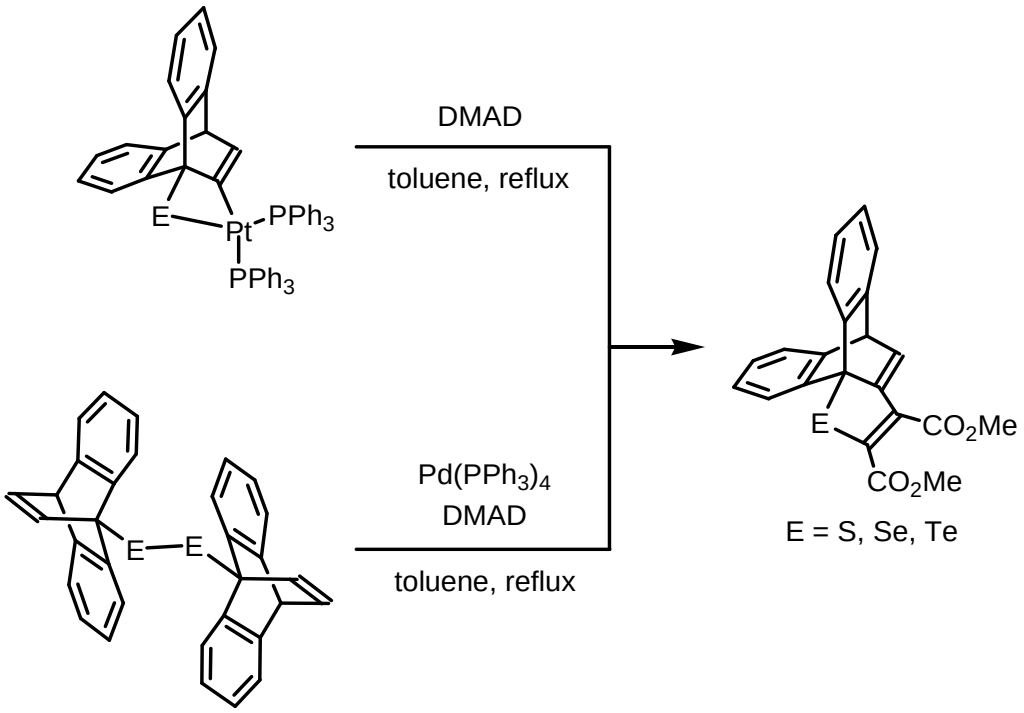

Scheme 1–5–2. Synthesis of 1,2-bis(methoxycarbonyl)-1-chalcogeno-1,3-butadiene derivatives.

1–6 Studies in the Master Thesis

1–6–1 Fluorescent 1-Thio- and 1-Seleno-1,3-butadienes synthesized via an Intramolecular Cycloaddition

1-Chalcogeno-1,3-butadiene derivatives showed unprecedented strong fluorescence, however their syntheses were inefficient and low versatility. To develop effective synthesis and expand the substitution versatility of the 1-chalcogeno-1,3-butadiene derivative, the author worked out an alternative synthetic strategy, an intramolecular cycloaddition of (9-anthrylchalcogeno)enyne between a 9-anthryl and an alkynyl moieties, in which it is straightforward path to construct the dibenzobarrelene scaffold accompanying an additional ring system in one process.[23]

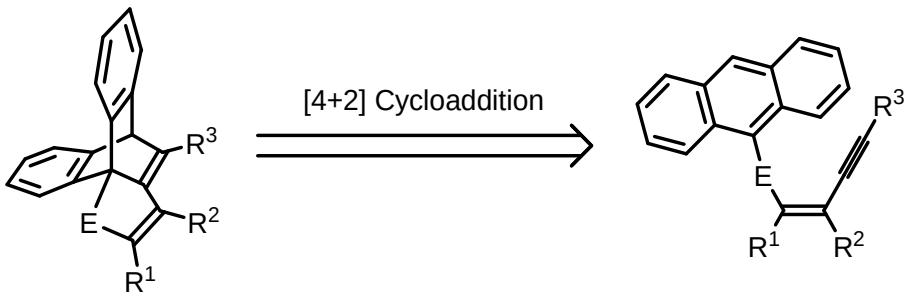

Scheme 1–6–1. Intramolecular cycloaddition of (9-anthrylchalcogeno)enyne.

For the preparation of (9-anthrylchalcogeno)enyne, 9-anthrylchalcogenolate which was generated by the reduction of di-9-anthryl dichalcogenide with $NaBH_4$ in EtOH and THF, was allowed to react with 1,4-diphenyl-1,3-butadiyne at reflux (Scheme 1–6–2).[24] Unexpectedly, the reaction proceeded directly to the desired final products, 1,4-diphenyl-1-chalcogeno-1,3-butadiene derivatives in good yields, indicating that the enyne readily

underwent an intramolecular cycloaddition under the stated conditions.[25] Dipheny derivatives showed blue strong fluorescence both in solution and in the solid state as expected [$\lambda_{em}(CH_2Cl_2)$ = 479–509 nm, $\Phi_F(CH_2Cl_2)$ = 0.98–1.00, Φ_F(solid) = 0.22–0.81]. Oxidations of sulfur analogue by *m*-chloroperoxybenzoic acid (MCPBA) gave corresponding sulfoxide and sulfone, whose fluorescent wavelength shifted hypsochromically in comparison with those of starting material without drastic fluorescence quenching [$\lambda_{em}(CH_2Cl_2)$ = 459 and 509 nm, $\Phi_F(CH_2Cl_2)$ = 0.81 and 0.79, Φ_F(solid) = 0.39 and 0.67, respectively].

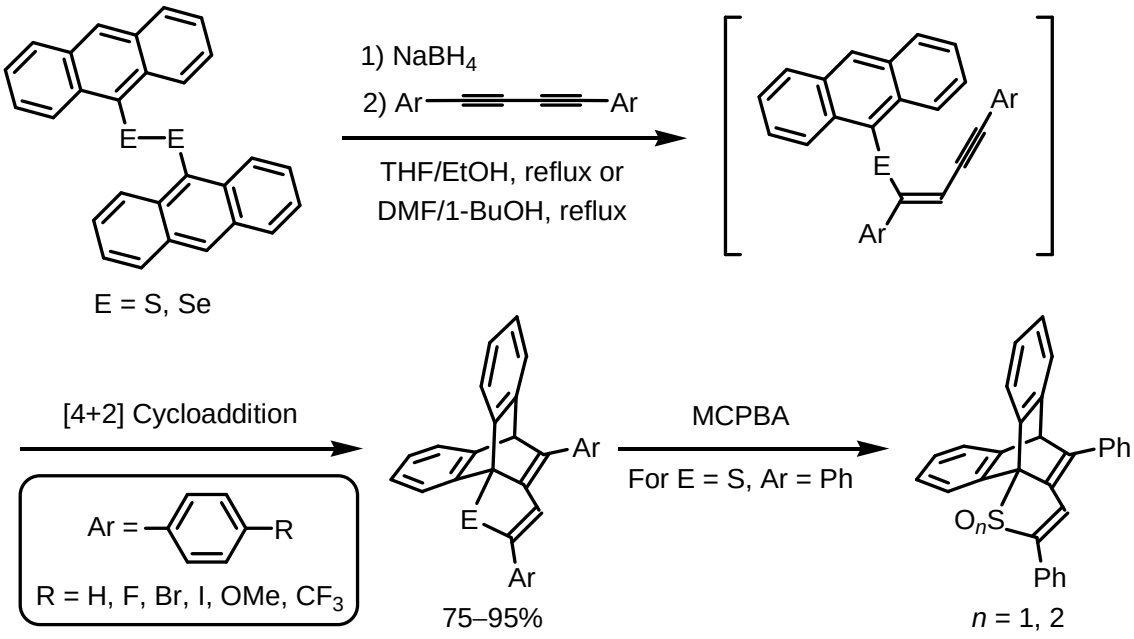

Scheme 1–6–2. Synthesis and oxidation of 1,4-diaryl-1-chalcogeno-1,3-butadiene.

1−6−2　Developed Intramolecular Cycloaddition

Para substituted diaryl derivatives (R = F, Br, I, OMe, and CF_3) could be synthesized conveniently by similar manner described in Scheme 1−6−2, and they also showed blue to green strong fluorescence. Particularly, fluorescence of sulfur analogue containing trifluoromethyl groups is strongest in the solid state among all derivatives.[25] In addition, [3,2-*b*]- and [2,3-*b*]thiophene-fused derivatives were obtained quantatively by intramolecular cyclizations of corresponding 2-alkynyl-3-(9-anthrylchalcogeno)-thiophenes and the geometrical isomer, respectively.[26]

In general, a naphthyl group as ynophile and a cyano group as dienophile exhibit intrinsically poor reactivity in Diels-Alder reaction, resulting in the requirement of high reaction temperature.[27,28] In contrast, intramolecular cycloadditions of (1-naphtylchalcogeno)enyne gave desired cycloadducts.[25] To drive the cyano-Diels-Alder reaction forward, we added boranes as Lewis acid to cyano-precursors and got borane adducted 4-chalcogeno-1-aza-1,3-butadiene derivatives.[29]

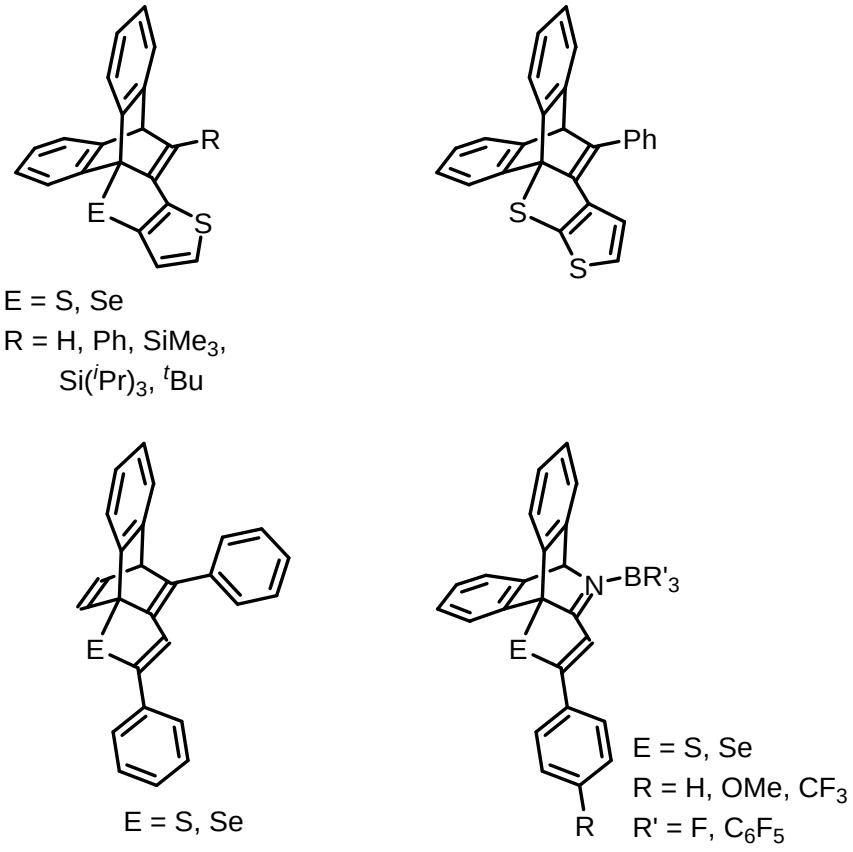

Figure 1–6–3. A series of 1-chalcogeno-1,3-butadiene derivatives.

1–7 This Work

As mentioned in this chapter, novel fluorescent 1-chalcogeno-1,3-butadiene derivatives have great potential to develop a new field in photoluminescence chemistry. The author believes that it is important to evince basic properties deeply and apply as an industrial fluorescent candidate for the development in this field. In this doctor's thesis, the author investigated elucidation of photophysical properties of 1-chalcogeno-1,3-butadiene derivatives and application to a hydrogen sulfide sensor.

In chapter 2, synthesis, structure, and photophysical properties of push-pull type 1-thio-1,3-butadienes containing diphenylamino groups as electronic donating group and sulfoxide or sulfone unit as electronic withdrawing group were described. Push-pull type compounds are often focused on achievement of red-shifted fluorescence which could be applied for bioimaging, night vision devices, and optical communications.

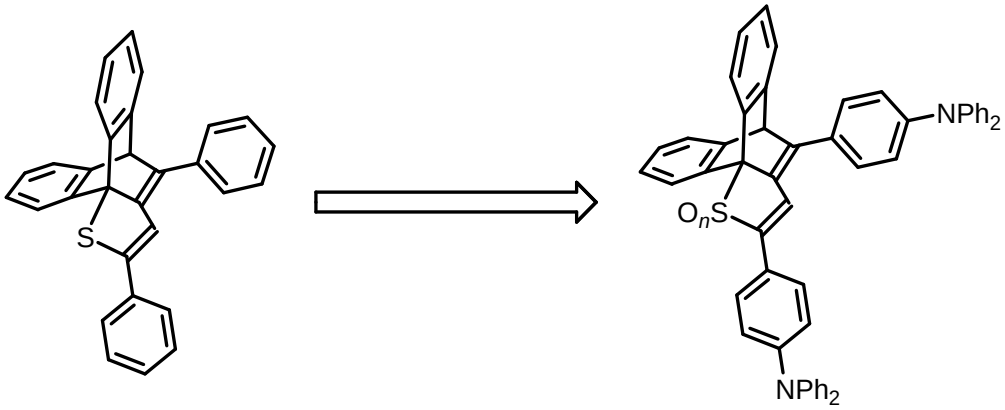

In chapter 3, synthesis, structure, and photophysical properties of 1-telluro-1,3-butadiene derivatives were examined to elucidate heavy-atom effect. Additionally, derivation utilizing tellurium atom as leaving group was carried out to create new

fluorophore. Herein, the author tried introduction of silicon atom into 1,3-butadiene moiety.

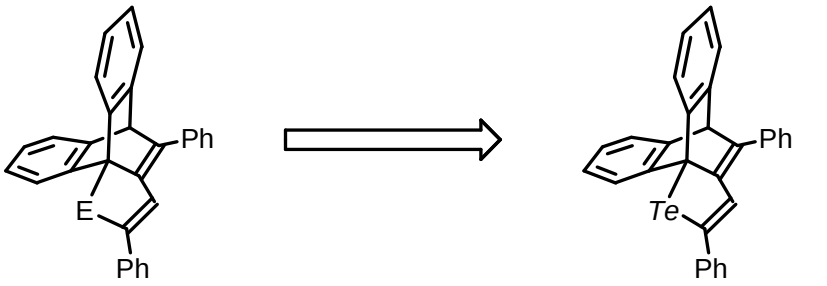

E = S, Se

Te = Te, TeO, $TeBr_2$

In chapter 4, the author applied 1-seleno-1,3-butadiene oxide for a reversible and turn-on type fluorescent probe for hydrogen sulfide via redox cycle between selenide and selenoxide. Moreover, a generation mechanism of selectivity for thiols was elucidated by a comparison of dibenzobarrelene derivative with benzobarrelene derivative. Reversible and turn-on probe for hydrogen sulfide with good reactivity, quantitatively, and selectivity could be achieved with only this cycle.

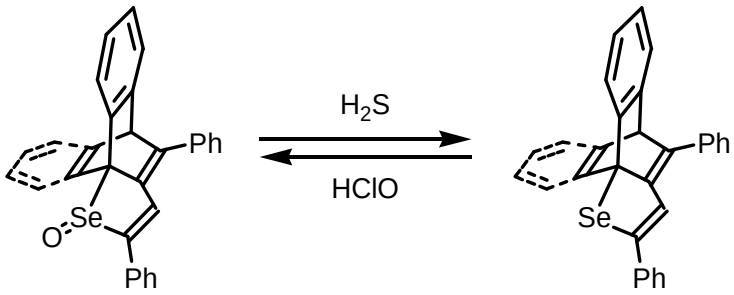

1–8 References

1. a) O. Shimonura, *Bioluminescence*, World Scientific, New Jersey, **2006**. b) O. Shimomura, *Angew. Chem. Int. Ed.* **2009**, *48*, 5590. c) M. Chalfie, *Angew. Chem. Int. Ed.* **2009**, *48*, 5603. d) R. Y. Tsien, *Angew. Chem. Int. Ed.* **2009**, *48*, 5612, and references cited therein.

2. *Organic Light-Emitting Devices*, (Eds: K. Müllen, and U. Scherf), Wiley-VCH, Weinheim, **2006**.

3. a) H. Yan, Z. Chen, Y. Zheng, C. Newman, J. R. Quinn, F. Dötz, M. Kastler, *Nature* **2009**, *457*, 679. b) H. Minemawari, T. Yamada, H. Matsui, J. Tsutsumi, S. Haas, R. Chiba, R. Kumai, T. Hasegawa, *Nature* **2011**, *475*, 364.

4. a) A. G. Emslie, F. T. Bonner, L. G. Peck, *J. Appl. Phys.* **1958**, *29*, 858. b) M. A. Herrera, A. P. Mathew, K. Oksman, *Carbohydr. Polym.* **2014**, *112*, 494. c) A. Eskandari, P. Sangpour, M. R. Vaezi, *Mater. Chem. Phys.* **2014**, *147*, 1204.

5. a) T. H. Liu, W. J. Shen, C. K. Yen, C. Y. Iou, H. H. Chen, B. Banumathy, C. H. Chen, *Synth. Met.* **2003**, *137*, 1033. b) Y. Kim, E. Oh, D. Choi, H. Lim, C. S. Ha, *Nanotechnology* **2004**, *15*, 149. c) B. X. Mi, Z. Q. Gao, M. W. Liu, K. Y. Chan, H. L. Kwong, N. B. Wong, C. S. Lee, L. S. Hung, S. T. Lee, *J. Mater. Chem.* **2002**, *12*, 1307. d) L. Türker, A. Tapan, S. Gümüş, *Polycyclic Aromat. Compd.* **2009**, *29*, 139. e) K. Okumoto, H. Kanno, Y. Hamada, H. Takahashi, K. Shibata, *Appl. Phys. Lett.* **2006**, *89*, 013502.

6. a) J. Yoshino, N. Kano, T. Kawashima, *Chem. Commun.* **2007**, 559. b) J. Yoshino, A. Furuta, T. Kambe, H. Itoi, N. Kano, T. Kawashima, Y. Ito, M. Asashima, *Chem. Eur. J.* **2010**, *16*, 5026. c) T. W. Hudnall, F. P. Gabbai, *J. Am. Chem. Soc.* **2007**, *129*, 11978. d)

M. H. Lee, T. Agou. J. Kobayashi, T. Kawashima, F. P. Gabbai, *Chem. Commun.* **2007**, 1133. e) Y. Kim, F. P. Gabbai, *J. Am. Chem. Soc.* **2009**, *131*, 3363.

7. a) S. Kyushin, M. Ikarugi, M. Goto, H. Hiratsuka, H. Matsumoto, *Organometallics* **1996**, *15*, 1067. b) M. Shimizu, K. Mochida, T. Hiyama, *Angew. Chem. Int. Ed.* **2008**, *47*, 9760. c) Y. Niko, S. Kawauchi, S. Otsu, K. Tokumaru, G. Konishi, *J. Org. Chem.* **2013**, *78*, 3196.

8. a) T. Baumgartner, R. Réau, *Chem. Rev.* **2006**, *106*, 4681. b) T. Baumgartner, T. Neumann, B. Wirges, *Angew. Chem. Int. Ed.* **2004**, *43*, 6197. c) T. Baumgartner, W. Bergmans, T. Kárpáti, T. Neumann, M. Nieger, L. Nyulászi, *Chem. Eur. J.* **2005**, *11*, 4687. d) Y. Dienes, M. Eggenstein, T. Neumann, U. Englert, T. Baumgartner, *Dalton Trans.* **2006**, 1424. e) T. Neumann, Y. Dienes, T. Baumgartner, *Org. Lett.* **2006**, *8*, 495. f) T. Baumgartner, W. Wilk, *Org. Lett.* **2006**, *8*, 503. g) S. Durben, Y. Dienes, T. Baumgartner, *Org. Lett.* **2006**, *8*, 5893. h) A. Fukazawa, M. Hara, T. Okamoto, E. C. Son, C. Xu, K. Tamao, S. Yamaguchi, *Org. Lett.* **2008**, *10*, 913.

9. a) S. Yamaguchi, K. Tamao, *Chem. Lett.* **2005**, *34*, 2. b) U. Salzner, J. B. Lagowski, P. G. Pickup, R. A. Poirier, K. *Synth. Met.* **1998**, *96*, 177.

10. a) L. Groenendaal, J. Dhaen, J. V. Luppen, E. Verdonck, F. Louwet, L. Leenders, *Synth. Met.* **2003**, 135–136, 115. b) A. Patra, Y. H. Wijsboom, S. S. Zade, M. Li, Y. Sheynin, G. Leitus, M. Bendikov, *J. Am. Chem. Soc.* **2008**, *130*, 6734. c) Y. H. Wijsboom, A. Patra, S. S. Zade, Y. Sheynin, M. Li, L. J. W. Shimon, M. Bendikov, *Angew. Chem. Int. Ed.* **2009**, *48*, 5443. d) T. Yamamoto, K. Takimiya, *J. Am. Chem. Soc.* **2007**, *129*, 2224. e) M. J. Kang, I. Doi, H. Mori, E. Miyazaki, K. Takimiya, M. Ikeda, H. Kuwabara, *Adv. Mater*. **2011**, *23*, 1222.

11. a) G. Barbarella, L. Favaretta, G. Sotgiu, M. Zambianchi, V. Fattori, M. Cocchi, F.

Cacialli, G. Gigli, R. Cingolani, *Adv. Mater.* **1999**, *23*, 1375. b) G. Barbarella, L. Favaretta, G. Sotgiu, M. Zambianchi, A. Bongini, M. Mastragostino, M. Anni, G. Gigli, R. Cingolani, *J. Am. Chem. Soc.* **2000**, *122*, 11971.

12. a) M. C. Suh, B. Jiang, T. D. Tilley, *Angew*. *Chem. Int. Ed.* **2000**, *39*, 2870. b) E. Amir, S. Rozen, *Angew. Chem. Int. Ed.* **2005**, *44*, 7374. c) T. M. Pappenfus, J. H. Melby, B. B. Hansen, D. M. Sumption, S. A. Hubers, D. E. Janzen, P. C. Ewbank, K. A. McGee, M. W. Burand, K. R. Mann, *Org. Lett.* **2007**, *9*, 3721. d) Y. Suzuki, T. Okamoto, A. Wakamiya, S. Yamaguchi, *Org. Lett.* **2008**, *10*, 3393. e) E. L. Dane, S. B. King, T. M. Swager, *J. Am. Chem. Soc.* **2010**, *132*, 7758.

13. K. N. Solov'ev, E. A. Borisevich, *Phys.-Usp*. **2005**, *48*, 231.

14. M. Zander, G. Kirsch, *Z. Naturforsch*. **1989**, *44a*, 205.

15. N. Hayashi, Y. Saito, H. Higuchi, K. Suzuki, *J. Phys. Chem. A* **2009**, *113*, 5342.

16. a) B. Wex, B. R. Kaafarani, E. O. Danilov, D. C. Neckers, *J. Phys. Chem. A* **2006**, *110*, 13754. b) K. Takimiya, Y. Konda, H. Ebata, N. Niihara, T. Otsubo, *J. Org. Chem.* **2005**, *70*, 10569.

17. M. W. Kryman, G. A. Schamerhorn, J. E. Hill, B. D. Calitree, K. S. Davies, M. K. Linder, T. Y. Ohulchanskyy, M. R. Detty, *Organometallics* **2014**, *33*, 2628.

18. H. Dreeskamp, E. Koch, M. Zander, *Chem. Phys. Lett.* **1975**, *31*, 251.

19. M. Zander, *Z. Naturforsch.* **1989**, *44a*, 1116.

20. Y. Yamaguchi, N. Nakata, A. Ishii, *Eur. J. Inorg. Chem.* **2013**, 5233.

21. D. L. Dexter, *J. Chem. Phys.* **1953**, *21*, 836.

22. A. Ishii, Y. Yamaguchi, N. Nakata, *Org. Lett.* **2011**, *13*, 3702.

23. E. Ciganek, *J. Org. Chem.* **1980**, *45*, 1497.

24. M. J. Dabdoub, A. C. M. Baroni, E. J. Leonardao, T. R. Gianeti, G. R. Hurtado,

Tetrahedron **2001**, *57*, 4271.

25. A. Ishii, T. Annaka, N. Nakata, *Chem. Eur. J.* **2012**, *18*, 6428.

26. A. Ishii, S. Kobayashi, Y. Aoki, T. Annaka, N. Nakata, *Heteroatom Chem.* **2014**, *25*, 658.

27. a) S. Trinof, A. S. Orahovats, *Helv. Chim. Acta* **1987**, *70*, 1732. b) E. Ciganek, M. A. Wuonola, *J. Heterocycl. Chem.* **1994**, *31*, 1251.

28. a) G. J. Janz, Cyanogen and Cyanogen-like Compounds as Dienophiles. In 1,4-Cycloaddition Reactions: The Diels-Alder Reaction in Heterocyclic Syntheses; Hamer, J., Ed.; Organic Chemistry, A Series of Monographs; Academic Press: New York, 1967; Vol. 8, pp 97−125. b) D. L. Boger, S. M. Weinreb. In Hetero Diels-Alder Methodology in Organic Synthesis; Wasserman, H. H., Ed.; Organic Chemistry, A Series of Monographs; Academic Press: San Diego, CA, 1987; Vol. 47, pp 146−150.

29. A. Ishii, Y. Aoki, N. Nakata, *J. Org. Chem.* **2014**, *79*, 7951.

Chapter 2

Syntheses, Structures, and Photophysical Properties of Extended π-Conjugative and Push-pull Type 1,4-Diaryl-1-thio-1,3-butadienes

2–1 Introduction

Strong red emission is important for applications in bioimaging, night vision devices, and optical communications.[1] In general, red-shifted emission has been achieved by the elongation of π-conjugation.[2] Solid-state strong emission is required for the device application, however, the emission quenching is often induced in extended π-conjugative compounds by the Dexter type energy transfer in the solid state.[3] Recently, we have developed a series of strong fluorescent 1,4-diaryl-1-chalcogeno-1,3-butadienes **1** incorporated in a rigid and bulky dibenzobarrelene skeleton.[4] However, their fluorescence colors are from blue to green and not extended to the region of orange and red [$\lambda_{em}(CH_2Cl_2)$ = 479–505 nm, λ_{em}(solid) = 466–514 nm]. The aim of this study is achievement of a largely red-shifted emission maintaining high fluorescent quantum yields by utilizing a derivation of sulfur analogue **1**. A donor-acceptor system is effective to elongate fluorescent wavelength, due to a large Stokes shift resulting from the intramolecular charge transfer (ICT) transition from the electron-donating group to electron-accepting group, as observed for 3-boryl-2,2'-bithiophenes **2** having donor aryl groups and acceptor boryl group.[5] The acceptor character of a sulfide can be significantly increased by oxidation leading to sulfoxide and sulfone groups.[6] In this chapter, we investigated push-pull type derivatives **3** and **4** having diphenylamino groups as the donor and a sulfoxide or a sulfone moiety as the acceptor.

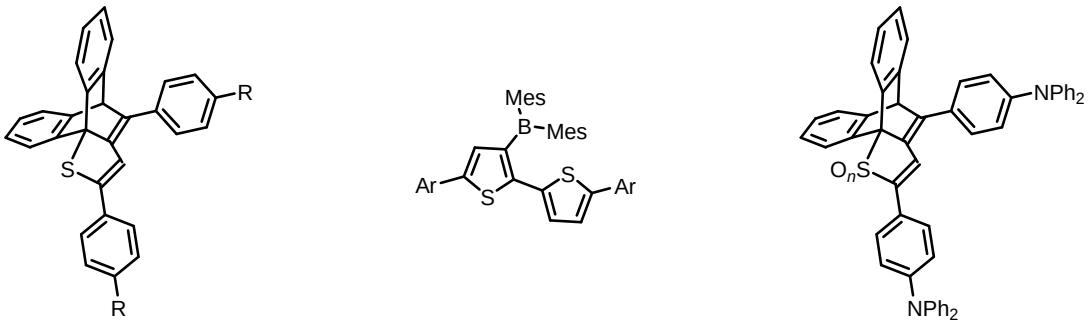

1: R = H, F, Br, I, OMe, CF_3, C≡CR'
R' = H, $SiMe_3$, Ph

2: Ar = H, Mes, Ph, *p*-carbazolylC_6H_4,
p-$Ph_2NC_6H_4$, 5-Ph_2N-2-thienyl

3: *n* = 1
4: *n* = 2

Figure 1. 1-Thio-1,3-butadiene derivatives **1**, 3-boryl-2,2'-bithiophenes **2**, and push-pull type derivatives **3** and **4**.

2–2 Syntheses and Structures of Push-pull Type 1-Thio-1,3-butadienes

As shown in Scheme 1, we carried out the synthesis and oxidations of diphenylamino derivative **5**. The Buchwald-Hartwig reactions of **1a** (R = Br) and **1b** (R = I) with diphenylamine afforded **5** in good yields as orange crystals. Oxidations of **5** with 1 or 2 molar equivalents of MCPBA smoothly proceeded in CH_2Cl_2 at room temperature to produce sulfoxide **3** (99%) and sulfone **4** (29%), respectively.

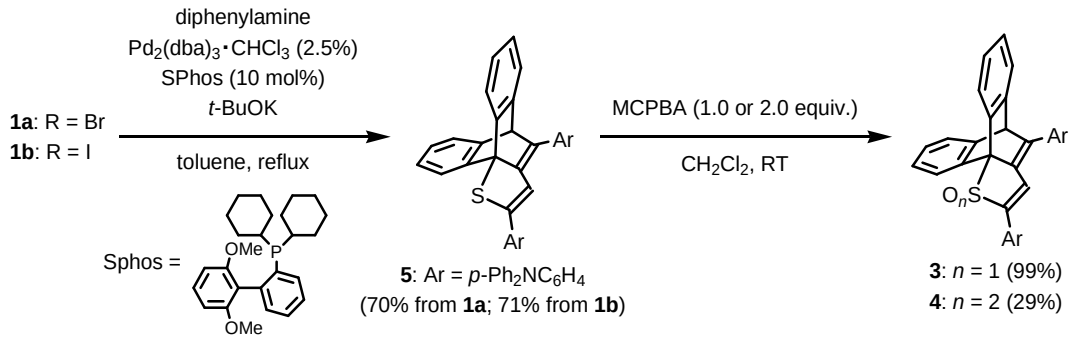

Scheme 1. Synthesis and oxidations of diphenylamino derivative **5**.

The structures of **3**–**5** were determined by spectroscopic methods and X-ray analysis for sulfoxide **3** (Figure 2). The 1,3-butadiene moiety in **3** is twisted (C2–C3–C4–C5: 168.4(3) Å) in contrast to the unsubstituted derivative **1c** (R = H) having planar 1-thio-1,3-butadiene moiety. As shown in Figure 3, **3** forms a close packing among three molecules in the crystal owing to a hydrogen-bonding between oxygen and H8, and several CH–π interactions such as H20–benzene ring (yellow), H26–benzene ring (green), H45–benzene ring (red), and H46–benzene ring (blue).

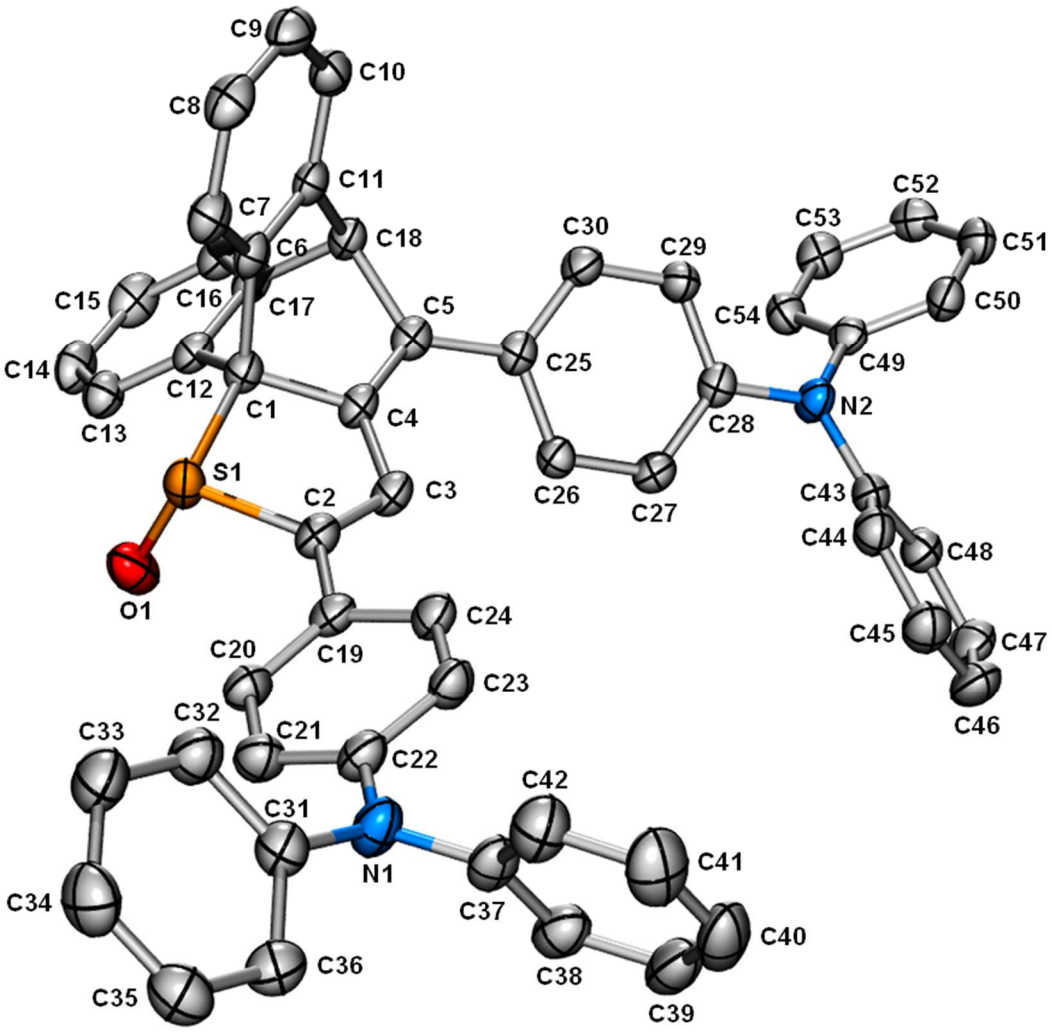

Figure 2. ORTEP drawing of sulfoxide **3** with 50% probability ellipsoids. Selected bond length (Å) and torsion angles (°): C1–S1: 1.848(3), S1–C2: 1.805(3), C2–C3: 1.341(4), C3–C4: 1.426(4), C1–C4: 1.536(3), C4–C5: 1.348(4), C2–C3–C4–C5: 168.4(3), C3–C2–C19–C24: 27.5(4), C4–C5–C25–C26: 33.7(4). *Crystal data:* $C_{54}H_{38}N_2OS \bullet C_7H_7$, MW = 854.05, monoclinic, space group $P2_1/n$, Z = 4, a = 14.9342(7), b = 12.9929(5), c = 23.7805(10) Å, β = 101.8670(10)°, V = 4515.7(3) Å^3, $D_{calcd.}$ = 1.256 g cm^{-3}, R_1 [$I > 2\sigma(I)$] = 0.0637, wR_2 (all data) = 0.1805 for 8394 reflections, 597 parameters, and 89 restraints for C_7H_7, GOF = 1.055.

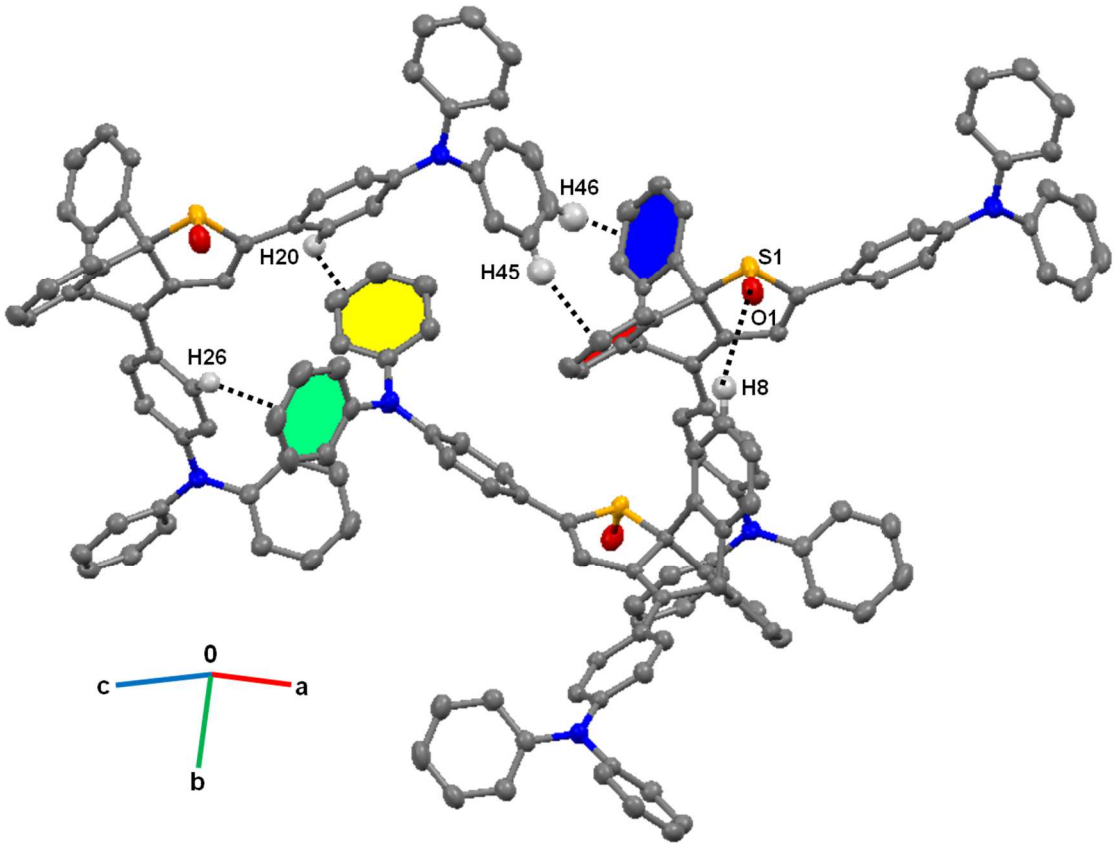

Figure 3. Crystal packing of sulfoxide **3**; O1–H8: 2.715 Å, H20–benzene ring A (yellow): 2.825 Å, H26–benzene ring B (green): 2.852 Å, H45–benzene ring C (red): 2.637 Å, H46–benzene ring (blue): 2.535 Å.

2–3 Properties of Push-pull Type 1-Thio-1,3-butadienes

Photophysical properties of **3–5** were studied in dilute CH_2Cl_2 solution (10^{-5} M) and in the solid state. The results are listed in Table 1, Figure 4, and 5 together with the data for unsubstituted derivative **1c** (R = H, in Figure 1). **3–5** showed yellow and/or orange fluorescence, and their absorption and emission maxima shifted bathochromically [$\lambda_{abs}(CH_2Cl_2)$ = 430–439 nm, $\lambda_{em}(CH_2Cl_2)$ = 522–562 nm] in comparison with **1c**. Interestingly, the fluorescence maxima of sulfoxide **3** and sulfone **4** in the solid state were more red-shifted than those in CH_2Cl_2 solution [**3**: λ_{em}(solid) = 559 nm, **4**: λ_{em}(solid) = 580 nm], which seems to be due to the intermolecular interactions in the solid state as shown in Figure 3.

In CH_2Cl_2, **3–5** exhibited strong fluorescence with almost quantitative quantum yields. Solid-state fluorescence quantum yields of **3–5** were from 0.13 to 0.48. The quantum yields of sulfoxide **3** and sulfone **4** were lower than those in solution owing to the strong intermolecular interactions as mentioned above. **3** and **4** showed most red-shifted orange fluorescence centered at 580 nm among reported 1,4-diaryl-1-chalcogeno-1,3-butadiene derivatives. The quantum yield of **4** was still high (0.48), although it is known that long-wavelength fluorophores usually tend to undergo severe luminescence quenching due to aggregation.[7]

Table 1. Photophysical and electrochemical properties of **1c** and **3**–**5**.[a]

	λ_{abs} [nm]	ε_{max} [M^{-1} cm^{-1}]	λ_{em} [nm][b]	Stokes shift [cm^{-1}]	Φ_F[b,c,d]	λ_{em}(solid) [nm][b,e]	Φ_F (solid)[b,c,e]	$+E_{1/2}$ [V][f]
1c	378	23000	491	6100	1.00	483	0.47	0.56
5	430	31400	522	4400	1.0	559	0.15	0.13 0.46
3	439	34900	554	5100	0.92	580	0.13	0.32
4	437	16300	562	5700	0.95	580	0.48	0.39

a) In CH_2Cl_2, unless otherwise noted. b) Exited at respective absorption maxima in CH_2Cl_2. c) Absolute fluorescence quantum yields were determined by using a calibrated integrating sphere system. d) Under argon. e) In the dried solid state. f) In CH_2Cl_2 vs Fc/Fc^+.

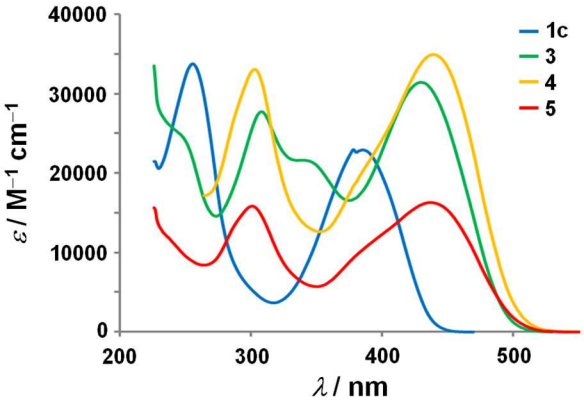

Figure 4. UV/Vis spectra of **1c** and **3**–**5** in CH_2Cl_2.

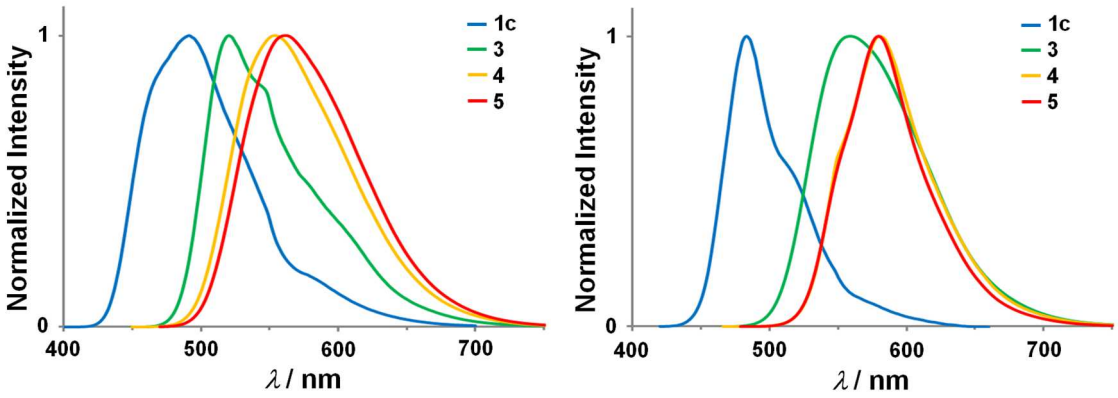

Figure 5. Fluorescence spectra of **1c** and **3**–**5** in CH_2Cl_2 (left) and in the solid state (right).

Stokes shifts of sulfoxide **3** (5100 cm^{-1}) and sulfone **4** (5700 cm^{-1}) in CH_2Cl_2 were

larger than sulfide **5** (4400 cm^{-1}), indicating that fluorescence of **3** and **4** are based on ICT. To consider the suitability of a conjugate system for CT process, the elucidation of solvatochromism is a simple and effective method.[8] As shown in Figure 6–8, positive solvatofluorescence was observed in the cases of **3** and **4**. While the longest absorption maxima of **3** and **4** barely changed in six solvents [**3**: $\lambda_{abs}(CH_2Cl_2)$ = 428–439 nm, **4**: $\lambda_{abs}(CH_2Cl_2)$ = 427–437 nm], their emission maxima shifted from 500 nm (C_6H_6) to 580 nm (CH_3CN) for **3** and from 510 nm (C_6H_6) to 600 nm (CH_3CN) for **4**. The Stokes shift of sulfoxide **3** were in the range from 3800 cm^{-1} in C_6H_6 (E_T^N: 0.111) to 5500 cm^{-1} in CH_3CN (E_T^N: 0.460), and those of sulfone **4** were from 4100 cm^{-1} in C_6H_6 to 6100 cm^{-1} in CH_3CN. For the reference, the Stokes shifts of sulfide **5** are in the range of 3900–4100 cm^{-1} under the same conditions. As shown in Figure 9, linear relationships are obtained between E^T_N values and the Stokes shift of **3** and **4** (**3**: R^2 = 0.9577, **4**: R^2 = 0.9241), supporting the CT process in **3** and **4**.

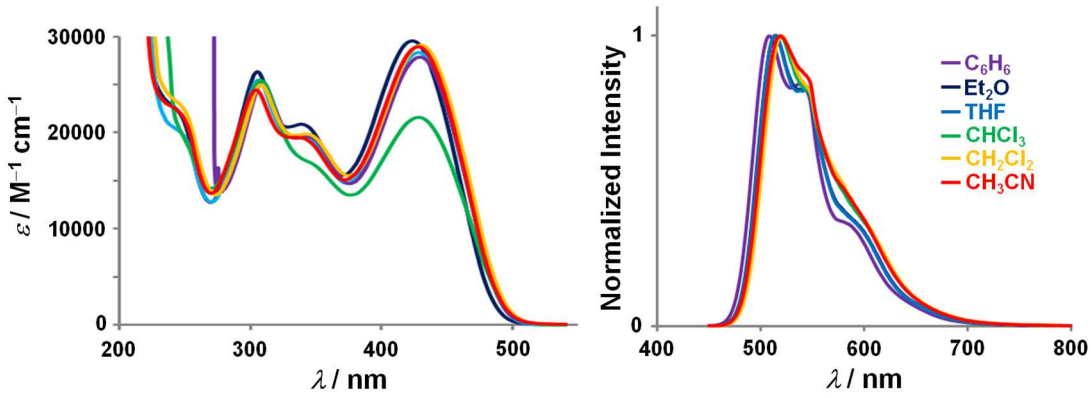

Figure 6. UV-vis (left) and fluorescence (right) spectra of **5** in various solvents.

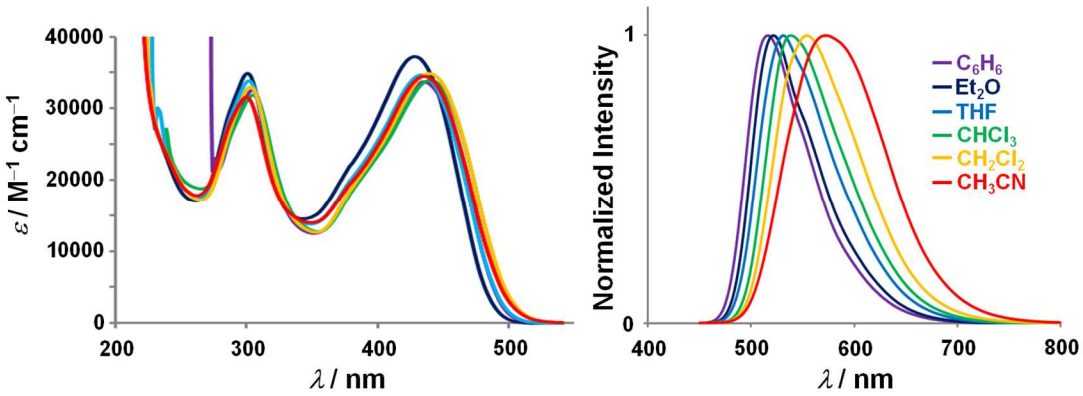

Figure 7. UV-vis (left) and fluorescence (right) spectra of **3** in various solvents.

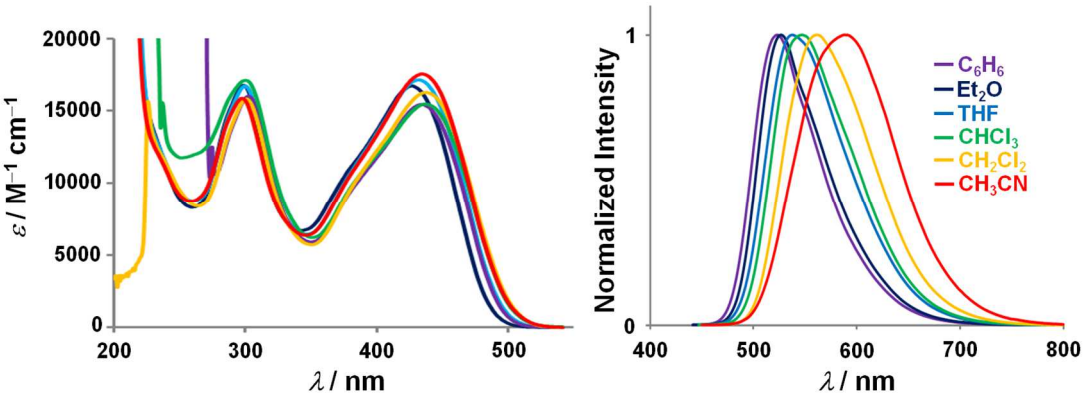

Figure 8. UV-vis (left) and fluorescence (right) spectra of **4** in various solvents.

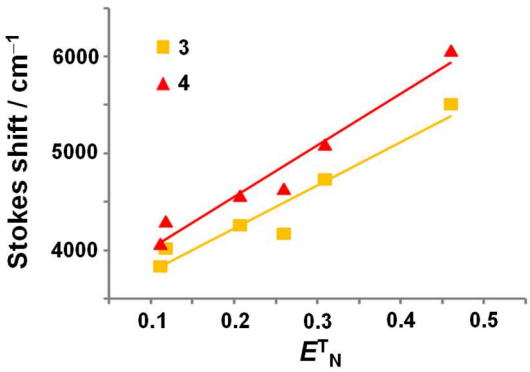

Figure 9. Relationship between E^{T}_{N} and Stokes shift of **3** and **4**.

We next carried out time-dependent (TD)-DFT calculations[9] at B3LYP/6–31G(d) level for sulfide **5** and sulfoxide **3** to consider excitation energies and their diagrams of HOMO and LUMO (Figure 10). LUMOs of **5** and **3** are localized in the central 1,4-diphenyl-1,3-butadiene moiety. HOMO of **5** is delocalized widely over the 4-[*p*-(diphenylamino)phenyl]-1,3-butadiene and the sulfur atom. HOMO of **3** is spread more widely around the 1,4-bis[*p*-(diphenylamino)phenyl]-1,3-butadiene moiety due to the electron-withdrawing character of sulfone unit. TD-DFT calculations indicate that the longest wavelengths of **5** and **3** are mainly due to the HOMO–LUMO transition. These contributions confirm a concomitant increase in charge separation and charge transfer ability in **5** comparing with **3**. The calculated excitation energy of **5** (2.92 eV, 424 nm) is close to that of **3** (2.93 eV, 423 nm), resembling the close longest absorption maxima of **5** (λ_{em} = 430 nm) and **3** (λ_{em} = 437 nm). The energy levels of HOMO and LUMO of **3** are lowered by the increase of the oxidation number of sulfur.

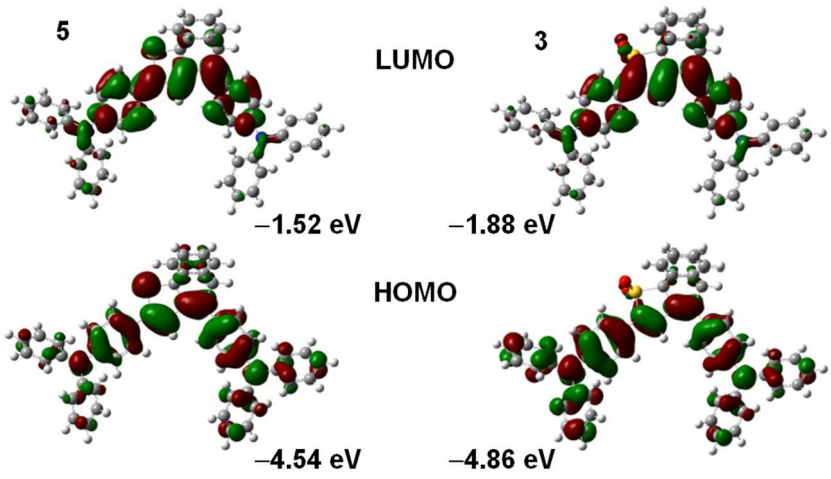

Figure 10. LUMO and HOMO of **5** (left) and **3** (right) obtained by TD-DFT calculations at the B3LYP/6–31G(d) level.

To study the electrochemistry of newly synthesized compounds **3**–**5** together with unsubstitued derivative **1c**, cyclic voltammetry was conducted in CH_2Cl_2 at room temperature (Table 1 and Figure 11). **1c** revealed reversible oxidation potential at $E_{1/2}$ of +0.56 V *vs.* Fc/Fc^+. Moreover, reversible cyclic voltammogram was observed for **5** ($E_{1/2}$ = +0.13, 0.46 V *vs.* Fc/Fc^+), which was shifted cathodically in comparison with **1c** and triphenylamine ($E_{1/2}$ = +1.13 V *vs* $DMFc/DMFc^+$).[10] Sulfoxide **3** and sulfone **4** also showed reversible cyclic voltammograms with $E_{1/2}$ of +0.32 and 0.39 V *vs.* Fc/Fc^+, respectively. Their values are shifted anodically with the increase of the oxidation number of sulfur in comparison with sulfide **5**, which are in good agreement with the TD-DFT calculations.

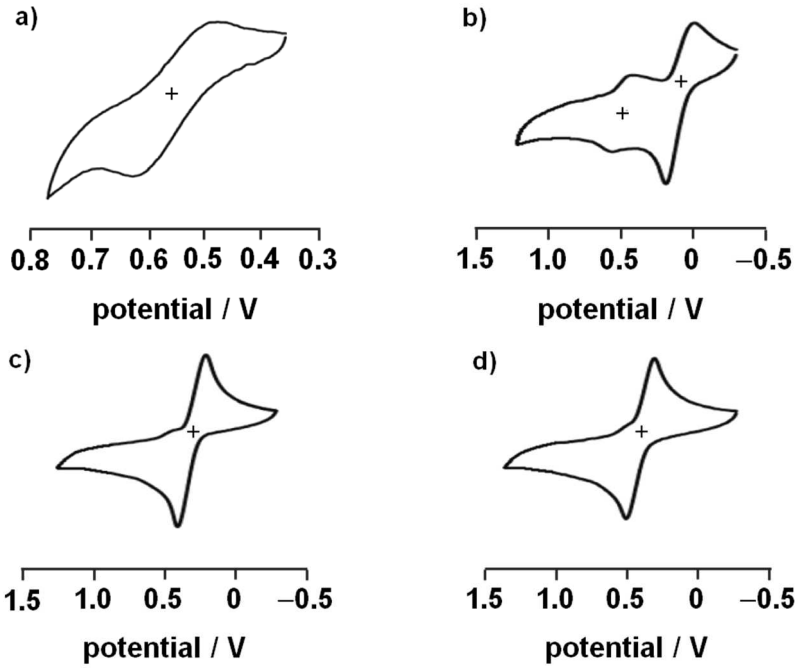

Figure 11. Cyclic voltammograms of a) **1c**, b) **5**, c) **3**, and d) **4** in CH_2Cl_2 solution with Bu_4NClO_4 as the electrolyte, potential *E* referenced *vs.* Fc/Fc^+.

2–4 Conclusion

We have demonstrated the synthesis of diphenylamino derivative **5** in high yield by cross coupling reactions of halo derivatives **1a** and **1b** and push-pull type derivatives **3** and **4** by the oxidation of **5**. Compounds **3**–**5** have red-shifted yellow and/or orange fluorescence in CH_2Cl_2 due to the π-elongation and/or intramolecular charge transfer. A close packing structure of sulfoxide **3** was in the crystalline state, leading to a more red-shifted fluorescence in the solid state than that in CH_2Cl_2 with decreasing fluorescence quantum yields. Push-pull type derivatives **3** and **4** showed solvatofluorescence with good correlations between the Stokes shifts and E^T_N values of solvent. Diphenylamino derivatives **3**–**5** exhibited reversible cyclic voltammograms with lower half-wave potentials than that of unsubstituted derivative **1c**, and those potentials shifted anodically with increase of the oxidation number of sulfur. This study shows promise of 1,4-diaryl-1-thio-1,3-butadienes incorporated in a rigid and bulky dibenzobarrelene skeleton as a material having controlled photo- and electrochemical properties with maintaining strong fluorescence.

2–5 Experimental Section

General Procedure

All melting points were determined on a Mel-Temp capillary tube apparatus and were uncorrected. ^{1}H and $^{13}C\{^{1}H\}$ NMR spectra were recorded on AVANCE-400 (400 MHz for ^{1}H and 101 MHz for ^{13}C) spectrometer using $CDCl_3$ as the solvent at room temperature. IR spectra were recorded on a Perkin Elmer System 2000 FT-IR spectrometer. UV-vis spectra were recorded on a JASCO V-560 spectrophotometer. Fluorescence spectra were recorded on a JASCO FP-6300 spectrofluorometer. Absolute photoluminescence quantum yields were measured by a calibrated integrating sphere system C10027 (Hamamatsu Photonics). Elemental analyses were carried out at the Molecular Analysis and Life Science Center of Saitama University. X-ray crystallography was performed with a Bruker AXS SMART diffractometer. The intensity data were collected at 103 K employing graphite-monochromated MoKα radiation (λ = 0.71073 Å) and the structures were solved by direct methods and refine by full-matrix least-squares procedures on F^2 for all reflections (SHELX-97).[11] Solvents were dried by standard methods and freshly distilled prior to use. Dehydrated toluene was purchased from Kanto Chemical Co., Inc. and used without further purification. Column chromatography was performed with silica gel (70–230 mesh) and the eluent is shown in parentheses.

2,4-Di[*p*-(diphenylamino)phenyl]-5*H*-5,9b[1',2']-benzenonaphto[1,2-*b*]thiophene (5)

From bromo derivative **1a** A solution of **1a** (362 mg, 0.63 mmol), diphenylamine (213 mg, 1.26 mmol), $Pd_2(dba)_3 \cdot CHCl_3$ (15 mg, 0.017 mmol), SPhos (2-Dicyclohexyl-phosphino-2',6'-dimethoxybiphenyl) (25 mg, 0.062 mmol), *t*-BuOK (213 mg, 1.89 mmol) in toluene (30 mL) was heated under reflux for 18 h under argon. Then, the solvent was removed under reduced pressure, and the mixture was extracted with CH_2Cl_2. The organic layer was washed with water and dried over anhydrous Na_2SO_4. After evaporation, the crude product was subjected to column chromatography (hexane/CH_2Cl_2 = 4/1) to give **5** (332 mg, 70%). From iodo derivative **1b** A solution of **1b** (73 mg, 0.11 mmol), diphenylamine (37 mg, 0.22 mmol), $Pd_2(dba)_3 \cdot CHCl_3$ (5.1 mg, 0.0056 mmol), SPhos (9.7 mg, 0.024 mmol), *t*-BuOK (37 mg, 0.33 mmol) in toluene (10 mL) was heated under reflux for 16 h under argon. Then, the solvent was removed under reduced pressure, and the mixture was extracted with CH_2Cl_2. The organic layer was washed with water and dried over anhydrous Na_2SO_4. After evaporation, the crude product was subjected to column chromatography (hexane/CH_2Cl_2 = 4/1) to give **5** (58 mg, 71%): orange crystals, mp 172–173 ˚C decomp (CH_2Cl_2/hexane). ^{1}H NMR (400 MHz) δ 5.53 (s, 1H), 6.75 (s, 1H), 6.96–7.13 (m, 18H), 7.17–7.29 (m, 12H), 7.36–7.39 (m, 2H), 7.49 (d, ^3J(H,H) = 8 Hz, 2H), 7.54–7.57 (m, 2H); ^{13}C{^{1}H} NMR (101 MHz) δ 56.2 (CH), 72.3 (C), 112.7 (CH), 122.5 (CH), 122.9 (CH), 123.0 (CH), 123.48 (CH), 123.52 (CH), 124.4 (CH), 124.9 (CH), 125.2 (CH), 126.0 (CH), 127.2 (CH), 127.3 (CH), 127.9 (C), 129.3 (CH), 129.4 (CH), 132.4 (C), 137.1 (C), 143.0 (C), 146.3 (C), 146.6 (C), 147.2 (C), 147.5 (C), 147.6 (C), 148.4 (C), 153.3 (C). Found: C, 86.29; H, 5.08; N, 3.66%. Anal. Calcd. for $C_{54}H_{38}N_2S$: C, 86.83; H, 5.13; N, 3.75%.

2,4-Di[*p*-(diphenylamino)phenyl]-5*H*-5,9b[1',2']-benzenonaphto[1,2-*b*]thiophene 1-Oxide (3)

A mixture of **5** (51 mg, 0.068 mmol) and MCPBA (95%) (13 mg, 0.072 mmol) was dissolved in CH_2Cl_2 (15 mL), and the mixture was stirred for 4.5 h. To the mixture were added aqueous Na_2SO_3 and aqueous $NaHCO_3$, and the mixture was extracted with CH_2Cl_2. The organic layer was washed with water and dried over anhydrous Na_2SO_4. After evaporation, the crude product was subjected to column chromatography (CH_2Cl_2) to give **3** (53 mg, 99%): Orange crystals, mp 185–187 ˚C decomp (hexane/CH_2Cl_2). ^{1}H NMR (400 MHz) δ 5.40 (s, 1H), 7.03–7.15 (m, 21H), 7.24–7.31 (m, 10H), 7.36–7.41 (m, 2H), 7.64–7.68 (m, 2H), 7.74–7.80 (m, 1H), 8.63–8.69 (m, 1H); ^{13}C{^{1}H} NMR (101 MHz) δ 56.4 (CH), 72.6 (C), 122.4 (CH), 122.5 (CH), 122.7 (CH), 123.0 (CH), 123.1 (CH), 123.2 (CH), 123.6 (CH), 123.8 (CH), 123.9 (CH), 124.9 (CH), 125.1 (3CH), 125.3 (CH), 126.2 (CH), 127.8 (CH), 127.9 (CH), 129.4 (2CH), 130.04 (C), 142.4 (C), 142.7 (C), 143.4 (C), 144.1 (C), 146.9 (C), 147.0 (2C), 147.2 (C), 148.2 (C), 148.8 (C), 149.7 (C) (one of quaternary carbon was not observed probably due to overlapping); IR (KBr) ν 1056 cm^{-1} (S=O). HRMS (ESI) Calcd. for $C_{54}H_{38}NO_2S \cdot Na$: M = 785.25971. Found 785.25947 (M^+ + Na^+).

2,4-Di[*p*-(diphenylamino)phenyl]-5*H*-5,9b[1',2']-benzenonaphto[1,2-*b*]thiophene 1,1-Dioxide (4)

A mixture of **5** (36 mg, 0.049 mmol) and MCPBA (95%) (10 mg, 0.112 mmol) was dissolved in CH_2Cl_2 (7 mL), and the mixture was stirred for 12.5 h. To the mixture were added aqueous Na_2SO_3 and aqueous $NaHCO_3$, and the mixture was extracted with CH_2Cl_2. The organic layer was washed with water and dried over anhydrous Na_2SO_4. After

evaporation, the crude product was subjected to column chromatography (CH_2Cl_2) to give **4** (11 mg, 29%): Orange crystals, mp 185–186 ˚C decomp (hexane/CH_2Cl_2). ^{1}H NMR (400 MHz) δ 5.35 (s, 1H), 7.03–7.15 (m, 18H), 7.18 (s, 1H), 7.23–7.31 (m, 12H), 7.36 (d, ^3J(H,H) = 7 Hz, 2H), 7.63 (d, ^3J(H,H) = 8 Hz, 2H), 8.53 (d, ^3J(H,H) = 8 Hz, 2H); ^{13}C{^{1}H} NMR (101 MHz) δ 56.9 (CH), 70.7 (C), 120.8 (C), 122.2 (CH), 122.4 (CH), 123.0 (CH), 123.4 (CH), 123.6 (CH), 123.8 (CH), 123.9 (CH), 125.1 (CH), 125.3 (2CH), 125.7 (CH), 127.6 (CH), 128.2 (CH), 128.4 (C), 129.5 (2CH), 137.2 (C), 140.8 (C), 142.8 (C), 145.3 (C), 146.0 (C), 146.9 (C), 147.1 (C), 148.7 (C), 149.2 (C); IR (KBr) ν 1310, 1138 cm^{-1} (O=S=O). Found: C, 83.04; H, 4.83; N, 3.57%. Anal. Calcd. for $C_{54}H_{38}N_2O_2S$: C, 83.26; H, 4.92; N, 3.60%.

2–6 References

1. Reviews on NIR chromophores and their applications: a) G. Qian, Z. Y. Wang, *Chem. Asian J.* **2010**, *5*, 1006. b) J. O. Escobedo, O. Rusin, S. Lim, R. M. Strongin, *Curr. Opin. Chem. Biol.* **2010**, *14*, 64. c) K. Kiyose, H. Kojima, T. Nagano, *Chem. Asian J.* **2008**, *3*, 506.

2. a) G. Barbarella, L. Favaretta, G. Sotgiu, M. Zambianchi, V. Fattori, M. Cocchi, F. Cacialli, G. Gigli, R. Cingolani, *Adv. Mater.* **1999**, *23*, 1375. b) G. Barbarella, O. Pudova, C. Arbizzani, M. Mastragostino, A. Bongini, *J. Org. Chem.* **1998**, *63*, 1742. c) G. Barbarella, L. Favaretta, G. Sotgiu, M. Zambianchi, A. Bongini, M. Mastragostino, M. Anni, G. Gigli, R. Cingolani, *J. Am. Chem. Soc.* **2000**, *122*, 11971.

3. D. L. Dexter, *J. Chem. Phys.* **1953**, *21*, 836.

4. A. Ishii, T. Annaka, N. Nakata, *Chem. Eur. J.* **2012**, *18*, 6428.

5. A. Wakamiya, K. Mori, S. Yamaguchi, *Angew. Chem. Int. Ed.* **2007**, *46*, 4273.

6. a) M. C. Suh, B. Jiang, T. D. Tilley, *Angew. Chem. Int. Ed.* **2000**, *39*, 2870. b) E. Amir, S. Rozen, *Angew. Chem. Int. Ed.* **2005**, *44*, 7374. c) T. M. Pappenfus, J. H. Melby, B. B. Hansen, D. M. Sumption, S. A. Hubers, D. E. Janzen, P. C. Ewbank, K. A. McGee, M. W. Burand, K. R. Mann, *Org. Lett.* **2007**, *9*, 3721. d) Y. Suzuki, T. Okamoto, A. Wakamiya, S. Yamaguchi, *Org. Lett.* **2008**, *10*, 3393.

7. a) J. Massin, W. Dayoub, J.-C. Mulatier, C. Aronica, Y. Bretonniere, C. Andraud, *Chem. Mater.* **2011**, *23*, 862. b) S. Y. Park, Y. Kubota, K. Funabiki, M. Shiro, M. Matsui, *Tetrahedron Lett.* **2009**, *50*, 1131. c) O. Fenwick, J. K. Sprafke, J. Binas, D. V. Kondratuk, F. Di Stasio, H. L. Anderson, F. Cacialli, *Nano Lett.* **2011**, *11*, 2451. d) G. Qian, Z. Zhong, M. Luo, D. Yu, Z. Zhang, Z. Y. Wang, D. Ma, *Adv. Mater.* **2009**, *21*, 111. e) G. Qian, Z.

Zhong, M. Luo, D. Yu, Z. Zhang, D. Ma, Z. Y. Wang, *J. Phys. Chem. C* **2009**, *113*, 1589.

f) C.-K. Lim, S. Kim, I. C. Kwon, C.-H. Ahn, S. Y. Park, *Chem. Mater.* **2009**, *21*, 5819.

8. C. Reichardt, *Chem. Rev.* **1994**, *94*, 2319.

9. M. J. Frisch, G. W. Trucks, H. B. Schlegel, G. E. Scuseria, M. A. Robb, J. R. Cheeseman, G. Scalmani, V. Barone, B. Mennucci, G. A. Petersson, H. Nakatsuji, M. Caricato, X. Li, H. P. Hratchian, A. F. Izmaylov, J. Bloino, G. Zheng, J. L. Sonnenberg, M. Hada, M. Ehara, K. Toyota, R. Fukuda, J. Hasegawa, M. Ishida, T. Nakajima, Y. Honda, O. Kitao, H. Nakai, T. Vreven, J. A. Montgomery Jr., J. E. Peralta, F. Ogliaro, M. Bearpark, I. J. Heyd, E. Brothers, K. N. Kudin, V. N. Staroverov, T. Keith, R. Kobayashi, J. Normand, K. Raghavachari, A. Rendell, J. C. Burant, S. S. Iyengar, J. Tomasi, M. Cossi, N. Rega, J. M. Millam, M. Klene, J. E. Knox, J. B. Cross, V. Bakken, C. Adamo, J. Jaramillo, R. Gomperts, R. E. Stratmann, O. Yazyev, A. J. Austin, R. Cammi, C. Pomelli, J. W. Ochterski, R. L. Martin, K. Morokuma, V. G. Zakrzewski, G. A. Voth, P. Salvador, J. J. Dannenberg, S. Dapprich, A. D. Daniels, O. Farkas, J. B. Foresman, J. V. Ortiz, J. Cioslowski, D. J. Fox, Gaussian 09, revision D.01; Gaussian, Inc.: Wallingford, CT, 2013.

10. T. Manifara, S. Rohania, R. Duqueb, C. Jenningsb, M. Sabanb, *Chem. Eng. Sci.* **2006**, *61*, 2590.

11. G. M. Sheldrick, SHELXL-97, Program for Crystal Structure Refinement; University of Göttingen: Göttingen, Germany, 1997.

Chapter 3

Synthesis, Structures, Photophysical Properties, and Derivations of 1,4-Diphenyl-1-telluro-1,3-butadienes

3–1 Introduction

The metalloid tellurium is a versatile element that forms the basis for several important materials, including catalysts, dyes, and optoelectronic compounds.[1] Tellurophene, the heavier analog of thiophene, has certain advantages, such as red-shifted optical absorption properties,[2] unique solid-state supramolecular structures through tellurium−tellurium interactions,[3] and high polarizability, relative to their lighter analogues due to the unique chemistry of tellurium. Organotellurium compounds can be derived from postsynthesis modification including oxidation and bromination at tellurium atom. Seferos reported a dramatic shift in optical properties of π-conjugated tellurophenes exposed to Br_2, which appears to be the result of coordination of Br atoms at their tellurium centers.[4]

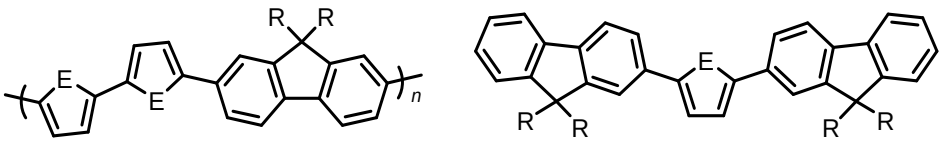

E = Te, $TeBr_2$, R = *n*-C_6H_{13}

Figure 1. π-Conjugated tellurophenes.

Vinylic tellurides can be derived from the tellurium-lithium exchange and the following reaction with electrophiles, providing functionalized alkenes.[5] Tokitoh and Mizuhata reported a synthesis of 1,2-dihydro-2-stannanaphthalenes as a precursor of 2-stannanaphthalene by the reaction of cyclic telluride with butyllithium and trihalostannanes.[6]

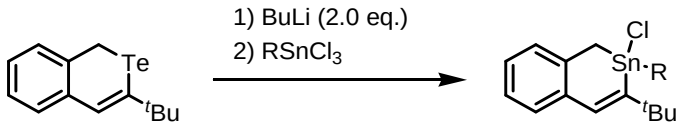

Scheme 1. Transformation of cyclic telluride to stannane.

The heavy-atom effect often plays a crucial role in nonradiative deactivation in a series of luminescent organic compounds, and in phosphorescence emission from transition metal complexes.[7] The effect induces an intersystem crossing from an exited singlet state to the exited triplet state caused by spin-orbit interaction of heavy atom.[8] As written in chapter 1, it has been reported that chalcogen-containing heteroaromatics such as benzo[b]chalcogenophenes,[9] dibenzo[b,d]chalcogenophenes,[10] benzo-[1,2-*b*:4,5-*b'*]dicalcogenophenes,[11] and chalcogenorhodamine derivatives[12] suffer drastic decreases in fluorescent quantum yields by changing the chalcogen atom from oxygen to sulfur, selenium, or tellurium. However, heavy-atom effect is not always effective when the energy difference between S_1 and the accepting triplet state is not small enough for intersystem crossing;[13] perylene, 3-bromo-, and 3,9-dibromo derivatives show fluorescence quantum yields of more than 0.95 at 295 K.[14] A recent topic of research is the photoluminescence of oxides of organotellurium compounds, and some *Te*-oxides of tellurorhodamine derivatives[12,15] and 1,1-dioxides of 2,5-diaryltellurophenes[16] have been reported to emit fluorescence with quantum yields of up to ~0.3 in buffered aqueous solutions at room temperature.

We have synthesized strong fluorescent 1-chalcogeno-1,3-butadienes **1**–**5**.[17–19] When a series of diesters measured in CH_2Cl_2 at room temperature, it was found that the fluorescence quantum yield (Φ_F) of **1** is quantitative, and that that of **2** is still high (Φ_F =

0.88), but that the tellurium derivative **3** is substantially non-fluorescent.[16,17] In contrast, both of diphenyl derivatives **4** and **5** emit blue fluorescence with almost quantitative quantum yield in CH_2Cl_2 at room temperature, even through **5** contains a selenium atom.[18] In **5**, the heavy-atom effect of selenium is ineffective for fluorescence quenching. These results prompted us to investigate the photophysical properties of the corresponding tellurium derivative **6**. In this chapter, the author reports the synthesis of **6**, following derivations, such as oxidation, bromination, and introduction of silicon atom to create of new emissive compounds, and the elucidation of their photophysical properties.

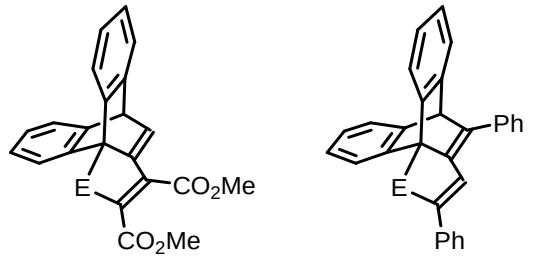

1: E = S (Φ_F = 1.00)
2: E = Se (Φ_F = 0.88)
3: E = Te (Φ_F = 0.004)

4: E = S (Φ_F = 1.00)
5: E = Se (Φ_F = 1.00)

Figure 2. 1-Chalcogeno-1,3-butadienes with fluorescence quantum yields.

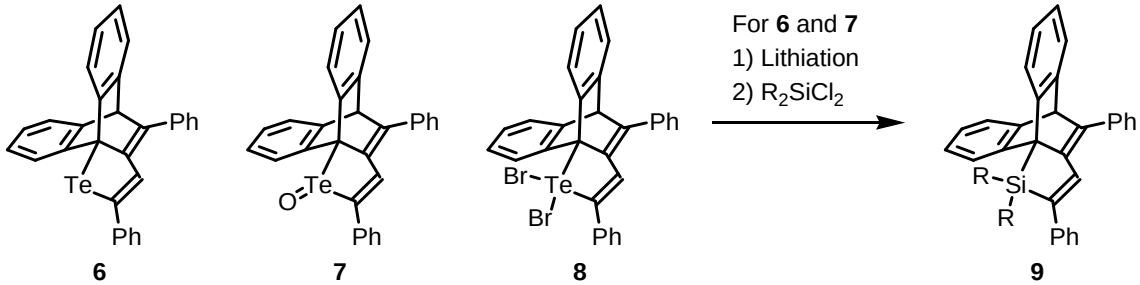

6 **7** **8** **9**

Scheme 2. Synthesis and Derivation of 1,4-dipheyl-1-telluro-1,3-butadienes.

3–2 Syntheses and Structures of 1,4-Diphenyl-1-telluro-1,3-butadienes

As shown in Scheme 3, telluride **6** was synthesized by a series of reactions similar to those for sulfur and selenium analogues **4** and **5**. Di(9-anthryl) ditelluride was reduced with $NaBH_4$ in bis(2-methoxyethyl)ether (diglyme) and 1-butanol, and the resulting tellurolate was allowed to react with diphenylbutadiyne, producing **6** in 62% yield. Oxidation of **6** with MCPBA in CH_2Cl_2 gave telluroxide **7** in 93% yield. The reaction of **6** with Br_2 in CH_2Cl_2 at room temperature yielded *Te,Te*-dibromide **8** almost quantitatively (94%) (Scheme 3).

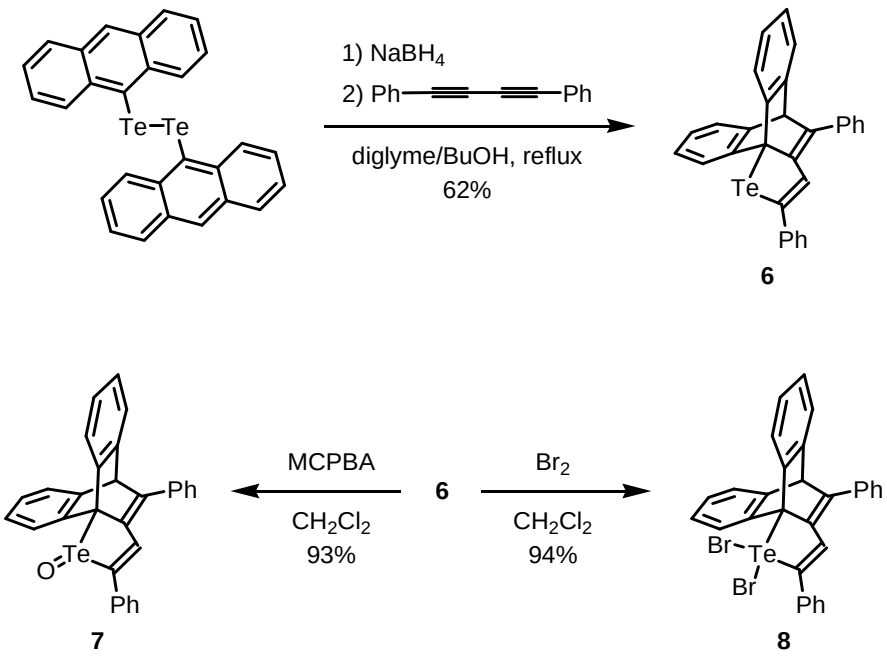

Scheme 3. Synthesis, oxidation, and bromination of 1-telluro-1,3-butadiene derivative **6**

The structures of **6**–**8** were determined by spectroscopic methods and X-ray crystallography (Figure 3–5). The 1-telluro-1,3-butadiene moieties (C2–C3–C4–C5) in

6–**8** are almost planar and the bond lengths are in similar ranges in comparison with those of sulfur and selenium analogues **4** and **5**.

Several CH–π interactions are observed in a crystalline structure of telluride **6** (Figure 6) in contrast to the dimeric structure in telluroxide **7** and dibromide **8** induced by intermolecular n(O)–σ*(Te–C) or n(Br)–σ*(Te–C) orbital interactions, respectively (Figure 7 and 8). The interatomic Te–O (2.590 Å) and Te–Br2 (3.641 Å) distances are 28% (0.99 Å) and 7% (0.27 Å) shorter than the sum of their van der Waals radii of Te (2.06 Å), O (1.52 Å), and Br (1.85 Å), respectively. In dibromide **8**, the n(Br)–σ*(Te–C) orbital interaction shortens intramolecular Te–Br2 bond in comparison with Te–Br1 bond [Te1–Br1: 2.6627(4), Te–Br2: 2.7434(4)]. This intermolecular interaction is weaker than that in 2,5-diphenyltellurophene *Te*,*Te*-dibromide, in which the interatomic distance between Te and Br is 2.673 Å with 175.33(5)° of the Br–Te–Br bond angle forming a polymeric structure.[4b] The bulky dibenzobarrelene skeleton prevents the formation of polymeric structure. The steric repulsion between Br atoms and benzene ring in dibenzobarrelene pushes the Br atoms to the opposite side leading to the bending [Br1–Te–Br2: 158.53(1)°].

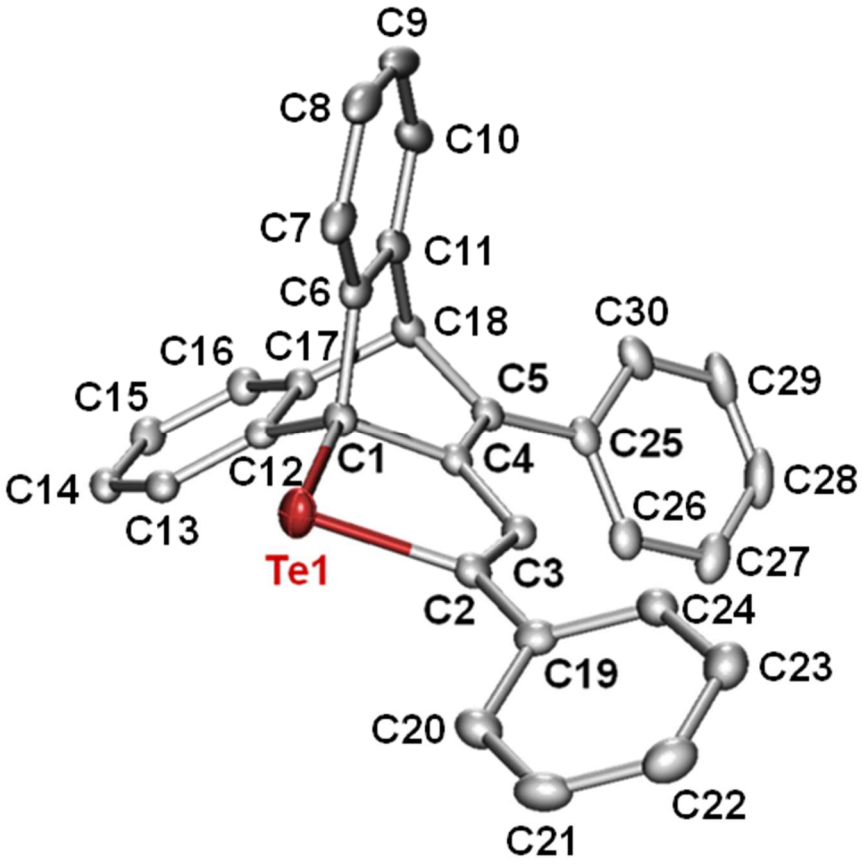

Figure 3. ORTEP drawing of **6** with 50% probability ellipsoids. Selected bond length (Å) and torsion angles (°): Te1–C2: 2.109(2), Te1–C1: 2.153(2), C1–C4: 1.549(3), C2–C3: 1.344(3), C3–C4: 1.438(3), C4–C5: 1.354(3), C2–C3–C4–C5, 176.2(2), C3–C2–C19–C24: 36.8(3), C4–C5–C25–C26: 36.6(2). *Crystal data*: $C_{30}H_{20}Te$, M_r = 508.06, monoclinic, $P2_1/c$, a = 13.5929(7), b = 12.1552(6), c = 13.0873(6) Å, β = 99.7420(10)°, V = 2131.16(18) Å^3, Z = 4, μ = 1.411 mm^{-1}, d_{calcd} = 1.583 g cm^{-3}, R_1 ($I > 2\sigma(I)$) = 0.0299, wR_2 = 0.0726 (all data) for 5061 reflections, 280 parameters, GOF = 1.073.

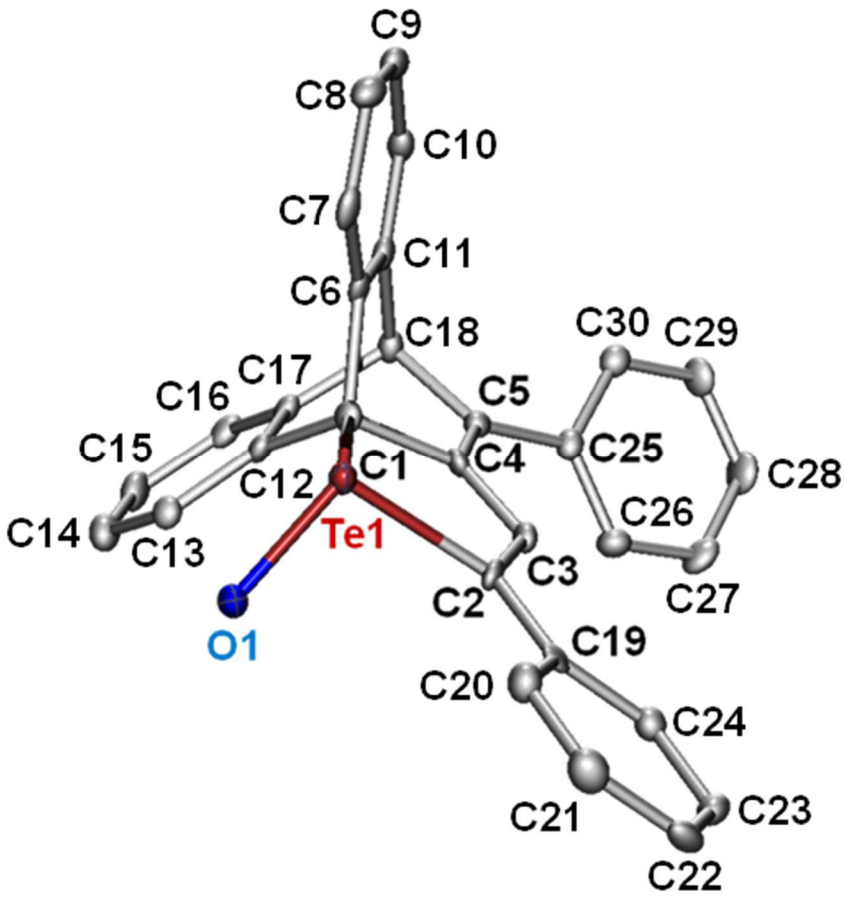

Figure 4. ORTEP drawing of **7** with 50% probability ellipsoids. Selected bond length (Å) and torsion angles (°): C1–Te1: 2.180(5), C2–C3: 1.354(6), C2–Te1: 2.137(4), C3–C4: 1.424(6), C4–C5: 1.353(7), Te1–O1, 1.860(3), C2–C3–C4–C5: 179.4(5), C3–C2–C19–C24: 12.6(7), C4–C5–C25–C26: 43.4(7). *Crystal data*: $C_{30}H_{20}OTe{\bullet}2CHCl_3$, M_r =762.80, triclinic, *P*–1, a = 11.0309(7), b = 11.3923(8), c = 13.0052(9) Å, α = 89.426(2), β = 67.896(2), γ= 88.106(2)°, V = 1513.38(18) Å^3, Z = 2, μ = 1.539 mm^{-1}, d_{calcd} = 1.674 g cm^{-3}, R_1 ($I > 2\sigma(I)$) = 0.0479, wR_2 = 0.1197 (all data) for 5591 reflections, 361 parameters, GOF = 1.055.

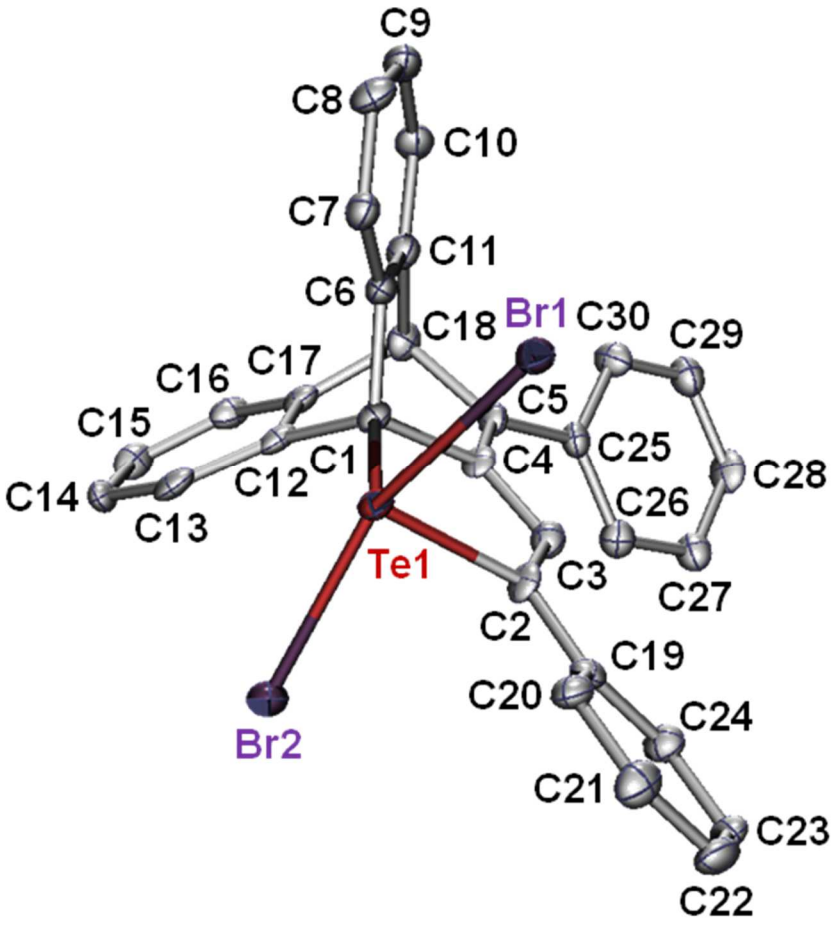

Figure 5. ORTEP drawing of **8** with 50% probability ellipsoids. Selected bond length (Å) and torsion angles (°): Te1–C2: 2.099(2), Te1–C1: 2.198(2), Te1–Br1: 2.6627(4), Te–Br2: 2.7434(4), C5–C4: 1.355(3), C4–C3: 1.435(3), C4–C1: 1.551(3), C2–C3: 1.340(3), Br1–Te1–Br2: 158.526(11), C5–C4–C3–C2: 179.3(3), C3–C2–C19–C24: 17.1(4), C4–C5–C25–C26: 39.8(4). *Crystal data*: $C_{30}H_{20}Br_2Te \bullet C_7H_8$, M_r = 760.01, triclinic, *P*–1, *a* = 11.1893(16), *b* = 11.4445(16), *c* = 12.9179(18) Å, α = 107.919(2), β = 105.3030(10), γ = 95.348(2)°, *V* = 1490.5(4) Å^3, *Z* = 2, μ = 3.704 mm^{-1}, d_{calcd} = 1.693 g cm^{-3}, R_1 ($I > 2\sigma(I)$) = 0.0225, wR_2 = 0.0420 (all data) for 5443 reflections, 425 parameters (242 restraints for C_7H_8), GOF = 1.015.

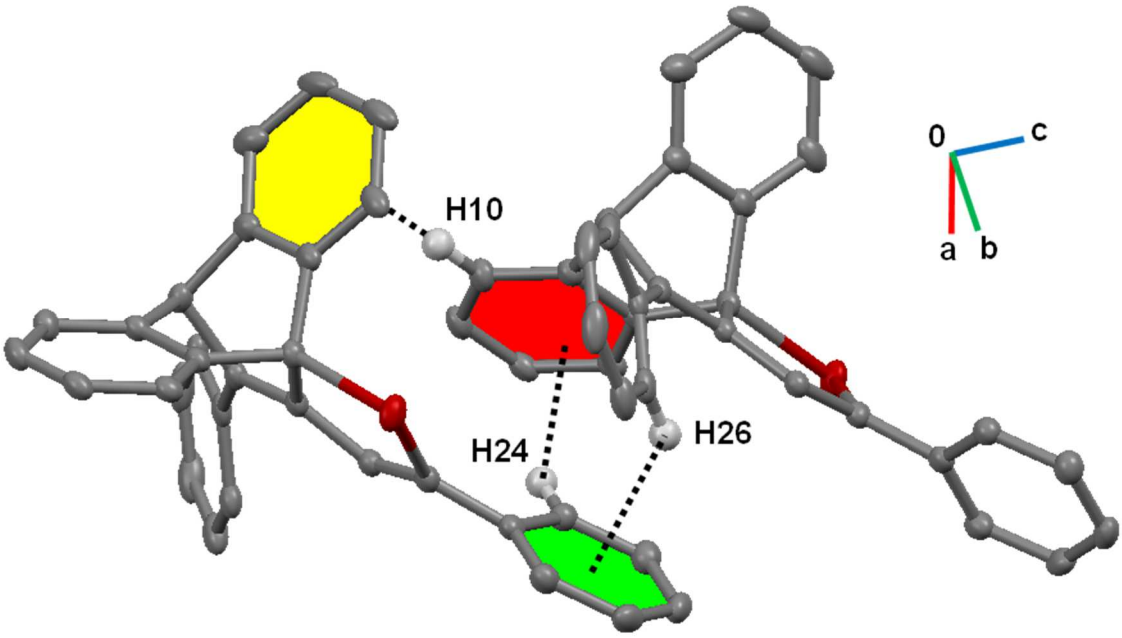

Figure 6. Crystal packing of **6**; H10–benzene ring (yellow): 2.728 Å, H24–benzene ring (red): 2738 Å, H26–benzene ring (green): 2.710 Å.

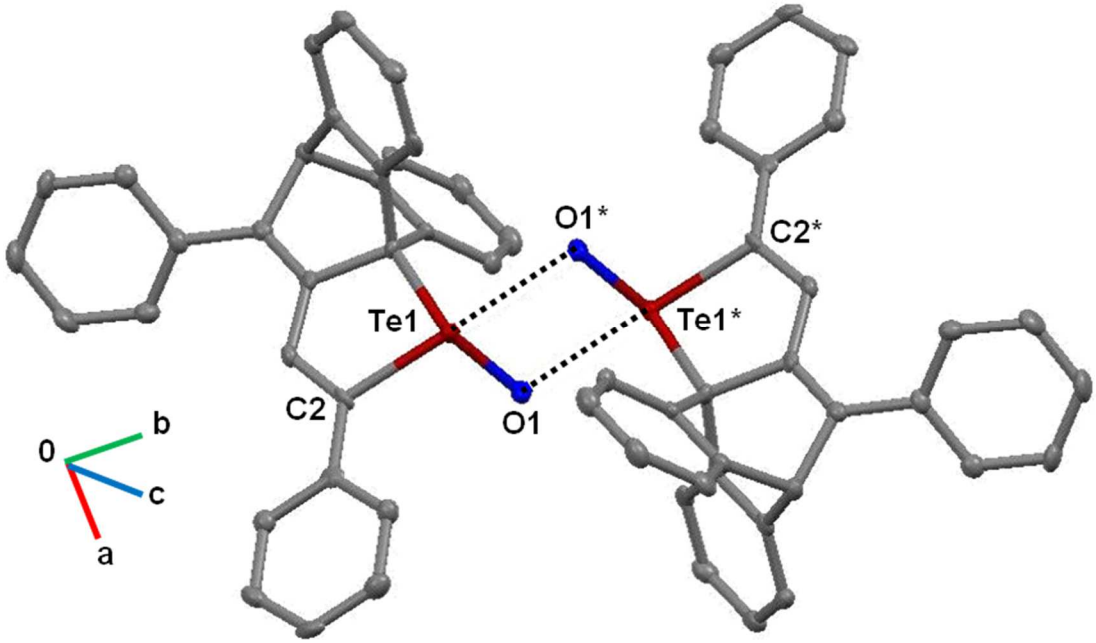

Figure 7. Crystal packing of **7**.

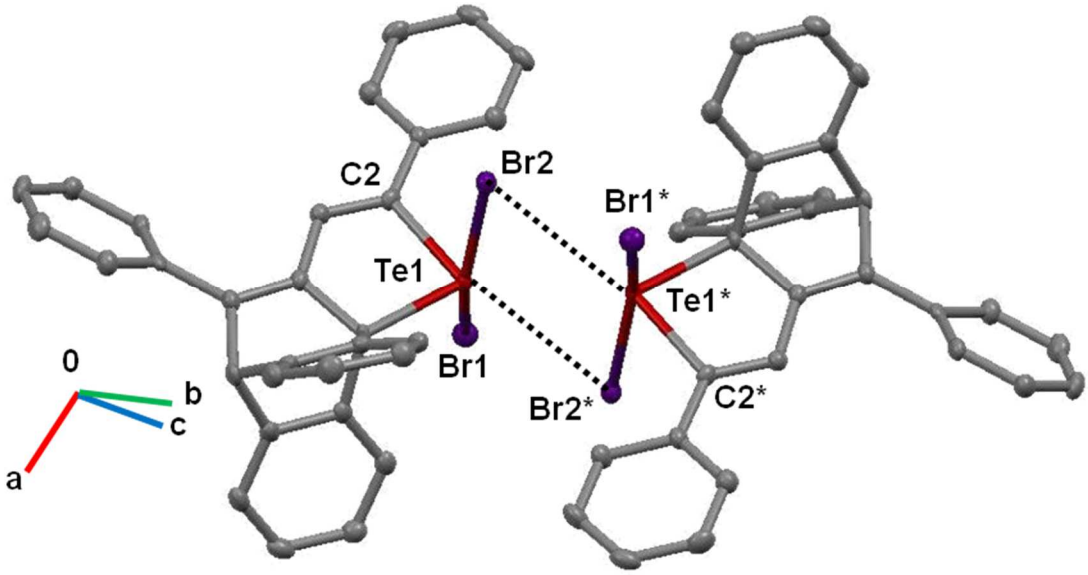

Figure 8. Crystal packing of **8**.

3–3 Silylations of 1,4-Diphenyl-1-telluro-1,3-butadienes

At first, we carried out lithiations of telluride **6** with *n*- or *t*-butyllithium, however the both reactions didn't undergo. Considering low reactivity came from too stable **6**, we next examined a lithiation of telluroxide **7**, having longer tellurium–carbon bonds than **6**, with *t*-butyllithium. This reaction gave silicon analogue **9** in trace (Scheme 3). The crude product included **6** mainly and unknown byproducts. We concluded the reduction of telluroxide **7** for telluride **6** and unstable dilithium compound as intermediate owing to the electronic repulsion between lithium atoms suffer inefficiency in this reaction. The silicon analogue **9** was identified only by ^{1}H-NMR spectroscopy and bright blue emission was observed in CH_2Cl_2.

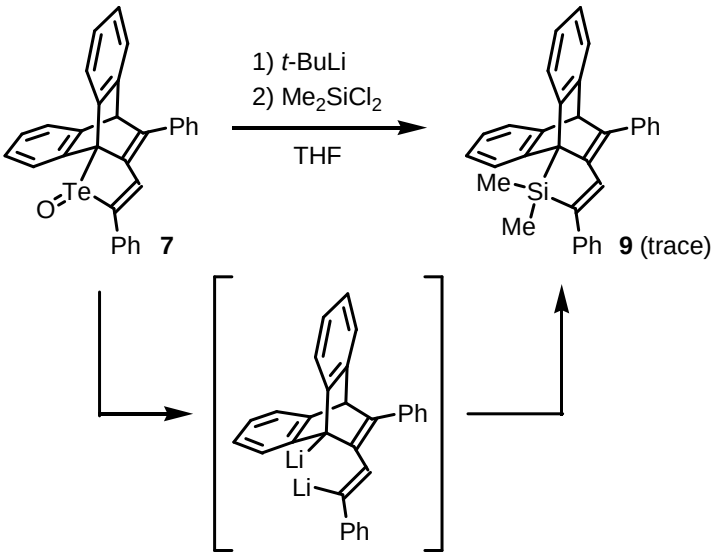

Scheme 3. Examination to synthsize silicon analogue **10**.

3–4 Photophysical Properties of 1,4-Diphenyl-1-telluro-1,3-butadienes

UV-vis spectra of **4**–**8** in 2-methyltetrahydrofuran (2-MeTHF) are shown in Figure 9, and their data are summarized in Table 1. Telluride **6** shows two absorption maxima at 406 and 377 nm, unlike the sulfur and selenium congeners **4** and **5**, which are monomodal. The longest absorption maximum of **6** is somewhat red-shifted compared with those of **4** (λ_{max} = 385 nm) and **5** (λ_{max} = 383 nm). Telluroxide **7** and dibromide **8** have the longest absorption maxima at 353 nm and 326 nm with a shoulder around 380 nm, respectively.

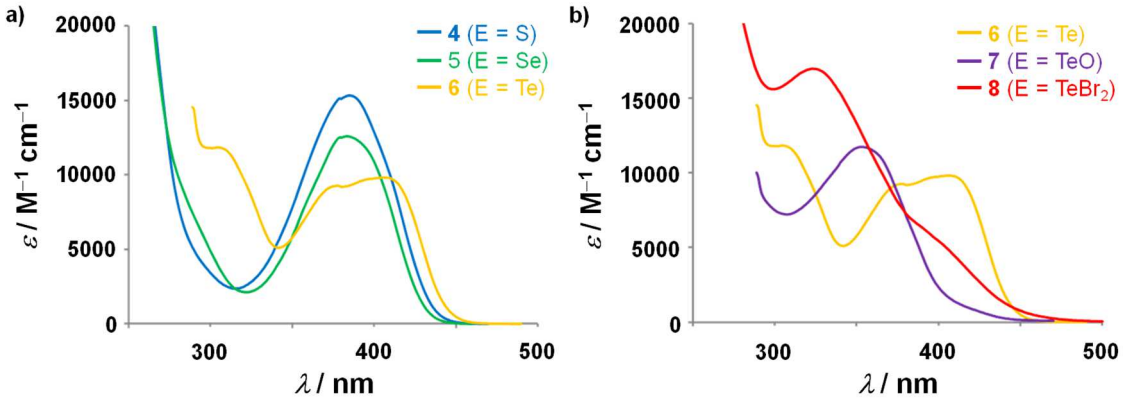

Figure 9. UV-vis spectra of a) chalcogenides **4**–**6** and b) tellurium derivatives **6**–**8** in 2-MeTHF.

TD-DFT calculations at the B3LYP/6-31G(d), LANL2DZ for Se, Te, and Br level were carried out to analyze the electronic spectra.[20–23] As shown in Teble 1 and Figure 10, two absorptions are calculated at 417 nm (2.98 eV) and 404 nm (3.07 eV) in telluride **6**, which are mainly due to HOMO–LUMO (f = 0.1521) and HOMO–LUMO+1 (f = 0.1020) transitions, respectively. The HOMO of **6** extends on the π-conjugated system comprising the lone pair on tellurium atom and the 1,3-butadiene moiety with small contributions

from benzene rings, and the LUMO is based on the anti-bonding π* orbital of the 1,4-diphenyl-1,3-butadiene moiety. Similar HOMO–LUMO transitions were calculated for the sulfur and selenium analogues **4** and **5**. Characteristic for **6** is the second low-energy excitation, in which the σ* orbital of Te–C bond participate generously in LUMO+1. It can be concluded that the low-lying LUMO+1 resulted in the bimodal absorption of **6**.

In the TD-DFT calculations of telluroxide **7**, the lowest excitation are observed at 3.22 eV (*f* = 0.1695) corresponding to 385 nm, which is mainly due to the HOMO–LUMO transition. This excitation is followed by the excitation mainly due to the HOMO−1–LUMO transition (3.29 eV, *f* = 0.1519). The diagram of LUMO+1 of **7** resembled that of **6**. In the case of dibromide **8**, the lowest-energy excitation is due to the HOMO–LUMO transition (*f* = 0.0859) with the energy of 2.73 eV (453 nm). This excitation is followed by two major excitations due to mainly HOMO−3–LUMO (*f* = 0.1250, 3.40 eV, 364 nm) and HOMO−1–LUMO (*f* = 0.1566, 3.53 eV, 351 nm) transitions. These excitations will lead to the broad absorption of **8** ranging from 300 to 500 nm. The HOMO, HOMO−1, and HOMO−3 are contributed from π-bonds of 1,3-butadiene and benzene rings, and the lone pairs on bromine. The LUMO consists of typical hypervalent three-center-four-electron σ* orbital.[20]

Table 1. Absorptions in 2-methyltetrahydrofuran and TD-DFT calculations of **4**–**8** at the B3LYP/6-31G(d), LANL2DZ for Se, Te, Br level.

	λ_{abs} [nm]	λ_{cal} [nm]	E [eV]	f	Main Transition
S **4**	385	400	3.10	0.4142	HOMO→LUMO (π–π^*)
Se **5**	383	400	3.10	0.3548	HOMO→LUMO (π–π^*)
Te **6**	406	417	2.98	0.1456	HOMO→LUMO (π–π^*)
	377	404	3.07	0.1081	HOMO→LUMO+1 (π–σ^*)
TeO **7**	362	385	3.21	0.1695	HOMO→LUMO
		377	3.29	0.1519	HOMO–1→LUMO
$TeBr_2$ **8**	sh	453	2.73	0.0859	HOMO→LUMO
	326	364	3.40	0.1250	HOMO–1→LUMO
		351	3.53	0.1566	HOMO–3→LUMO

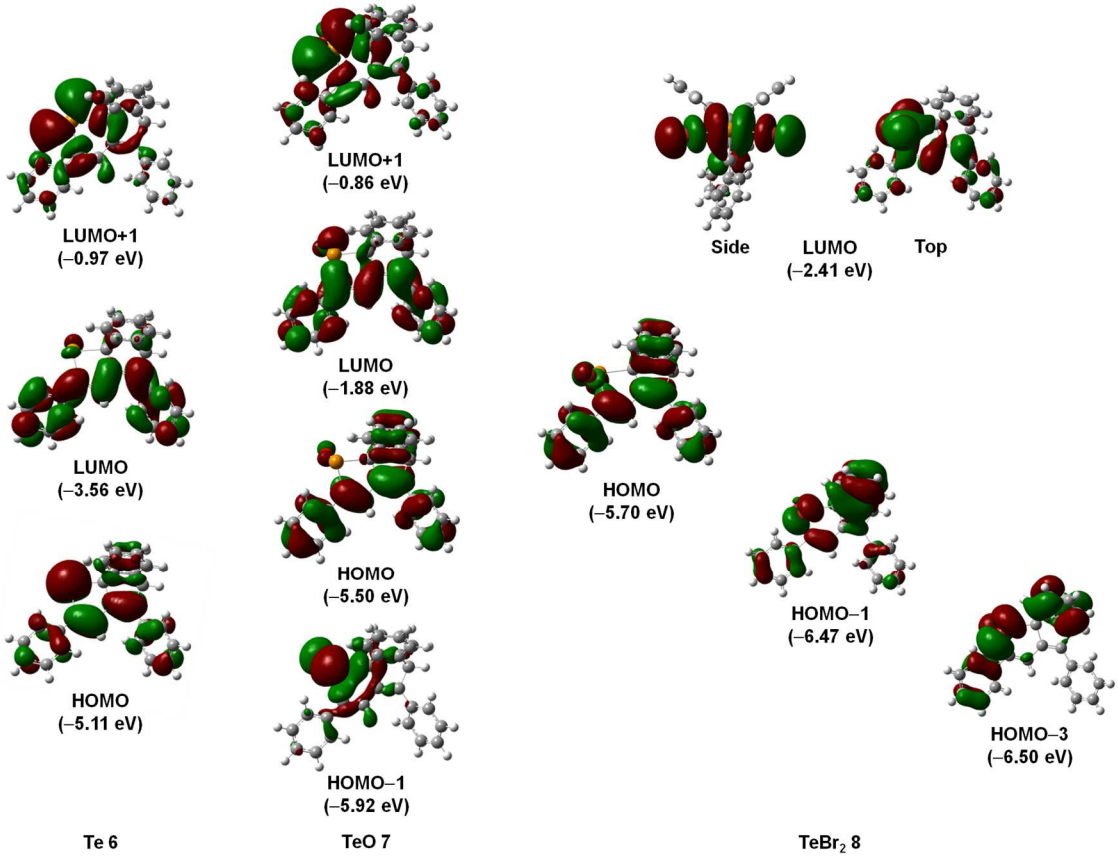

Figure 10. Diagram of frontier orbitals of **6**–**8** obtained by TD-DFT calculations at B3LYP/6-31G(d), LANL2DZ for Te and Br.

Fluorescence spectra in 2-MeTHF at room temperature and in glass state of 2-MeTHF at 77 K are shown in Figure 11 and 12, and their properties are summarized in Table 2. Telluride **6** has the shorter emission maximum at 459 nm with quite small quantum yield ($\Phi_{PL} < 0.01$) in 2-MeTHF comparing with sulfide **4** and selenide **5** (**4**: λ_{em} = 488 nm, Φ_{PL} = 0.91, **5**: λ_{em} = 477 nm, Φ_{PL} = 0.90) in 2-MeTHF at room temperature. This low luminescence quantum yield of **6** will be explained in terms of the heavy-atom effect of tellurium. Interestingly, **6** exhibited temperature dependent luminescence and emitted blue light with moderate quantum yield (Φ_F = 0.42) in glass state. In contrast to telluride **6**, the luminescence of telluroxide **7** and dibromide **8**, which contains a small amount of **6**, were none or very weak even in the glass state. To assign the luminescence of **6**, its emission life time was measured. The emission life time is in the nanosecond order, strongly suggesting that its emission is fluorescence and not phosphorescence. Temperature dependent quantum yields of fluorescence have been reported;[7,13,24] for example, the quantum yield of 9-bromoanthracene changed from 0.018 at 295 K to almost unity at 110 K.[7,25] And the phenomena have been explained by the presence of the thermally activated intersystem crossing from a lowest excited singlet stale (S_1) to an adjusted higher excited triplet state (T_n).[7,13,25c,26] This will be the case for the remarkable increase of the quantum yield of **6** at 77 K, while its moderate quantum yield suggests that the temperature independent intersystem crossing is competitively operative there.[26a]

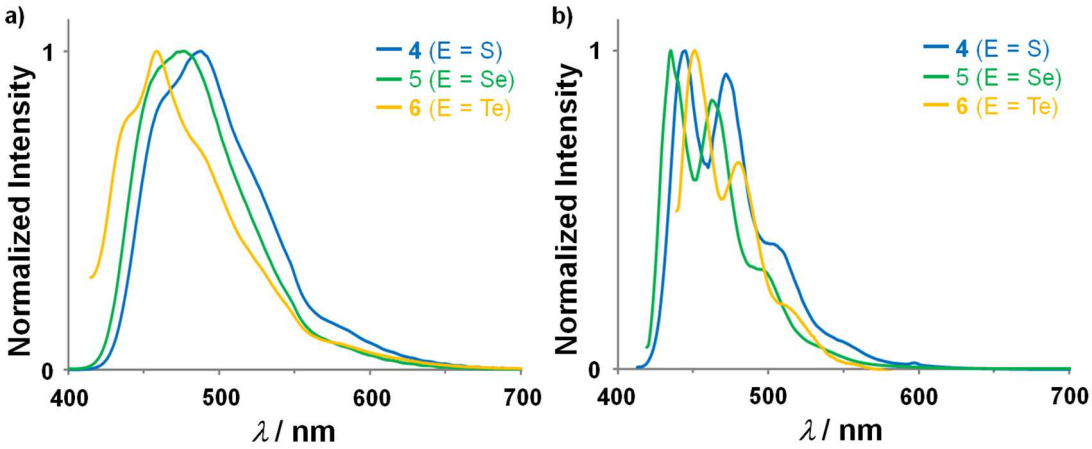

Figure 11. Fluorescence spectra of chalcogenide **4**–**6** at a) room temperature and b) 77 K in 2-MeTHF.

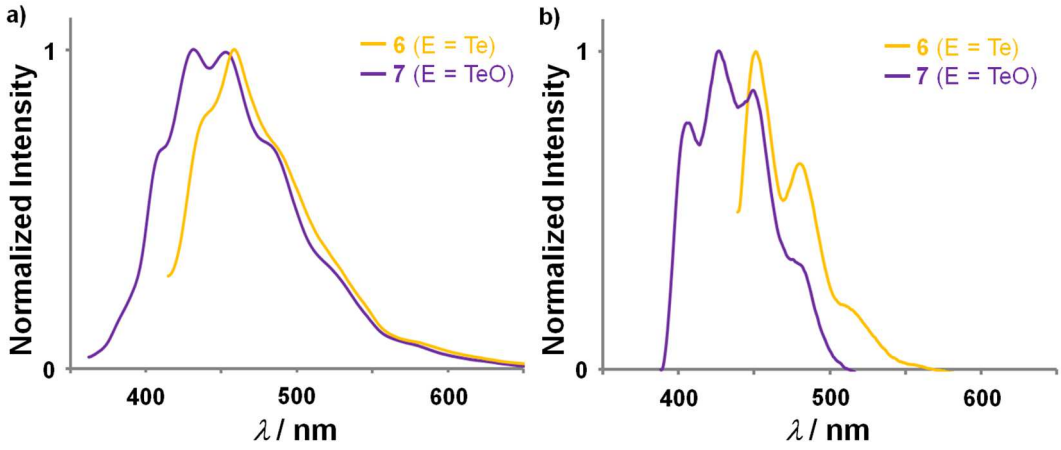

Figure 12. Fluorescence spectra of telluride **6** and telluroxide **7** at a) room temperature and b) 77 K in 2-MeTHF.

Table 2. Luminescent properties of 10^{-5} M **4**–**8** in 2-Methyltetrahydrofuran.

	λ_{em} [nm] at RT	λ_{em} [nm] at 77 K	Φ_{PL} at RT	Φ_{PL} at 77 K	τ_{PL} [ns] at RT	τ_{PL} [ns] at 77 K
S **4**	488	445, 472	0.91	0.85	5.05[b]	N. D.[c]
Se **5**	477	435, 462	0.90	0.87	4.87[b]	N. D.[c]
Te **6**	459	451, 480	< 0.01	0.42	0.14, 5.04	0.80, 3.69
TeO **7**	431, 453	406, 426, 449	0.01	0.02	N. D.[c]	N. D.[c]
$TeBr_2$ **8**	N. E.[a]	451, 480	N. E.[a]	0.04	N. D.[c]	N. D.[c]

a) No emission. b) In CH_2Cl_2. c) Not determined.

3–5 Conclusion

1,4-Diphenyl-1-telluro-1,3-butadiene derivative **6** incorporated in a dibenzobarrelene skeleton was successfully synthesized by intramolecular Diels-Alder reaction as key reaction. Telluroxide **7** and *Te,Te*-dibromide **8** were prepared by oxidation and bromination of **6**, respectively. The lithiation and the following reaction with dichlorosilane didn't undergo well, giving silicon analogue **9** in trace only from **7**. We found that telluride **6** reveals temperature-dependent fluorescence; it is fluorescent with moderate quantum yield in the glass state of 2-MeTHF at 77 K, whereas it is barely fluorescent at room temperature, unlike the sulfur and selenium congeners **4** and **5**, due to the heavy-atom effect of tellurium. Although further detailed photophysical studies on their exited states, it can be considered that the temperature-dependent fluorescence character is attributed to the thermally activated intersystem crossing from a lowest excited singlet state to an adjusted higher excited triplet state.

3–6 Experimental Section

General Procedures

All melting points were determined on a Mel-Temp capillary tube apparatus and were uncorrected. ^{1}H and ^{13}C were recorded on a Bruker Avance-400 spectrometer (400 MHz and 101 MHz, respectively) and ^{77}Te NMR spectra were obtained on a Bruker AVANCE-500 (158 MHz) spectrometer using $CDCl_3$ as the solvent at room temperature. IR spectra were recorded on a Perkin Elmer System 2000 FT-IR spectrometer. UV-Vis spectra were recorded on a HITACHI U-1900 spectrophotometer. Fluorescence spectra were recorded on a JASCO FP-6300 spectrofluorometer. Absolute photoluminescence quantum yields were measured on a calibrated integrating sphere system C10027 (Hamamatsu Photonics). Emission lifetimes were measured on a Hamamatsu Photonics Quantaurus-Tau. Elemental analyses were carried out at the Molecular Analysis and Life Science Center of Saitama University. X-ray crystallography was performed with a Bruker AXS SMART diffractometer. The intensity data were collected at 103 K employing graphite-monochromated MoKα radiation (λ = 0.71073 Å) and the structures were solved by direct methods and refine by full-matrix least-squares procedures on F^2 for all reflections (SHELX-97).[27] Solvents were dried by standard methods and freshly distilled prior to use. Dehydrated THF was purchased from Kanto Chemical Co., Inc. and 2-methyltetrahydrofuran was purchased from Sigma-Aldrich Co. LLC and used without further purification. Column chromatography was performed with silica gel (70–230 mesh) and the eluent is shown in parentheses. Preparative gel permeation liquid chromatography (GPC) was performed on an LC-918 (Japan Analytical Industry Co., Ltd.) equipped with JAIGEL 1H and 2H columns (eluent: $CHCl_3$).

Synthesis of Di(9-anthryl) Ditelluride

To a solution of 9-bromoanthracene (1.00 g, 3.89 mmol) in THF (10 mL) at −78 °C was added *t*-BuLi (1.65 M in pentane, 4.6 mL, 7.58 mmol) under argon. The mixture was stirred for 30 min at −78 °C, and tellurium powder (471 mg, 7.58 mmol) was added. The mixture was stirred for 11.5 h at room temperature. After stirring for 1 h at room temperature in the air for oxidation, the mixture was filtered through a pad of Celite® with CH_2Cl_2. The extract was washed with water, dried over anhydrous Na_2SO_4, and evaporated to dryness. The residue was purified by reprecipitation from CH_2Cl_2/hexane to give di(9-anthryl) ditelluride (920 mg, 78%): Brown crystals, mp 196 °C decomp ^{1}H NMR (400 MHz) δ 6.92–7.02 (m, 4H), 7.24–7.35 (m, 4H), 7.82 (d, ^3J(H,H) = 8.4 Hz, 4H), 8.21 (d, ^3J(H,H) = 8.4 Hz, 4H), 8.34 (s, 1H); ^{13}C NMR (100.7 MHz) δ 115.5 (C), 125.1 (CH), 126.2 (CH), 128.7 (CH), 130.6 (CH), 130.9 (C), 135.3 (CH), 137.4 (C); ^{125}Te NMR (158 MHz, $CDCl_3$) δ176.8. Found: C, 55.34; H, 2.92%. Anal. Calcd. for $C_{28}H_{18}Te_2$: C, 55.16; H, 2.98%.

Synthesis of 2,4-Diphenyl-5*H*-5,9b[1',2']-benzenonaphto[1,2-*b*]tellurophene (6)

A solution of di(9-anthryl) ditelluride (116 mg, 0.19 mmol) and 1,4-diphenyl-1,3-butadiyne (78 mg, 0.38 mmol) in diglyme (14 mL) was added slowly to a solution of $NaBH_4$ (22 mg, 0.59 mmol) in BuOH (7 mL) at 0 °C under argon. After stirring for 30 min at 0 °C, the mixture was heated under reflux for 20 h, and then the reaction was quenched by addition of saturated ammonium chloride solution. The mixture was extracted with CH_2Cl_2, and the extract was washed with water, dried over anhydrous Na_2SO_4, and evaporated to dryness. The residue was subjected to column chromatography (hexane/CH_2Cl_2 = 4/1) to give **6** (121 mg, 62%): Yellow crystals, mp

145 °C (CH_2Cl_2/hexane). ^{1}H NMR (400 MHz) δ 5.46 (s, 1H), 7.02–7.10 (m, 4H), 7.22–7.41 (m, 13H), 7.46–7.52 (m, 2H); ^{13}C NMR (101 MHz) δ 57.6 (CH), 63.2 (C), 123.1 (CH), 125.6 (CH), 126.3 (CH), 126.5 (CH), 127.2 (CH), 127.4 (CH), 127.5 (CH), 128.3 (CH), 128.5 (CH), 128.7 (CH), 129.0 (CH), 131.6 (C), 139.25 (C), 139.29 (C), 144.4 (C), 146.5 (C), 148.0 (C), 158.1 (C); ^{125}Te NMR (158 MHz) δ 496.9. Found: C, 71.03; H, 4.14. Anal. Calcd. for $C_{30}H_{20}Te$: C, 70.92; H, 3.97.

Oxidation of telluride 6 with MCPBA

A mixture of telluride **6** (60 mg, 0.12 mmol) and MCPBA (95%) (32 mg, 0.18 mmol) was dissolved in CH_2Cl_2 (5 mL), and the mixture was stirred for 1 h. To the mixture were added aqueous Na_2SO_3 and aqueous $NaHCO_3$, and the mixture was extracted with CH_2Cl_2. The extract was washed with water, dried over anhydrous Na_2SO_4, and evaporated to dryness. The residue was washed with Et_2O (10 mL) and dried to give 2,4-diphenyl-5*H*-5,9b[1',2']-benzenonaphto[1,2-*b*]tellurophene 1-oxide (**7**) (57 mg, 93%): Pale yellow crystals, mp 209 °C decomp (ether). ^{1}H NMR (400 MHz) δ 5.35 (s, 1H), 6.93–7.16 (m, 4H), 7.28–7.46 (m, 10H), 7.57–7.66 (m, 3H), 7.71 (s, 1H), 8.53 (d, ^3J(H,H) = 7.2 Hz, 1H); ^{13}C NMR (101 MHz) δ 57.3 (CH), 69.2 (C), 123.9 (CH), 123.5 (CH), 124.0 (2CH), 125.1 (CH), 125.3 (CH), 125.4 (CH), 126.3 (CH), 127.5 (CH), 127.6 (CH), 128.4 (CH), 128.6 (CH), 128.7 (CH), 128.9 (CH), 136.8 (C), 137.8 (C), 138.1 (CH), 143.7 (C), 144.9 (C), 145.0 (C), 147.9 (C), 148.1 (C), 150.5 (C), 153.5 (C); IR (KBr) ν 696 cm^{-1} (Te=O). Found: C, 68.37; H, 3.75. Anal. Calcd. for $C_{30}H_{20}OTe$: C, 68.75; H, 3.85.

Bromination of telluride 6 with Br_2

A solution of Br_2 in CH_2Cl_2 (0.39 M, 0.5 mL, 0.20 mmol) was added to a solution of

telluride **6** (93 mg, 0.18 mmol) in CH_2Cl_2 (7 mL) at room temperature, and the mixture was stirred for 1 h in the dark. Hexane was added to the mixture to precipitate the product, and the resulting precipitates were washed with hexane and dried to give 2,4-diphenyl-5*H*-5,9b[1',2']-benzenonaphto[1,2-*b*]-tellurophene 1,1-dibromide (**8**) (115 mg, 94%): Orange crystals, mp 165 °C decomp (purified by GPC). ^{1}H NMR (400 MHz) δ 5.36 (s, 1H), 7.02–7.10 (m, 4H), 7.32–7.51 (m, 10H), 7.60–7.66 (m, 2H), 8.00–8.07 (m, 2H); ^{13}C NMR (101 MHz) δ 57.5 (CH), 79.0 (C), 123.1 (CH), 124.9 (CH), 126.2 (CH), 127.7 (CH), 127.8 (CH), 128.6 (CH), 128.9 (CH), 129.1 (CH), 129.3 (CH), 129.8 (CH), 132.9 (C), 133.0 (CH), 137.8 (C), 143.2 (C), 145.6 (C), 151.1 (C), 151.6 (C), 153.4 (C); ^{125}Te NMR (158 MHz) δ 1029.5. Found: C, 54.42; H, 3.04. Anal. Calcd for $C_{30}H_{20}Br_2Te$: C, 53.95; H, 3.02.

Synthesis of 2,4-Diphenyl-5*H*-5,9b[1',2']-benzenonaphto[1,2-*b*]dimethylsilole (9)

To a solution of **7** (25 mg, 0.048 mmol) in THF (3 mL) at −78 °C was added *t*-BuLi (1.77 M in pentane, 0.16 mL, 0.28 mmol) under argon. The mixture was stirred for 1 h at −78 °C, and dimethyldichlorosilane (0.03 mL, 0.31 mmol) was added. The mixture was stirred for 1.5 h at room temperature, and then the reaction was quenched by addition of saturated ammonium chloride solution. The mixture was extracted with CH_2Cl_2, and the extract was washed with water, dried over anhydrous Na_2SO_4, and evaporated to dryness. The residue was subjected to column chromatography (hexane/CH_2Cl_2 = 4/1) and following gel permeation chromatography to give **9** in trace: yellow crystals, ^{1}H NMR (400 MHz) δ 1.00 (s, 6H), 5.31 (s, 1H), 6.93–7.03 (m, 4H), 7.18–7.43 (m, 13H) , 7.51–7.58 (m, 2H).

3–7 References

1. a) M. R. Detty, H. R. Luss, *Organometallics* **1986**, *5*, 2250. b) K. A. Leonard, F. Zhou, M. R. Detty, *Organometallics* **1996**, *15*, 4285. c) D. E. Higgs, M. I. Nelen, M. R. Detty, *Org. Lett.* **2001**, *3*, 349, d) T. S. Butcher, M. R. Detty, *J. Org. Chem.* **1999**, *64*, 5677. d) M. Abe, M. R. Detty, O. O. Gerlits, D. K. Sukumaran, *Organometallics* **2004**, *23*, 4513. e) B. Zhang, W. Hou, X. Ye, S. Fu, Y. Xie, *Adv. Funct. Mater.* **2007**, *17*, 486. f) L. Manna, D. J. Milliron, A. Meisel, E. C. Scher, A. P. Alivisatos, *Nat. Mater.* **2003**, *2*, 382. g) J. Chu, X. Li, P. Xu, *J. Mater. Chem.* **2011**, *21*, 11283. h) S. A. Gamboa, P. J. Sebastian, X. Mathew, H. Nguyen-Cong, P. Chartier, *Sol. Energy Mater. Sol. Cells* **1999**, *59*, 115. i) A. M. Smith, S. Nie, *Acc. Chem. Res.* **2010**, *43*, 190.

2. a) Y. Narita, I. Hagiri, N. Takahashi, K. Takeda, *Jpn. J. Appl. Phys. 1* **2004**, *43*, 4248. b) Y. Narita, K. Takeda, *Jpn. J. Appl. Phys. 1* **2006**, *45*, 2628. c) A. Muranaka, S. Yasuike, C. Y. Liu, J. Kurita, N. Kakusawa, T. Tsuchiya, M. Okuda, N. Kobayashi, Y. Matsumoto, K. Yoshida, D. Hashizume, M. Uchiyama, *J. Phys. Chem. A* **2009**, *113*, 464.

3. a) R. D. McCullough, G. B. Kok, K. A. Lerstrup, D. O. Cowan, *J. Am. Chem. Soc.* **1987**, *109*, 4115. b) M. Bendikov, F. Wudl, D. F. Perepichka, *Chem. Rev.* **2004**, *104*, 4891. c) F. Wudl, E. Aharon-Shalom, *J. Am. Chem. Soc.* **1982**, *104*, 1154.

4. a) A. A. Jahnke, G. W. Howe, D. S. Seferos, *Angew. Chem. Int. Ed.* **2010**, *49*, 10140. b) T. M. McCormick, A. A. Jahnke, A. J. Lough, D. S. Seferos, *J. Am. Chem. Soc.* **2012**, *134*, 3542.

5. a) G. Zeni, D. S. Lüdtke, R. B. Panatieri, A. L. Braga, *Chem. Rev.* **2006,** *106*, 1032. b) M. J. Dabdoub, V. B. Dabdoub, M. A. Pereira, *J. Org. Chem.* **1996,** *61*, 9503. c) M. J. Dabdoub, A. Justino, P. G. Guerrero Jr., *Organometallics* **1998,** *17*, 1901. d) C. C.

Schneider, H. Caldeira, B. M. Gay, D. F. Back, G. Zeni, *Org. Lett.* **2010**, *12*, 936.

6. Y. Mizuhata, T. Sasamori, N. Takeda, N. Tokitoh, *J. Am. Chem. Soc.* **2006**, *128*, 1050.

7. K. N. Solov'ev, E. A. Borisevich, *Phys.-Usp.* **2005**, *48*, 231.

8. M. Zander, G. Kirsch, *Z. Naturforsch.* **1989**, *44a*, 205.

9. N. Hayashi, Y. Saito, H. Higuchi, K. Suzuki, *J. Phys. Chem. A* **2009**, *113*, 5342.

10. B. Wex, B. R. Kaafarani, E. O. Danilov, D. C. Neckers, *J. Phys. Chem. A* **2006**, *110*, 13754.

11. a) K. Takimiya, Y. Konda, H. Ebata, N. Niihara, T. Otsubo, *J. Org. Chem.* **2005**, *70*, 10569. b) B. Wex, B. R. Kaafarani, E. O. Danilov, D. C. Neckers, *J. Phys. Chem. A* **2006**, *110*, 13754.

12. M. W. Kryman, G. A. Schamerhorn, J. E. Hill, B. D. Calitree, K. S. Davies, M. K. Linder, T. Y. Ohulchanskyy, M. R. Detty, *Organometallics* **2014**, *33*, 2628.

13. H. Dreeskamp, E. Koch, M. Zander, *Chem. Phys. Lett.* **1975**, *31*, 251.

14. M. Zander, *Z. Naturforsch.* **1989**, *44a*, 1116.

15. a) Y. Koide, M. Kawaguchi, Y. Urano, K. Hanaoka, T. Komatsu, M. Abo, T. Terai, T. Nagano, *Chem. Commun.* **2012**, *48*, 3091. b) M. W. Kryman, G. Schamerhorn, K. Yung, B. Sathyamoorthy, D. Sukumaran, T. Y. Ohulchanskyy, J. B. Benedict, M. R. Detty, *Organometallics* **2013**, *32*, 4321.

16. a) T. M. McCormick, E. I. Carrera, T. B. Schon, D. S. Seferos, *Chem. Comm.* **2013**, *49*, 11182. b) M. Kaur, D. S. Yang, K. Choi, M. J. Cho, D. H. Choi, *Dyes Pigm.* **2014**, *100*, 118.

17. A. Ishii, Y. Yamaguchi, N. Nakata, *Org. Lett.* **2011**, *13*, 3702.

18. Y. Yamaguchi, N. Nakata, A. Ishii, *Eur. J. Inorg. Chem.* **2013**, 5233.

19. A. Ishii, T. Annaka, N. Nakata, *Chem. Eur. J.* **2012**, *18*, 6428.

20. R. E. Stratmann, G. E. Scuseria, M. J. Frisch, *J. Chem. Phys.* **1998**, *109*, 8218.

21. R. Bauernschmitt, R. Ahlrichs, *Chem. Phys. Lett.* **1996**, *256*, 454.

22. M. E. Casida, C. Jamorski, K. C. Casida, D. R. Salahub, *J. Chem. Phys.* **1998**, *108*, 4439.

23. M. J. Frisch, G. W. Trucks, H. B. Schlegel, G. E. Scuseria, M. A. Robb, J. R. Cheeseman, G. Scalmani, V. Barone, B. Mennucci, G. A. Petersson, H. Nakatsuji, M. Caricato, X. Li, H. P. Hratchian, A. F. Izmaylov, J. Bloino, G. Zheng, J. L. Sonnenberg, M. Hada, M. Ehara, K. Toyota, R. Fukuda, J. Hasegawa, M. Ishida, T. Nakajima, Y. Honda, O. Kitao, H. Nakai, T. Vreven, J. A. Montgomery Jr., J. E. Peralta, F. Ogliaro, M. Bearpark, I. J. Heyd, E. Brothers, K. N. Kudin, V. N. Staroverov, T. Keith, R. Kobayashi, J. Normand, K. Raghavachari, A. Rendell, J. C. Burant, S. S. Iyengar, J. Tomasi, M. Cossi, N. Rega, J. M. Millam, M. Klene, J. E. Knox, J. B. Cross, V. Bakken, C. Adamo, J. Jaramillo, R. Gomperts, R. E. Stratmann, O. Yazyev, A. J. Austin, R. Cammi, C. Pomelli, J. W. Ochterski, R. L. Martin, K. Morokuma, V. G. Zakrzewski, G. A. Voth, P. Salvador, J. J. Dannenberg, S. Dapprich, A. D. Daniels, O. Farkas, J. B. Foresman, J. V. Ortiz, J. Cioslowski, D. J. Fox, Gaussian 09, revision D.01; Gaussian, Inc.: Wallingford, CT, 2013.

24. K. -y. Akiba, In Organo Main Group Chemistry, John Wiley & Sons, Hoboken, New Jersey, 2011, p. 33.

25. a) E. J. Bowen, B. A. Sahu, *J. Phys. Chem.* **1959**, *4*, 63. b) W. R. Ware, R. A. Baldwin, *J. Chem. Phys.* **1965**, *43*, 1194, c) R. G. Bennett, P. J. McCartin, *J. Chem. Phys.* **1966**, *44*, 1969.

26. a) K. Hamanoue, T. Nakayama, K. Ikegaya, K. Ibuki, *J. Photochem. Photobiol. A: Chem.* **1993**, *74*, 147. b) G. Favaro, M. R. di Nunzio, P. L. Gentili, A. Romani, R. S. Becker, *J. Phys. Chem. A* **2007**, *111*, 5948. c) K. Hamanoue, S. Tai, T. Hidaka, T.

Nakayama, M. Kimoto, H. Teranishi, *J. Phys. Chem.* **1984**, *88*, 4380.

27. G. M. Sheldrick, SHELXL-97, Program for Crystal Structure Refinement; University of Göttingen: Göttingen, Germany, 1997.

Chapter 4

Reversible and Turn-on Fluorescent Probes for Hydrogen Sulfide via redox cycle between Selenide and Selenoxide

4–1 Introduction

Hydrogen sulfide (H_2S) is well-known for repugnant rotten egg smell and as a toxic gas. On the other hand, H_2S has been discovered as the third gaseous transmitter such as nitric oxide and carbon monoxide.[1] H_2S is generated from enzymatic processes in mammalian organs and tissues, including relaxation of vascular smooth muscles, mediation of neurotransmission, inhibition of insulin signaling, and regulation of inflammation and O_2 sensing.[3–6] Previous studies have shown that H_2S affects the cardiovascular functions, central nervous systems, and energy metabolism.[7] Abnormal levels of H_2S can cause disease such as gastric mucosal injury, liver cirrhosis, and Alzheimer's disease.[8–10]

Currently, the major detections for H_2S were colorimetric and electrochemical analysis, gas chromatography, and sulfide precipitation.[11–14] However, these methods gave variable results owing to the rapid catabolism of H_2S. In contrast to these detection technologies, the nondestructive fluorescent analysis offers advantages with higher sensitivity, quantitativity, and selectivity in situ observation. Recently, fluorescent probes for H_2S have been reported, utilizing the reactions such as a) reduction of azide, b) nucleophilic reaction, and c) precipitation of copper sulfide (Scheme 1).[15–17] These reaction-based probes reveal good sensing abilities for H_2S with turn-on fluorescence, but do not have reversibility to non-fluorescence. On the other hand, fluorescent on-off redox systems (selenide/selenoxide) were developed between hypochlorous acid (HClO) and H_2S.[18] Non-fluorescent selenide is oxidized with HClO selectively, and following selective reduction with H_2S underwent.

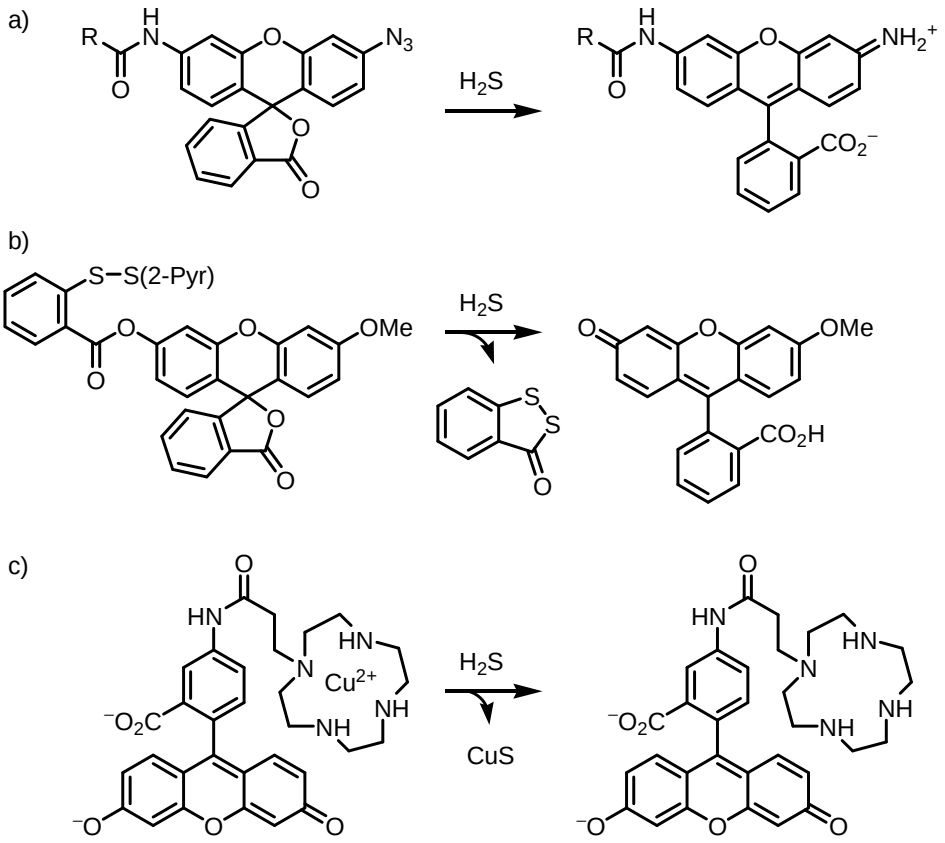

Scheme 1. Fluorescent probes for H_2S based on a) reduction of azide, b) nucleophilic reaction, and c) precipitation of copper sulfide.

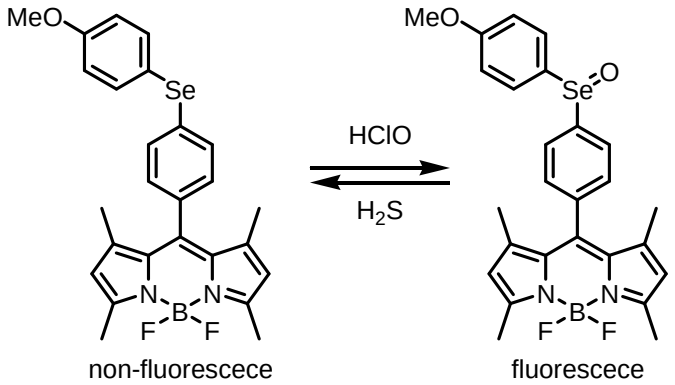

Scheme 2. Selenide/selenoxide redox cycle between HClO oxidation and H_2S repair.

Endogenous HClO is an important member of reactive oxygen species (ROS), which has been known to be essential for several biological functions, and produced from H_2O_2 and Cl^- by the enzyme myeloperoxidase.[19–21] In cells, HClO works as an antibacterial species killing a wide range of pathogens, however, excess HClO causes critical oxidative stress to cholesterol, fatty acid groups, proteins, DNA, and RNA.[22]

A few reversible fluorescent probes for redox process and turn-on fluorescent probes for H_2S have been reported individually,[23] but fluorescent probe possessing both properties has not been established yet. We have already discovered selenide/selenoxide redox cycle between MCPBA oxidation of 1,2-bis(methoxycarbonyl)-1-seleno-1,3-butadiene derivative **1** and PPh_3 reduction of corresponding selenoxide **2** (Scheme 3).[24] **1** showed strong fluorescence in contrast to weak fluorescence of **2** [**1**: $\Phi_F(CH_2Cl_2) = 0.86$, **2**: $\Phi_F(CH_2Cl_2) = 0.03$]. However, this redox cycle has a few problems; low reactivity in the oxidation of **1** owing to the two electrophilic methoxycarbonyl groups, and instability of selenoxide **2**.

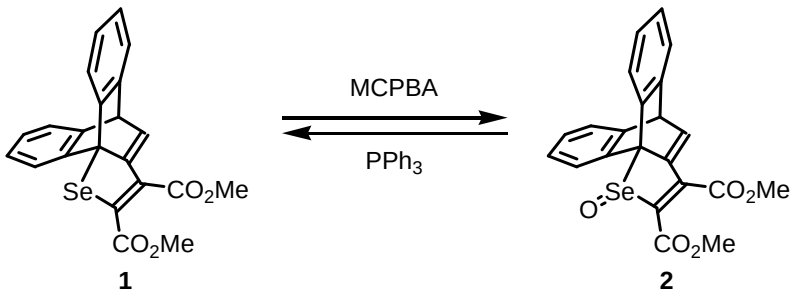

1 **2**

Scheme 3. Redox cycle between 1,2-di(methoxycarbonyl)-1-seleno-1,3-butadiene derivative **1** and its oxide **2**.

Meanwhile, we also developed the convenient synthesis of 1,4-diphenyl-1-seleno-1,3-butadiene derivatives **3** and **4** incorporated in a dibenzobarrelene (Dbb) and benzobarrelene (Bb), respectively.[25] Herein, we report turn-on type fluorescent probes for H_2S induced by redox cycles between selenides, **3** and **4**, and corresponding selenoxides, **5** and **6**, which also possess high sensitivity, quantitativity, and selectivity, and reversibility by the oxidation with HClO (Scheme 4).

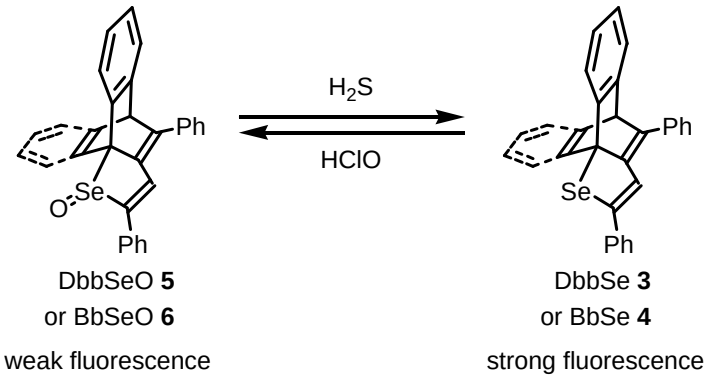

Scheme 4. Fluorescent probes for H_2S/HClO induced by the redox cycles between 1,4-diphenyl-1-seleno-1,3-butadiene derivatives, **3** and **4**, and their oxides, **5** and **6**.

4–2 Syntheses and Structures of 1,4-Diphenyl-1-seleno-1,3-butadiene 1-Oxides

First of all, we examined the synthesis of selenoxides **5** and **6** by the oxidation of selenides **3** and **4** with MCPBA to give **5** and **6** in high yields (Scheme 5). Both fluorescences of **5** and **6** were diminished in comparison with those of **3** and **4**.

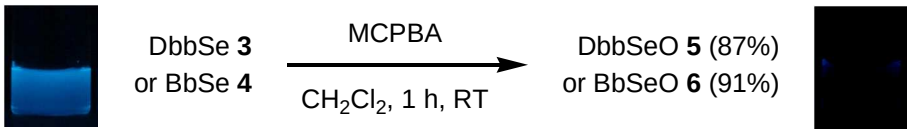

Scheme 5. Oxidation of selenides **3** and **4** with the pictures of 1:1 CH_3CN/H_2O solution of DbbSe **3** and DbbSeO **5** under irradiation of 365 nm light.

The structures of **5** and **6** were determined by spectroscopic methods and X-ray crystallography (Figure 1 and 2). The 1,3-butadiene moieties (C2–C3–C4–C5) in **5** and **6** are almost planar and the bond lengths are in similar ranges except for those of carbon–selenium bonds in comparison with those of **3** [**5**: C1–Se1: 1.988(3), Se1–C2: 1.942(3), **3**: C1–Se1: 1.9613(18), Se1–C2: 1.9226(19)].

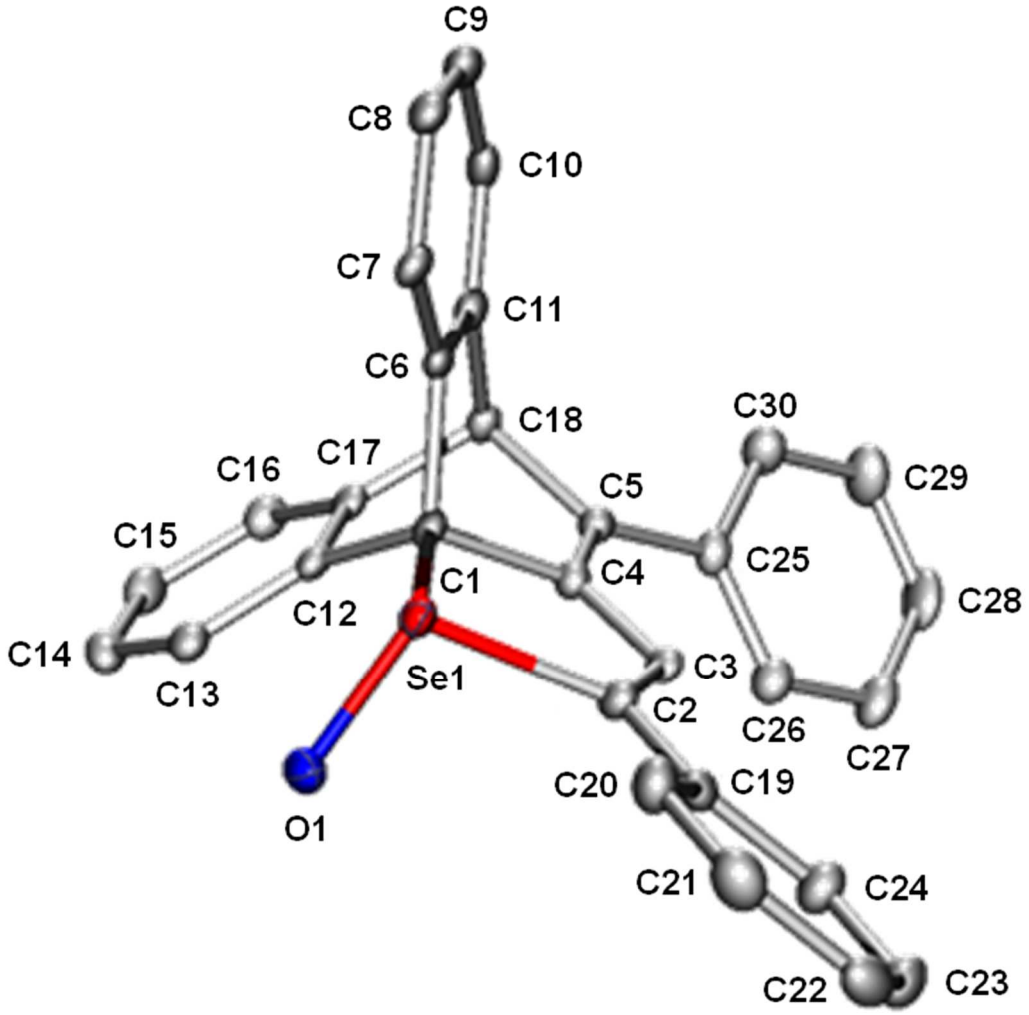

Figure 1. ORTEP drawing of DbbSeO **5** with 50% probability ellipsoids. Selected bond length (Å) and torsion angles (°): O1–Se1: 1.672(2), C1–Se1: 1.988(3), Se1–C2: 1.942(3), C2–C3: 1.339(4), C3–C4: 1.440(4), C1–C4: 1.536(4), C4–C5: 1.346(4), C2–C3–C4–C5: 173.2(3), C3–C2–C19–C24: 19.6(5), C4–C5–C33–C38: 36.8(5). *Crystal data*: $C_{30}H_{20}OSe \bullet C_2H_2Cl_6$, M_W = 714.16, monoclinic, space group $P2_1/c$, Z = 2, a = 10.3946(6), b = 11.3394(7), c = 12.8696(8) Å, α = 90.7040(10)°, β = 98.331(2)°, γ = 92.8220(10)°, V = 1498.80(16) Å^3, $D_{calcd.}$ = 1.582 g cm^{-3}, R_1 [$I > 2\sigma(I)$] = 0.0463, wR_2 (all data) = 0.1196 for 10230 reflections, 597 parameters, GOF = 1.011.

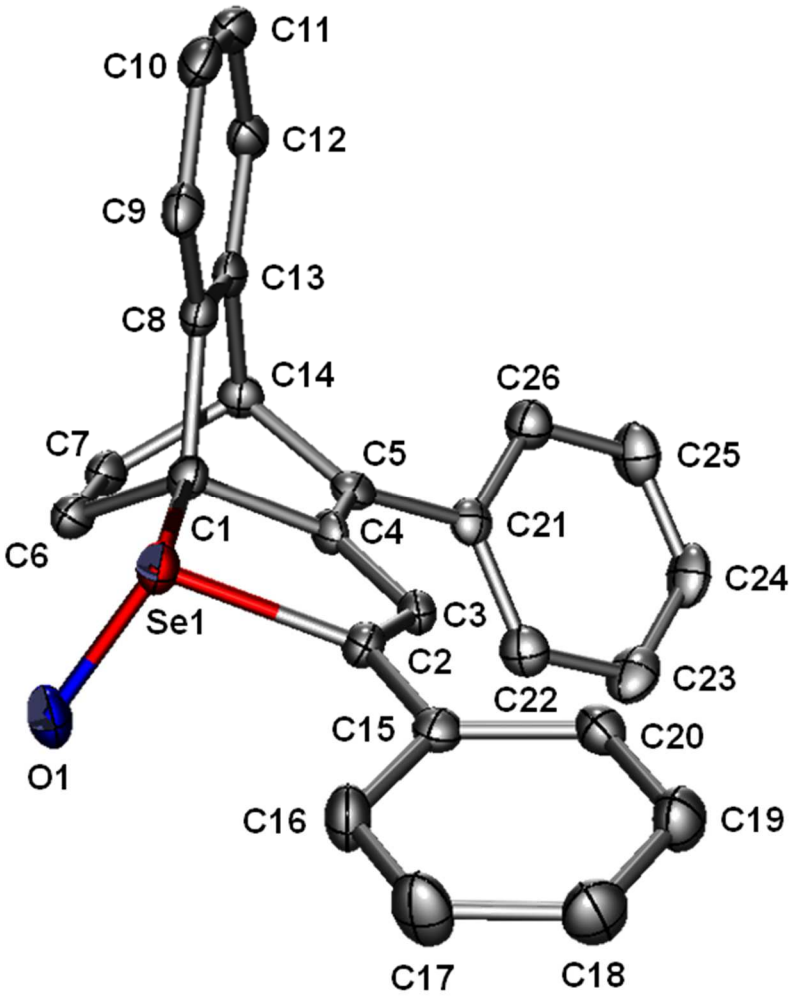

Figure 2. ORTEP drawing of BbSeO **6** with 50% probability ellipsoids. Selected bond length (Å) and torsion angles (°): O1–Se1: 1.675(2), C1–Se1: 1.979(3), Se1–C2: 1.945(3), C2–C3: 1.345(5), C3–C4: 1.437(5), C1–C4: 1.527(5), C4–C5: 1.334(5), C2–C3–C4–C5: 179.0(4), C3–C2–C15–C20: 27.4(6), C4–C5–C21–C26: 41.8(5). *Crystal data*: $C_{26}H_{18}OSe•O$, M_W = 441.36, monoclinic, space group $P2_1$, Z = 2, a = 0.1234(6), b = 12.7495(8), c = 9.6022(6) Å, β = 116.3210(10)°, V = 1001.12(11) Å^3, $D_{calcd.}$ = 1.464 g cm^{-3}, R_1 [$I > 2\sigma(I)$] = 0.0330, wR_2 (all data) = 0.0745 for 5806 reflections, 597 parameters, and 1 restraints for O, GOF = 1.038.

As shown in Figure 3 of DbbSe **3** and Figure 4 of DbbSeO **5**, **5** formed dimeric structure in crystalline owing to two intermolecular n(O)–σ*(Se–C) orbital interactions in contrast to the observation of several CH–π interactions in **3**.[26] A close packing structure of BbSeO **6** was formed in the crystal through a CH–π interaction of H3–benzene ring painted in yellow, and three hydrogen-bondings between oxygen and H12, H14, and H26, respectively (Figure 5).

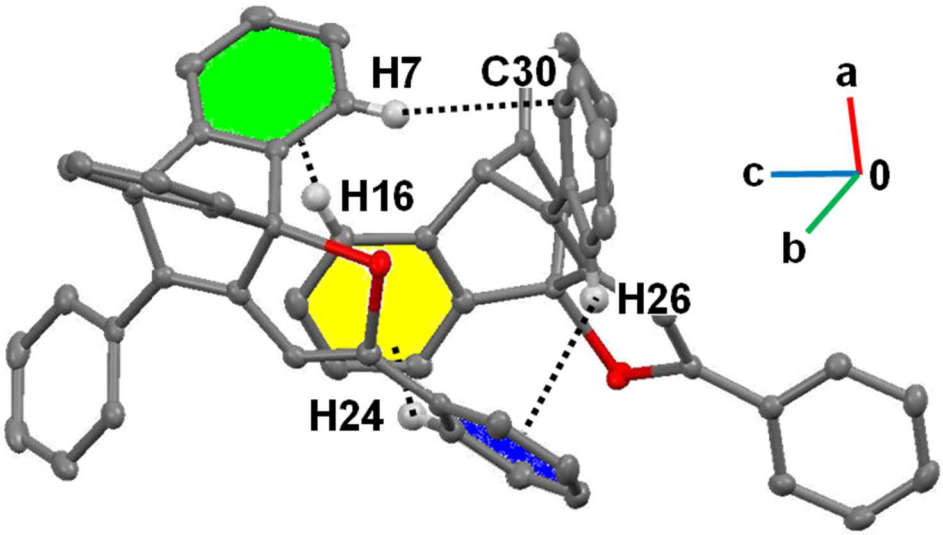

Figure 3. Crystal packing of DbbSe **3**: H7–C30: 2.834 Å, H16–benzene ring A (green): 2.823 Å, H24–benzene ring B (yellow): 2.763 Å, H26–benzene ring C (blue): 2.758 Å.

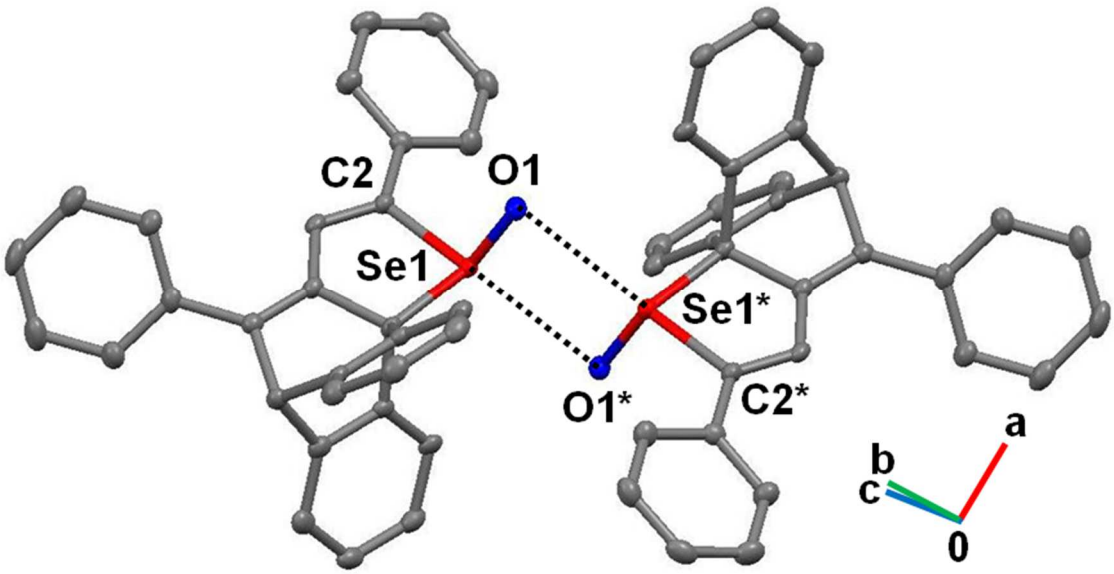

Figure 4. Crystal packing of DbbSeO **5**: O1–Se1*: 2.968 Å.

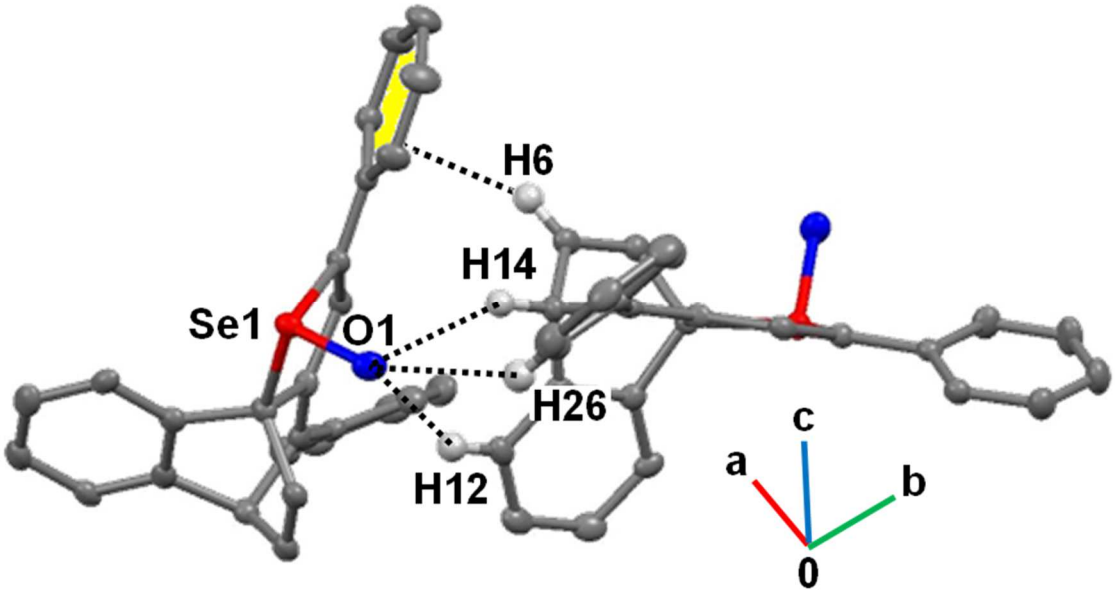

Figure 5. Crystal packing of BbSeO **6**: O1–H12: 2.663 Å, O1–H14: 2.596 Å, O1–H26: 2.627 Å, H6–benzene ring (yellow): 2.728 Å.

4–3 Photophysical Properties of 1,4-Diphenyl-1-seleno-1,3-butadienes

Photophysical properties of **3**–**6** were studied in dilute CH_2Cl_2, CH_3CN, 1:1 CH_3CN/H_2O solutions (10^{-5} M), and in the solid state, listed in Table 1, 2, and Figure 6. Absorption maxima of selenoxides **5** and **6** were shifted hypsochromically with drastic fluorescent quenching in solution. Fluorescence wavelengths of selenoxides **5** and **6** in CH_3CN/H_2O were red-shifted in comparison with those in CH_3CN owing to hydrogen-bonding interactions to H_2O. In CH_3CN/H_2O, fluorescence quantum yields of DbbSe **3** and BbSe **4** are 13- and 143-folds higher than those of corresponding selenoxides **5** and **6**, respectively, indicating that these redox cycles revealed large fluorescent on-off character. Solid-state fluorescence quantum yields of **3**–**5** were lower than those in solution owing to the strong intermolecular interactions as shown in Figure 3 and 4. In contrast, fluorescence of BbSeO **6** in the solid state was enhanced to 0.21 comparing to those in organic solvents. These results were attributed to a crystallization-induced emission (CIE)[27] as observed in BbSO, sulfur analogue of **6**.[25]

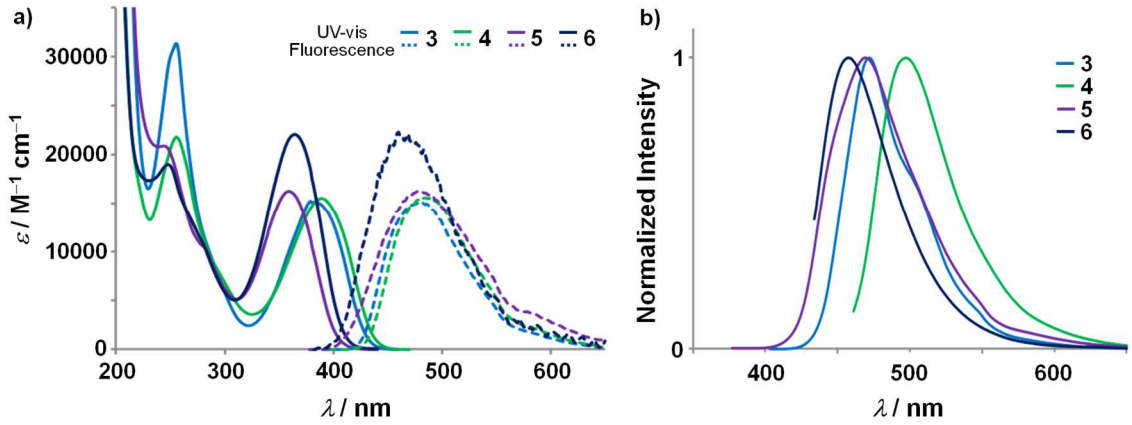

Figure 6. a) UV-vis and fluorescence spectra of **3**–**6** in 1:1 CH_3CN/H_2O and b) in the solid state.

Table 1. Photophysical Properties of DbbSe **3** and DbbSeO **5**.[a]

	Compound	λ_{abs} [nm]	ε [$M^{-1}cm^{-1}$]	λ_{em} [nm][b]	$\Phi_F^{b,d,f}$	$\Phi_F^{b,e,f}$
3	CH_2Cl_2	384	16000	479	1.00	–
	CH_3CN	382	15300	479	1.00	0.83
	CH_3CN/H_2O (1:1)	383	15200	480	–	0.89
	solid	–	–	472	–	0.22[c]
5	CH_2Cl_2	357	16900	457	0.34	–
	CH_3CN	355	14800	457	0.24	0.24
	CH_3CN/H_2O (1:1)	359	16300	480	–	0.07
	solid	–	–	469	–	0.03[c]

a) All solutions were adjusted at 10^{-5} M. b) Exited at respective absorption maxima. c) Exited at respective excited maxima. d) Under argon. e) Under air. f) Absolute fluorescence quantum yields were determined by using a calibrated integrating sphere system..

Table 2. Photophysical Properties of BbSe **4** and BbSeO **6**.[a]

	Compound	λ_{abs} [nm]	ε [$M^{-1}cm^{-1}$]	λ_{em} [nm][b]	$\Phi_F^{b,d,f}$	$\Phi_F^{b,e,f}$
4	CH_2Cl_2	391	15700	475	1.00	–
	CH_3CN	389	15500	485	1.00	0.74
	CH_3CN/H_2O (1:1)	389	15600	484	–	0.86
	solid	–	–	475	–	0.27[c]
6	CH_2Cl_2	362	22000	455	0.017	–
	CH_3CN	360	22000	451	0.007	0.006
	CH_3CN/H_2O (1:1)	364	22100	463	–	0.006
	solid	–	–	458	–	0.21[c]

a) All solutions were adjusted at 10^{-5} M. b) Exited at respective absorption maxima. c) Exited at respective excited maxima. d) Under argon. e) Under air. f) Absolute fluorescence quantum yields were determined by using a calibrated integrating sphere system.

Since there are large difference between fluorescence of selenides and selenoxides, we next carried out the adjustment of the ratio of mixed solvents (Figure 6). In the case of selenides **3** and **4**, fluorescent intensities were increased slightly as addition of H_2O by 50%, following continuous addition lowered intensities owing to aggregation. In contrast, the intensities of selenoxides **5** and **6** decreased immediately after addition of H_2O, resulting that 1:1 ratio leads largest fluorescent difference between selenide and selenoxide (Figure 7).

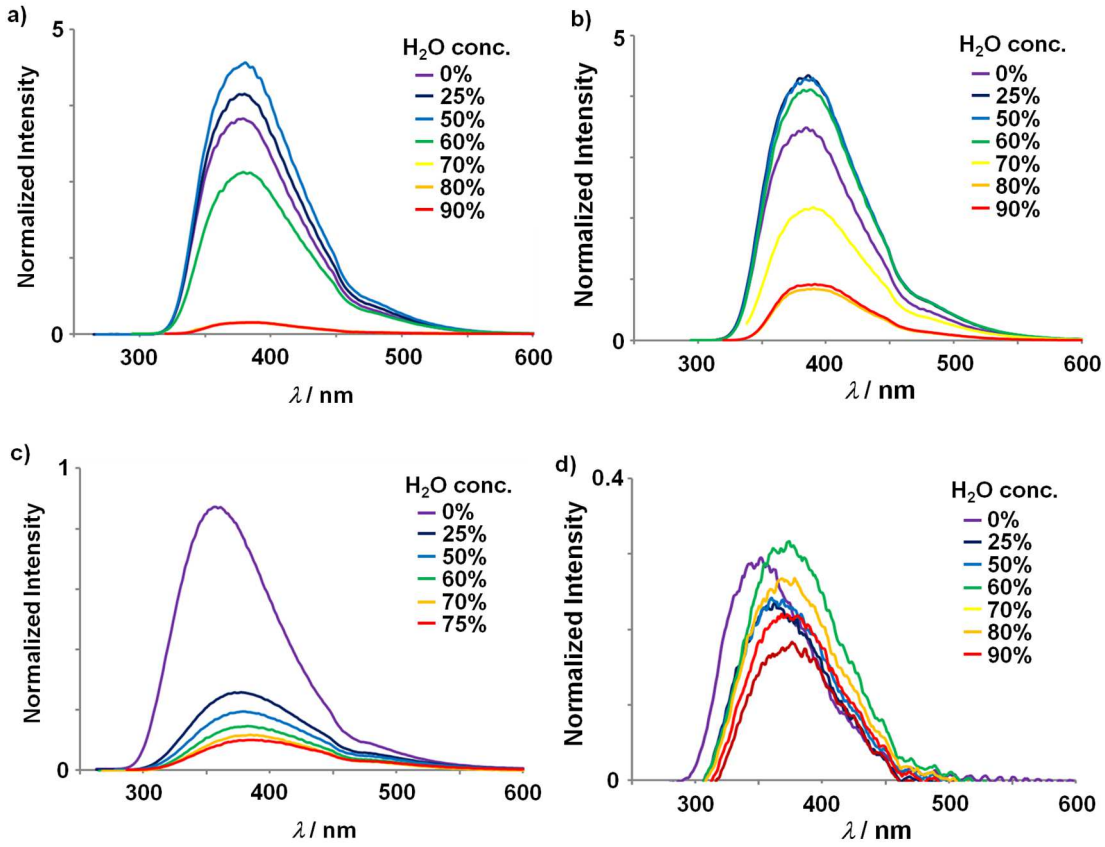

Figure 7. Fluorescence spectra of a) DbbSe **3**, b) BbSe **4**, c) DbbSeO **5**, and d) BbSeO **6** in CH_3CN/H_2O

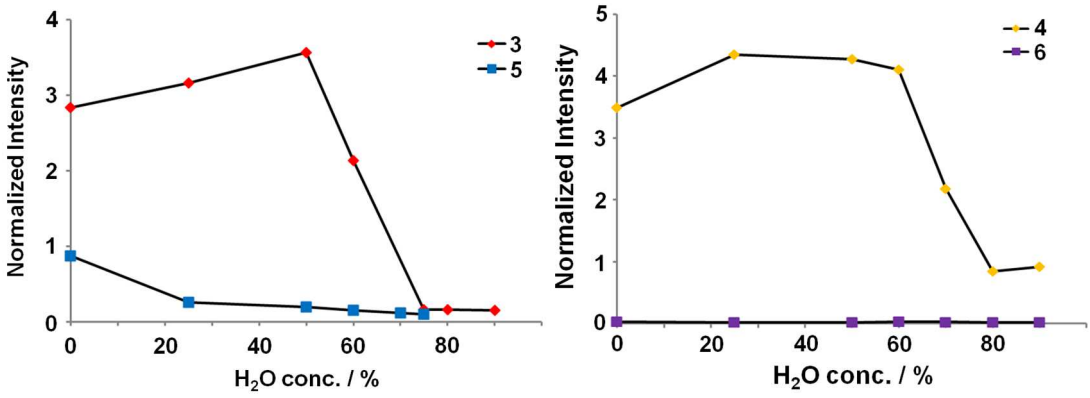

Figure 8. The titration curves of fluorescent intensity of **3** and **5** (left) and **4** and **6** (right) plotted against the solvent composition at fluorescence maxima.

4–4 Sensing Abilities

The probe for H_2S demands sensitivity, and selectivity for other biothiols especially for L-cysteine (Cys) and reduced gulthathione (GSH). To elucidate both characters, we examined the reductions of **5** and **6** with reductants such as H_2S (using NaHS as an equivalent), Cys, and GSH in 10 mM pH 7.4 phosphate buffer saline (PBS) including 50% CH_3CN under several conditions (Scheme 6).

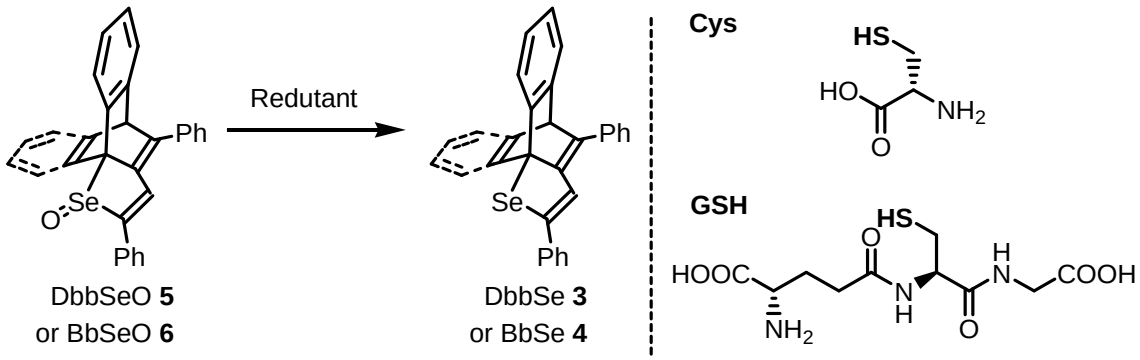

Scheme 6. Reductions of selenoxides **5** and **6**.

Plausible reduction of selenoxide requires the use of 2 equivalents thiol.[28] As displayed in Table 3, the reductions of DbbSeO **5** underwent immediately and quantitatively under using 2 equivalents NaHS (Run 1), and the solutions of reaction mixture showed strong fluorescence after addition of NaHS quite quickly. However, the yields of reduction using equilibrium NaHS were 60% and 80% in Run 2 and 3, respectively, indicating that the rest of selenoxide was reduced by sulfur byproducts. On the other hand, reduction was not affected by the concentration of selenoxide, solvent ratio, and temperature (Run 4–6).

Table 3. Reaction screenings in the reaction of BbSeO **5** and BbSeO **6** with NaHS.

Run	Conc. [M]	NaHS [eq.]	PBS [%]	Temp.	Time [h]	Yield [%]
1	2.3×10^{-4}	2	50	RT	0.5	100
2	2.3×10^{-4}	1	50	RT	0.5	60
3	2.3×10^{-4}	1	50	RT	16	80
4	2.7×10^{-4}	1	50	40 ºC	0.5	62
5	2.3×10^{-4}	1	25	RT	0.5	74
6	2.3×10^{-3}	1	25	RT	0.5	75

The reaction yields using Cys and GSH deceased in comparison with the rapid reduction by NaHS as shown in Table 4. There are two reasons to generate selectivity. The first one is pKa of thiol group in reductants (Cys: 8.3, GSH: 9.0).[28,29] They are hard to ionize under neutral condition, leading to lower reactivity than that of NaHS. The other is the bulkiness of selenoxides and thiols. Their reactivity were lowered as the bulkiness around sulfur in reductant become larger, and the selectivity of BbSeO **6** also decreased comparing with bulkier DbbSeO **5**. As considering reactivity and selectivity are dependent on bulkiness of thiols and selenoxides, we presumed the reaction mechanism of reduction of selenoxide shown in scheme 5. An intermediate in the reaction of dibenzobarrelene derivative has two steric hindrances between *o*-position proton of benzene rings in dibenzobarrelene skeleton and substituents, -SR and -OH, on selenium atom, leading to decrease reactivity and generate following selectivity.

Table 4. NMR yields of 230 μM selenides **3** and **4** in the reactions of selenoxides **5** and **6** with 2 equivalents biothiols

	Reductant	Yield [%]		Reductant	Yield [%]
	NaHS	100		NaHS	100
DbbSeO **5**	Cys	36	BbSeO **6**	Cys	54
	GSH	8		GSH	18

*The reactions were carried out in 10 mM pH 7.4 PBS containing 50% CH_3CN within 30 min at room temperature

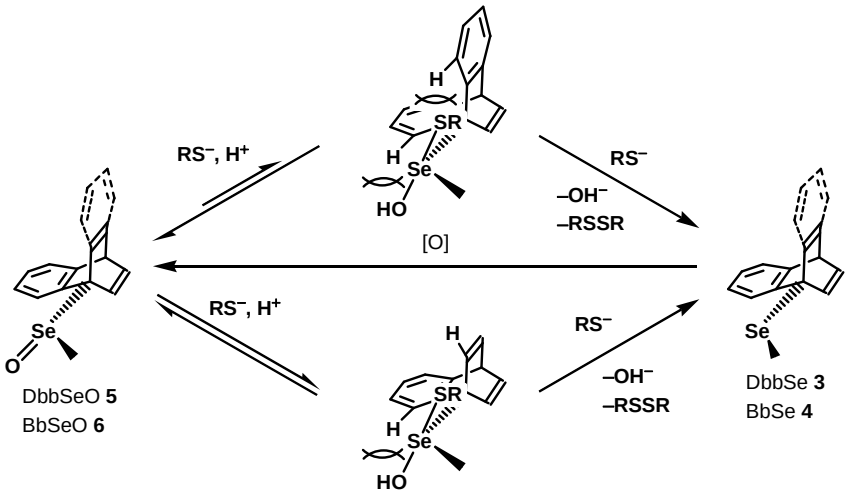

Scheme 5. Plausible mechanism of redox cycles between selenoxide and selenide.

We measured spectroscopy to study sensing ability of selenoxides **5** and **6**. As shown in Figure 9 and 10, additions of 50–300 μM NaHS to the 50 μM CH_3CN/PBS (1:1) solution of **5** and **6** led to increase the longest wavelength absorbance of selenides **3** (383 nm) and **4** (389 nm) in UV-vis spectra and the intensities in fluorescence spectra at 480 nm and 483 nm, respectively, with [NaHS] being dense.

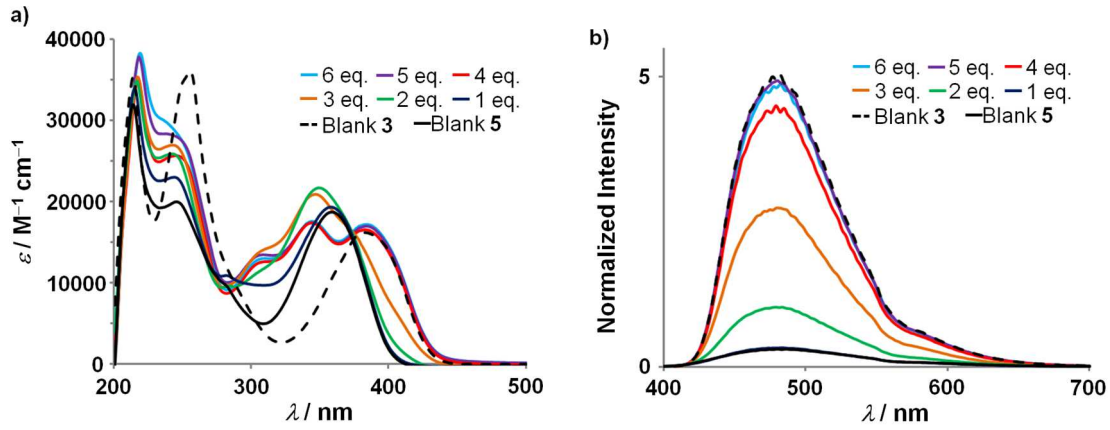

Figure 9. a) UV-vis and b) fluorescence spectra monitoring the reactions of 50 μM DbbSeO **5** with 50–300 μM NaHS in 10 mM pH 7.4 PBS containing 50% CH_3CN with excitation at 383 nm at 30 min

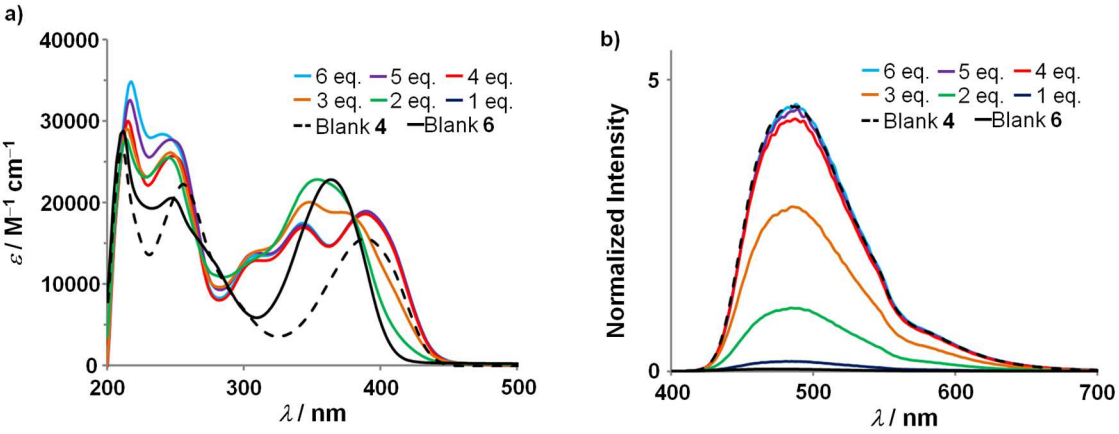

Figure 10. a) UV-vis and b) fluorescence spectra monitoring the reactions of 50 μM BbSeO **6** with 50–300 μM NaHS in 10 mM pH 7.4 PBS containing 50% CH_3CN with excitation at 389 nm at 30 min.

Fluorescence intensity was observed with naked eyes brightly and acquired a constant value in approximately 15 min for each concentration of NaHS (Figure 11a and 12a). In

addition, there was good linearity of fluorescent intensity against [NaHS] among 1–4 equivalent at 30 min, and regression equations were F_{max} = 1.42 × [NaHS] – 1.40 (R2 = 0.97) for DbbSeO **5** and F_{max} = 1.41 × [NaHS] – 1.43 (R2 = 0.99) for BbSeO **6** (Figure 11b and 12b). The selectivity of DbbSeO **5** was tested within 15 min, resulting weak or no fluorescence in the reactions with Cys and GSH, respectively (Figure 13a). In contrast, the fluorescent intensities in the reaction of BbSeO **6** with Cys and GSH increased earlier than that of **5**, demonstrating that higher selectivity of **5** is induced by the bulkiness of the selenoxide and thiol. These results showed good sensitivity, quantitativity, and selectivity of DbbSeO **5** as fluorescent probe for H_2S under simulated physiological conditions.

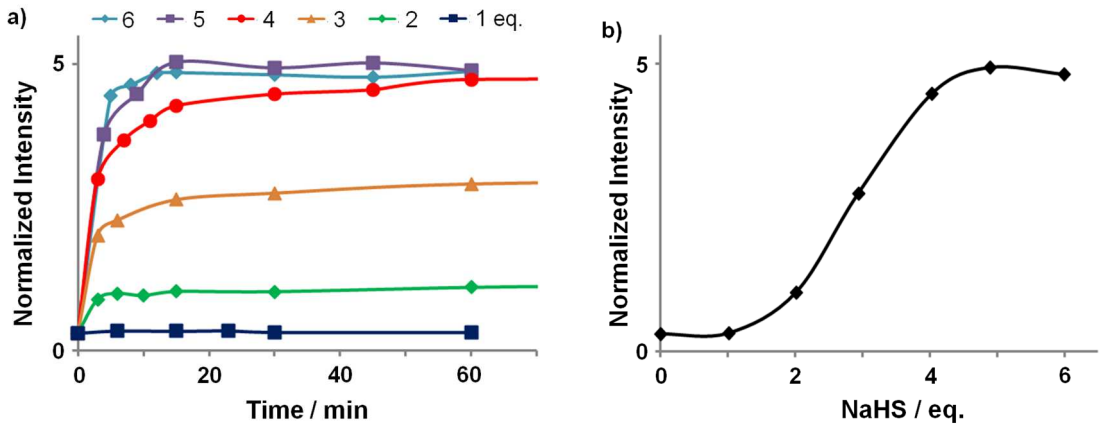

Figure 11. a) Kinetic profiles of the reaction of 50 μM DbbSeO **5** with 50–300 μM NaHS, observed by fluorescent intensity at 480 nm. b) The titration curve plotted by fluorescent intensity at 480 nm after 30 min.

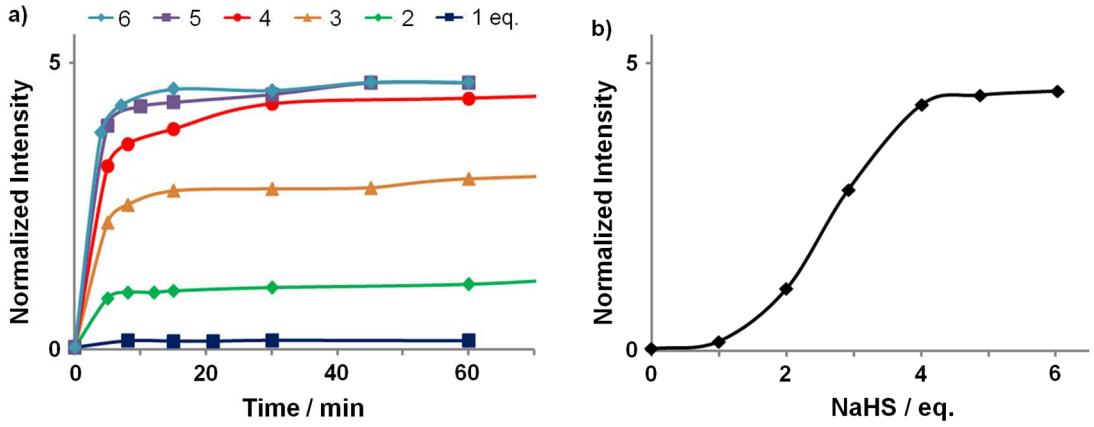

Figure 12. a) Kinetic profiles of the reaction of 50 μM BbSeO **6** with 50–300 μM NaHS, observed by fluorescent intensity at 483 nm. b) The titration curve plotted by fluorescent intensity at 483 nm after 30 min.

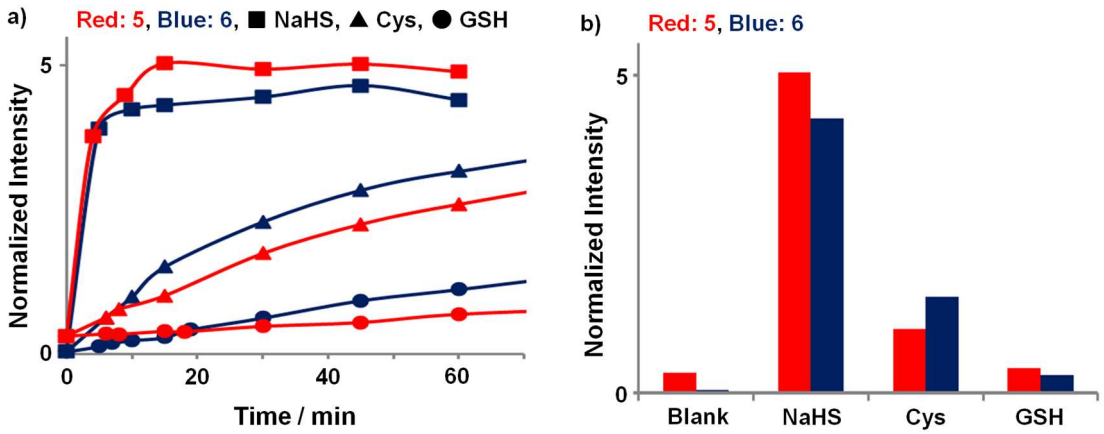

Figure 13. a) Kinetic profiles of the reaction of 50 μM selenoxides **5** (red) and **6** (blue) with 250 μM NaHS (■), Cys (▲), and GSH (●) observed by fluorescent intensity at 480 nm. b) Comparison of the fluorescence intensity of **5** (red) and **6** (blue) with the addition of different reductants after 15 min.

To construct the redox cycle, we examined oxidation of 50 μM DbbSe **3** with HClO (using NaClO as the equivalent), H_2O_2, *t*-BuO_2H, and $ONOO^-$ (prepared by the reaction of isoamylnitrite with H_2O_2 under basic condition)[30] in 10 mM pH 7.4 PBS containing 50% CH_3CN. The NaClO oxidations underwent immediately and quantitatively [F_{max} = −1.18 × [NaClO] + 4.97 (R2 = 0.997)] with fluorescent disappearing shown in Figure 14. In the cases of H_2O_2, *t*-BuO_2H, and $ONOO^-$, solutions kept emitting strongly without fluorescent quenching within 15 min (Figure 15), indicating good selectivity in oxidation pathway. Addition of NaClO after the reduction of DbbSeO **5** with 250 μM H_2S also gave a linear relationship [F_{max} = −1.11 × [NaClO] + 14.6 (R2 = 0.990)] between fluorescent intensity and NaHS equivalence (Figure 16). These results suggested that the probe DbbSeO **5** could be applied to monitor the redox cycle between H_2S reduction and HClO oxidation.

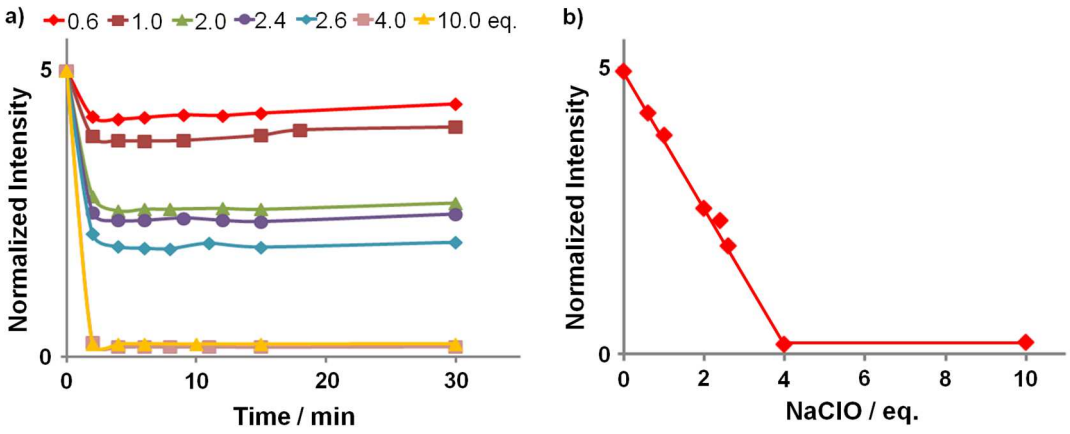

Figure 14. a) Kinetic profiles of the reaction of 50 μM DbbSe **3** with 30–500 μM NaClO, observed by fluorescent intensity at 480 nm. b) The titration curve plotted by fluorescent intensity at 480 nm after 15 min.

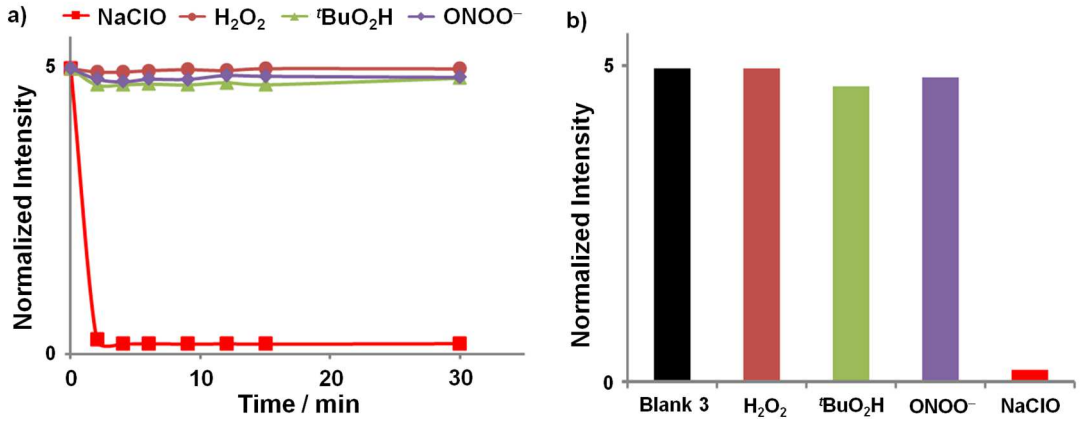

Figure 15. a) Kinetic profiles of the reaction of 50 μM DbbSe **3** with 200 μM NaClO (■), H_2O_2 (●), $^tBuO_2H$ (▲), and $ONOO^-$ (◆) observed by fluorescent intensity at 480 nm. b) Comparison of the fluorescence intensity of DbbSe **3** with the addition of different oxidant after 15 min.

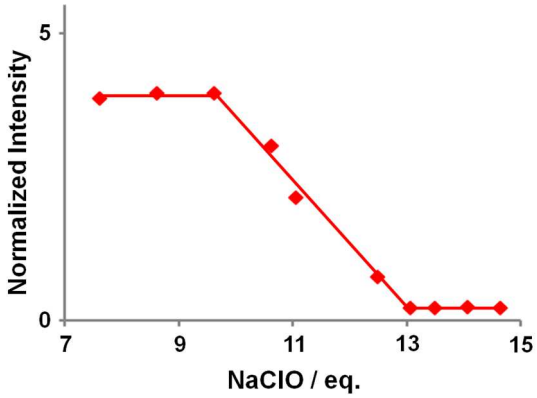

Figure 16. Fluorescence response at 480 nm in addition of NaClO at 15 min to the mixture of 50 μM DbbSeO **5** with 250 μM H_2S.

4–5 Conclusion

In summary, we have reported new reversible and turn-on fluorescent probes for H_2S induced a redox cycle between 1,4-diphenyl-1-seleno-1,3-butadines **3** and **4** incorporated in a dibenzo- or benzobarrelene skeletons and corresponding selenoxides **5** and **6**. DbbSeO **5** can detect hydrogen sulfide sensitively, quantitatively, and selectively among biothiols such as H_2S, Cys, and GSH. This selectivity could be increased by the steric repulsion between bulky dibenzobarrelene skeleton and thiol. In addition, oxidation pathway is constructed immediately, quantitatively, and selectively by the addition of HClO. The author believes that DbbSeO **5** could be applied to monitor the redox cycle between H_2S reduction and HClO oxidation under simulated physiological conditions, and are going to develop fluorescent probe having water-solubility, near infrared emission, and perfect selectivity.

4–6 Experimental Section

General Procedure

All melting points were determined on a Mel-Temp capillary tube apparatus and were uncorrected. ^{1}H, $^{13}C\{^{1}H\}$, $^{77}Se\{^{1}H\}$ NMR spectra were recorded on AVANCE-400 (400 MHz for ^{1}H and 101 MHz for ^{13}C) and AVANCE-500T (95.4 MHz for ^{77}Se) spectrometer using $CDCl_3$ as the solvent at room temperature. IR spectra were recorded on a Perkin Elmer System 2000 FT-IR spectrometer. UV-vis spectra were recorded on a JASCO V-560 spectrophotometer. Fluorescence spectra were recorded on a JASCO FP-6300 spectrofluorometer. Absolute photoluminescence quantum yields were measured by a calibrated integrating sphere system C10027 (Hamamatsu Photonics). Elemental analyses were carried out at the Molecular Analysis and Life Science Center of Saitama University. X-ray crystallography was performed with a Bruker AXS SMART diffractometer. The intensity data were collected at 103 K employing graphite-monochromated MoKα radiation (λ = 0.71073 Å) and the structures were solved by direct methods and refine by full-matrix least-squares procedures on F^2 for all reflections (SHELX-97).[31] Solvents were dried by standard methods and freshly distilled prior to use. Phosphate buffer saline was purchased from Wako Pure Chemical Industries, Ltd.

2,4-Diphenyl-5*H*-5,9b[1',2']-benzenonaphto[1,2-*b*]selenophene 1-Oxide (5)

A mixture of **3** (60 mg, 0.13 mmol) and MCPBA (95%) (36 mg, 0.20 mmol) was dissolved in CH_2Cl_2 (5 mL), and the mixture was stirred for 1 h. To the mixture were added aqueous Na_2SO_3 and aqueous $NaHCO_3$, and the mixture was extracted with CH_2Cl_2. The organic layer was washed with water and dried over anhydrous Na_2SO_4. After removal of the solvent of the filtrate in vacuo, the residue was purified by reprecipitation from CH_2Cl_2 and hexane solution to give **5** (54 mg, 87%): Pale yellow crystals, mp 192−193 ˚C decomp (hexane/$CHCl_3$). ^{1}H NMR (400 MHz) δ 5.41 (s, 1H), 7.02–7.17 (m, 4H), 7.33–7.49 (m, 11H), 7.62–7.67 (m, 1H), 7.71–7.78 (m, 2H), 8.89 (d, ^3J(H,H) = 6.8 Hz, 1H); ^{13}C NMR (101 MHz, $CDCl_3$) δ 57.0 (CH), 73.2 (C), 122.4 (CH), 123.2 (CH), 125.3 (CH), 125.4 (CH), 125.5 (CH), 126.6 (CH), 127.0 (CH), 127.2 (CH), 128.7 (CH), 128.9 (2CH), 129.2 (2CH), 129.5 (CH), 133.1 (C), 137.1 (C), 142.9 (2C), 143.1 (C), 147.3 (C), 148.3 (C), 150.4 (C), 150.9 (C); ^{77}Se NMR (95.4 MHz, $CDCl_3$) δ 992.2; IR (KBr) ν 818 cm^{-1} (Se=O). Found: C, 75.61; H, 4.15%. Anal. Calcd. for $C_{30}H_{20}OSe$: C, 75.79; H, 4.24%.

2,4-Diphenyl-5*H*-5,9b[1',2']-ethenonaphto[1,2-*b*]selenophene 1-Oxide (6)

A mixture of **4** (511 mg, 1.25 mmol) and MCPBA (95%) (340 mg, 1.87 mmol) was dissolved in CH_2Cl_2 (20 mL), and the mixture was stirred for 1 h. To the mixture were added aqueous Na_2SO_3 and aqueous $NaHCO_3$, and the mixture was extracted with CH_2Cl_2. The organic layer was washed with water and dried over anhydrous Na_2SO_4. After removal of the solvent of the filtrate in vacuo, the residue was purified by reprecipitation from CH_2Cl_2 and hexane solution to give **6** (483 mg, 91%): Orange crystals, mp 195−197 ˚C decomp (hexane/$CHCl_3$). ^{1}H NMR (400 MHz) δ 5.35 (dd, ^3J(H,H) = 5.6 Hz, ^4J(H,H) = 1.6 Hz, 1H), 7.02–7.14 (m, 2H), 7.15 (dd, ^3J(H,H) = 7.2 Hz, ^3J(H,H) = 5.6 Hz, 1H), 7.32–7.46 (m, 11H), 7.56 (dd, ^3J(H,H) = 1.6 Hz, ^3J(H,H) = 7.56 Hz, 1H), 7.72–7.78 (m, 2H); ^{13}C NMR (101 MHz, $CDCl_3$) δ 55.5 (CH), 77.2 (C), 121.3 (CH), 122.8 (CH), 124.7 (CH), 125.8 (CH), 126.90 (CH), 126.91 (CH), 128.5 (CH), 128.9 (CH), 129.2 (CH), 129.3 (CH), 129.5 (CH), 133.3 (CH), 133.4 (C), 137.2 (C), 138.1 (CH), 143.1 (C), 147.1 (C), 149.0 (C), 151.2 (C), 151.7 (C); ^{77}Se NMR (95.4 MHz, $CDCl_3$) δ 933.5; IR (KBr) ν 817 cm^{-1} (Se=O). HRMS (ESI) Calcd. for $C_{26}H_{18}OSe\cdot H$: M = 427.05956. Found 427.06342 ($M^+ + H^+$).

4–6 References

1. a) E. Lowicka, J. Beltowski, *Pharmacol. Rep.* **2007**, *59*, 4. b) M. Lavu, S. Bhushan, D. Lefer, *J. Clin. Sci.* **2011**, *120*, 219. (c) M. Whiteman, P. K. Moore, *J. Cell. Mol. Med.* **2009**, *13*, 488.

2. G. D. Yang, L. Y. Wu, B. Jiang, W. Yang, J. S. Qi, K. Cao, Q. H. Meng, A. K. Mustafa, W. T. Mu, S. M. Zhang, S. H. Snyder, R. Wang, *Science* **2008**, *322*, 587.

3. K. Abe, H. Kimura, *J. Neurosci.* **1996**, *16*, 1066.

4. a) Y. Kaneko, Y. Kimura, H. Kimura, I. Niki, *Diabetes* **2006**, *55*, 1391. b) W. Yang, G. D. Yang, X. M. Jia, L. Y. Wu, R. Wang, *J. Physiol.* **2005**, *569*, 519.

5. a) L. Li, M. Bhatia, Y. Z. Zhu, Y. C. Zhu, R. D. Ramnath, Z. J. Wang, F. B. M. Anuar, M. Whiteman, M. Salto-Tellez, P. K. Moore, *FASEB J.* **2005**, *19*, 1196. (b) R. C. O. Zanardo, V. Brancaleone, E. Distrutti, S. Fiorucci, G. Cirino, J. L. Wallace, *FASEB J.* **2006**, *20*, 2118.

6. Y. J. Peng, J. Nanduri, G. Raghuraman, D. Souvannakitti, M. M. Gadalla, G. K. Kumar, S. H. Snyder, N. R. Prabhakar, *Proc. Natl. Acad. Sci. U.S.A.* **2010**, *107*, 10719.

7. O. Kabil, R. Banerjee, *J. Biol. Chem.* **2010**, *285*, 21903.

8. S. Fiorucci, E. Antonelli, E. Distrutti, G. Rizzo, A. Mencarelli, S. Orlandi, R. Zanardo, *Gastroenterology* **2005**, *129*, 1210.

9. S. Fiorucci, E. Antonelli, A. Mencarelli, S. Orlandi, B. Renga, G. Rizzo, E. Distrutti, V. Shah, A. Morelli, *Hepatology* **2005**, *42*, 539.

10. a) K. Eto, T. Asada, K. Arima, T. Makifuchi, H. Kimura, *Biochem. Biophys. Res. Commun.* **2002**, *293*, 1485, b) K. Qu, S. Lee, J. Bian, C. Low, P. Wong, *Neurochem. Int.* **2008**, *52*, 155.

11. A. Tangerman, *J. Chromatogr. B* **2009**, *877*, 3366.

12. T. Ubuka, *J. Chromatogr. B.* **2002**, *781*, 227.

13. J. E. Doeller, T. S. Isbell, G. Benavides, J. Koenitzer, H. Patel, R. P. Patel, J. R. Lancaster Jr., *Anal. Biochem.* **2005**, *341*, 40.

14. N. Karbanee, R. P. van Hille, A. E. Lewis, *Ind. Eng. Chem. Res.* **2008,** *47*, 1596.

15. a) H. Peng, Y. Cheng, C. Dai, A. L. King, B. L. Predmore, D. J. Lefer, B. Wang, *Angew. Chem. Int. Ed.* **2011**, *50*, 9672. b) S. Chen, Z. Chen, W. Ren, H. Ai, *J. Am. Chem. Soc.* **2012**, *134*, 9589. c) A. R. Lippert, E. J. New, C. J. Chang, *J. Am. Chem. Soc.* **2011**, *133*, 10078.

16. a) W. Xuan, C. Sheng, Y. Cao, W. He, W. Wang, *Angew. Chem. Int. Ed.* **2012**, *51*, 2282. b) C. Liu, B. Peng, S. Li, C. M. Park, A. R. Whorton, M. Xian, *Org. Lett.* **2012**, *14*, 2184. c) C. Liu, J. Pan, S. Li, Y. Zhao, L. Y. Wu, C. E. Berkman, A. R. Whorton, M. Xian, *Angew. Chem.* **2011**, *123*, 10511.

17. a) K. Sasakura, K. Hanaoka, N. Shibuya, Y. Mikami, Y. Kimura, T. Komatsu, T. Ueno, T. Terai, H. Kimura, T. Nagano, *J. Am. Chem. Soc.* **2011**, *133*, 18003. b) X. Yaoa, Y. Y. Guob, J. X. Rua, C. Xua, Y. M. Liua, W. W. Qina, G. L. Zhanga, X. L. Tanga, W. S. Liu, *Sens. Actuators B* **2014**, *198*, 20.

18. a) B. Wang, P. Li, F. Yu, P. Song, X. Sun, S. Yang, Z. Lou, K. Han, *Chem. Commun.*, **2013**, *49*, 1014. b) Z. Lou, P. Li, Q. Panab K. Han, *Chem. Commun*, **2013**, *49*, 2445. c) B. Wang, P. Li, F. Yu, J. Chen, Z. Qu, K. Han, *Chem. Commun.*, **2013**, *49*, 5790.

19. a) B. Halliwell, M. Whiteman, *Br. J. Pharmacol.* **2004**, *142*, 231, b) B. Halliwell, *Trends Biochem. Sci.* **2006**, *31*, 509.

20. a) A. Gomes, E. Fernandes, J. Lima, *J. Biochem. Biophys. Methods* **2005**, *65*, 45. b) D. Oushiki, H. Kojima, T. Terai, M. Arita, M. Hanaoka, K. Hanaoka, Y. Urano, T. Nagano,

J. Am. Chem. Soc. **2010**, *132*, 2795. c) K. Cui, D. Zhang, G. Zhang, D. Zhu, *Tetrahedron Lett.* **2010**, *51*, 6052. d) A. Bizyukin, L. Korkina, B. Velichkovskii, *Bull. Exp. Biol. Med.* **1995**, *119*, 347.

21. D. Pattison, M. Davies, *Biochemistry* **2006**, *45*, 8152.

22. a) E. Podrez, H. A. Soud, S. Hazen, *Free Radical Biol. Med.* **2000**, *28*, 1717. b) D. Pattison, M. Davies, *Chem. Res. Toxicol.* **2001**, *14*, 1453. c) D. Pattison, M. Davies, *Biochemistry* **2006**, *45*, 8152.

23. a) F. Yu, P. Li, P. Song, B. Wang, J. Zhao, K. Han, *Chem. Commun.* **2012**, *48*, 4980. b) E. Miller, S. Bian, C. Chang, *J. Am. Chem. Soc.* **2007**, *129*, 3458. c) Y. Yamada, Y. Tomiyama, A. Morita, M. Ikekita, S. Aoki, *ChemBioChem* **2008**, *9*, 853. c) F. Yu, P. Li, G. Li, G. Zhao, T. Chu, K. Han, *J. Am. Chem. Soc.* **2011**, *133*, 11030. d) Y. Koide, M. Kawaguchi, Y. Urano, K. Hanaoka, T. Komatsu, M. Abo, T. Terai, T. Nagano, *Chem. Commun.* **2012**, *48*, 3091.

24. A. Ishii, T. Annaka, N. Nakata, *Org. Lett.* **2011**, *13*, 3702.

25. a) A. Ishii, T. Annaka, N. Nakata, *Chem. Eur. J.* **2012**, *18*, 6428. b) A. Ishii, Y. Aoki, N. Nakata, *J. Org. Chem.* **2012**, *18*, 6428.

26. Selected examples of orbital interaction between oxygen and σ* orbital in chalcogen–carbon bond; a) S. Hayashi, H. Wada, T. Ueno, W. Nakanishi, *J. Org. Chem.* **2006**, *71*, 5574. b) J. Beckmann, D. Dakternieks, A. Duthie, F. Ribot, M. Schürmann, N. A. Lewcenko, *Organometallics* **2003**, *22*, 3257. c) M. W. Kryman, G. A. Schamerhorn, K. Yung, B. Sathyamoorthy, D. K. Sukumaran, T. Y. Ohulchanskyy, J. B. Benedict, M. R. Detty, *Organometallics* **2013**, *32*, 4321.

27. For reviews, see a) Y. Hong, J. W. Y. Lam, B. Z. Tang, *Chem. Commun.* **2009**, 4332. b) J. Liu, J. W. Y. Lam, B. Z. Tang, *J. Inorg. Organomet. Polym.* **2009**, *19*, 249.

28. Y. Yuan, M. H. Knaggs, L. B. Poole, J. S. Fetrow, F. R. Salsbury Jr., *J. Biomol. Struct. Dyn.* **2010**, *28*, 51.

29. A. L. Bowman, L. Ridder, I. M. C. M. Rietjens, J. Vervoort, A. J. Mulholland, *Biochemistry* **2007**, *46*, 6353.

30. R. M. Uppu, *Anal. Biochem.* **2006**, *354*, 165.

31. G. M. Sheldrick, SHELXL-97, Program for Crystal Structure Refinement; University of Göttingen: Göttingen, Germany, 1997.

Chapter 5

Conclusion and Outlook

The author succeeded in the syntheses and applications of novel fluorescent 1-chalcogeno-1,3-butadiene derivatives, and opened a new field in photoluminescence chemistry.

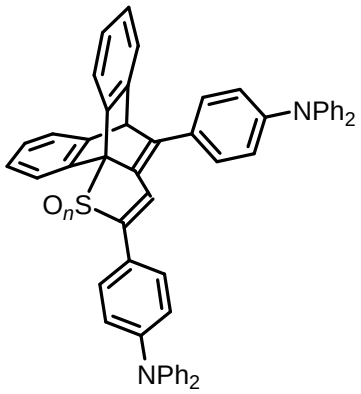

Chapter 2
Push-pull Type Derivatives (*n* = 1, 2)
Orange Fluorescence Based on CT Transition

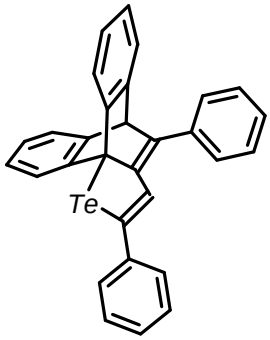

Chapter 3
Tellurium Analogues (*Te* = Te, TeO, $TeBr_2$)
Temperature-dependent Fluorescence

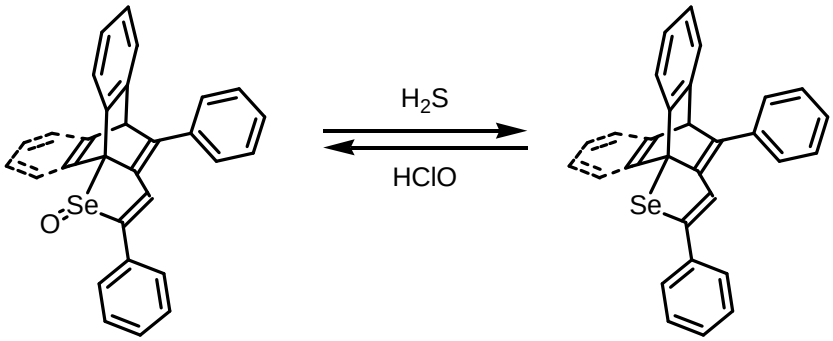

Chapter 4
Seleoxide/Selenide Redox Cycles
Reversible and Turn-on Type Fluorescent Probe for H_2S

We have demonstrated the synthesis of push-pull type derivatives including diphenylamino groups as electron-donating group and sulfoxide or sulfone unit as electon-withdrawing group by the oxidation of corresponding sulfide analogue. These oxides showed red-shifted, comparing with sulfide analogue, orange fluorescence and

solvatofluorescence. An elucidation of solvatofluorescence and TD-DFT calculations supported fluorescence of push-pull type derivatives are based on the intramolecular charge transfer transition. However, the red and near infrared emission has not be established yet in our compounds. We have already started to create more red-shifted emission by utilizing other push-pull type derivatives.

We got successful to synthesize 1-telluro-1,3-butadienes and to elucidate their photophysical properties. Telluride analogue showed temperature-dependent fluorescence; it is fluorescent with moderate quantum yield in the glass state of 2-MeTHF at 77 K, whereas it is barely fluorescent at room temperature, unlike the sulfide and selenide analogues, due to the heavy-atom effect of tellurium. Although further detailed photophysical studies on their exited states, it can be considered that the temperature-dependent fluorescence character is attributed to the thermally activated intersystem crossing from a lowest excited singlet state to an adjusted higher excited triplet state.

The reversible and turn-on type fluorescent probes for H_2S could be constructed in redox cycle between reduction of selenoxide and oxidation of selenide with HClO. These probes also showed the high sensitivity, quantitativity, and selectivity for other biothiols, L-cysteine and glutathione. Their selectivity was induced by the steric repulsion between bulky dibenzobarrelene skeleton and thiols, supported by the comparison between dibenzobarrelene and benzobarrelene derivatives. Oxidation of NaClO was underwent immediately, quantitatively, and selectively. The author believes our system could be applied to monitor the redox cycle between H_2S reduction and HClO oxidation under simulated physiological conditions, and are going to develop fluorescent probe having water-solubility, near infrared emission, and perfect selectivity.

Acknowledgments

The author could summarize my studies in this thesis that has been carried out under the direction of Prof. *Akihiko Ishii* at Saitama University during the period of April 2012 to March 2015.

The author wishes to express his sincere gratitude to Prof. *Akihiko Ishii* for his kind guidance, helpful suggestion, and hearty encouragement throughout this work.

The author is grateful to Dr. Norio Nakata for his useful advice, suggestions, kind encouragement, measurement and instruction of X-ray crystallographic analysis.

The author wishes to thank Dr. *Sylviane Sabo-Etienne* and all members of her group for discussions, collaborations, and kind assistance.

The author would like to acknowledge to Prof. *Toshiyuki Takayanagi*, Prof. *Masaichi Saito*, Assoc. Prof. *Yoshiaki Sugihara*, and Assoc. Prof. *Toshio Hasegawa* for helpful discussions from various points of view.

The author thanks Mr. *K. Hosokawa*, Mr. *H. Watanabe*, and Mr. *K. Aoshima* (Hamamatsu Photonics K. K.) for measuring the emission lifetime.

The author acknowledges the Japan Society for the Promotion of Science (JSPS) for a fellowship for young scientists.

Finally, the author would like to express deep appreciation to parents, Mr. *Hiroshi Annaka* and Mrs. *Katsuko Annaka*, brothers, Mr. *Kosuke Annaka* and *Shogo Annaka*, other families, and loved Ms. *Kaori Matsumoto* for their constant assistance and affectionate encouragement.

The author is grateful for many discussions and kind assistance to all members of Ishii's laboratory.

Professor *Akihiko Ishii*

Assistant Professor *Norio Nakata*

Dr. *Tomoyuki Toda* , Dr. *Yuki Yamaguchi*, Mr. *Takashige Ikeda*, Ms. *Nanami Kato*

Mr. *Shun Fkazawa*, Ms. *Yoko Fujiwara*, Mrs. *Hitomi Toda*, Ms. *Eriko Toyoda*

Mr.*Yuichiro Nemoto*, Mr. *Noriyuki Furukawa*, Ms. *Suzuka Yamamoto*

Ms. *Kanako Asajima*, Mr. *Takanori Ito*, Ms. *Chizuru Komatsubara*, Mr. *Yusuke Saito*

Mr. *Keita Ikuma*, Mr. *Fumihiko Kawauchi*, Ms. *Tsuiman Kao*, Mr. *Shota Kobayashi*

Mr. *Yutaro Aoki*, Ms. *Jing An*, Mr. *Izuru Suzuki*, Ms. *Noriko Sekizawa*

Mr. *Hiroki Mikami*, Mr. *Hiroki Abe*, Mr. *Hiroki Kobayashi*, Mr. *Yukihiro Makishima*

Ms. *Hanako Yamamoto*, Mr. *Laurent Bacque*, Mr. *Tasuku Ogasawara*, Ms. *Chika Shibata*,

Ms. *Mari Shibata*, Mr. *Narimi Hosoda*, Mr. *Takanori Watanabe*

Ms. *Estefania da Costa Baptista*, Mr. *Yusuke Oshima*, Ms. *Sawako Shoda*

Ms. *Miki Toyoda*, Ms. *Yuri Hirai*, Mr. *Andreas Meißner*

Tatsuro Annaka

Saitama University

March, 2015

List of publications

Publications for this thesis

1. ‘Synthesis and Photophysical Properties of Extended π-Conjugative and Push-pull Type 1,4-Diaryl-1-thio-1,3-butadienes’ T. Annaka, N. Nakata, A. Ishii, *Bull. Chem. Soc. Jpn.* DOI:10.1246/bcsj.20140351.

2. ‘Synthesis, Structures, and Temperature-Dependent Photoluminescence of 1,4-Diphenyl-1-telluro-1,3-butadiene Incorporated in a Dibenzobarrelene Skeleton and Derivatives’ T. Annaka, N. Nakata, A. Ishii, *Organometallics* under revision.

3. ‘Reversible Fluorescence Probes Based on Selenide/Selenoxide System for Redox Cycle Between H_2S and HClO’ T. Annaka, N. Nakata, A. Ishii, manuscript in preparation.

Other publications

1. ‘Convenient Syntheses and Photophysical Properties of 1-Thio- and 1-Seleno-1,3-Butadiene Fluorophores in Rigid Dibenzobarrelene and Benzobarrelene Skeletons’, A. Ishii, T. Annaka, N. Nakata, *Chem. Eur. J.* **2012**, *18*, 6428.

2. ‘Thiophene-Fused 3-Methylene-2,3-dihydrochalcogenophenes: Fluorescent Dyes Incorporated in a Rigid Dibenzobarrelene Skeleton’ A. Ishii, S. Kobayashi, Y. Aoki, T. Annaka, N. Nakata, *Heteroatmchem.* **2014**, *25*, 658.

3. ‘Silane Deuteration Catalyzed by Ruthenium Bis(dihydrogen) Complexes or Simple Metal Salts’ K. A. Smart, E. M. Martin, T. Annaka, M. Grellier, S. S. Etienne, *Adv. Synth. Catal.* **2014**, *356*, 759.